A review article presented by Dr. Matteo Bonomo from the MOF Group at the Department of Chemistry, University of Turin, Italy in collaboration with the GAME Lab Group at the Politecnico di Torino, Italy.

Recent advances in eco-friendly and cost-effective materials towards sustainable dye-sensitized solar cells

The most significant and impactful strategies recently adopted by the scientific community to enhance the sustainability of materials in classical components of dye-sensitised solar cells, a topic of utmost importance, are reviewed. These include sensitizers, redox couples, electrolytes and counter electrodes, which are critically presented and discussed in terms of environmental impact and cost, along with their smart syntheses and deposition procedures for practical scaling-up.

As featured in:

See Matteo Bonomo *et al.*, *Green Chem.*, 2020, **22**, 7168.

ROYAL SOCIETY OF CHEMISTRY

rsc.li/greenchem

Registered charity number: 207890

Green Chemistry

ROYAL SOCIETY OF CHEMISTRY

CRITICAL REVIEW

View Article Online
View Journal | View Issue

Cite this: *Green Chem.*, 2020, **22**, 7168

Recent advances in eco-friendly and cost-effective materials towards sustainable dye-sensitized solar cells

Nicole Mariotti, [a] Matteo Bonomo, *[a,b] Lucia Fagiolari, [c] Nadia Barbero, [a,b] Claudio Gerbaldi, [c] Federico Bella [c] and Claudia Barolo [a,b,d]

Dye-sensitized solar cells (DSSCs), as emerging photovoltaic technology, have been thoroughly and extensively investigated in the last three decades. Since their first appearance in 1991, DSSCs have gained increasing attention and have been classified as feasible alternatives to conventional photovoltaic devices due to their numerous advantages, such as cheap and simple preparation methods, the possibility of being integrated in buildings and astonishing performances under indoor and diffuse illumination conditions. Photoconversion efficiencies of up to 14% and 8% have been obtained for lab-scale devices and modules, respectively. Albeit the efforts made, these values seem arduous to be outdone, at least under simulated solar radiation. Nevertheless, recent lab-scale systems have demonstrated photoconversion efficiencies of up to 33% under indoor illumination (*i.e.* 1000 lux) leading to an actual *Renaissance* (or *Revival*) of these devices. It is worth mentioning that scientists in this field are developing innovative materials aiming at long-term and efficient devices, being the concept of sustainability often set apart. However, in light of effective commercialization of this technology, stability, efficiency and sustainability should be considered as the essential keywords. Nowadays, DSSCs are finding a "new way back" towards sustainability and rather a huge number of reports have focused on the preparation of green and cost-effective materials to replace the standard ones. In this scenario, the present review aims to give an overview of the most adopted strategies to enhance the sustainability of materials in classical DSSC components (*e.g.* sensitizer, redox couple, electrolyte and counter-electrode), including smart synthesis and deposition procedures, which currently represent utmost important topics in the scientific community.

Received 31st March 2020,
Accepted 30th July 2020

DOI: 10.1039/d0gc01148g

rsc.li/greenchem

1. Introduction

With a world population that is now about to reach eight billion people and a forecast of even ten billion by the middle of this century, we need to appropriately answer the question of how humanity will be able to fulfill its energy needs in the near future. To date, most of the global electricity production has been entrusted to fossil fuels, which – in addition to being non-renewable – generate large quantities of carbon dioxide, the greenhouse gas that has now become a real threat to our global ecosystem.[1,2] The Intergovernmental Panel on Climate Change (IPCC) declared that the energy supply sector is the largest contributor to global greenhouse gas emissions (considering energy extraction, conversion, storage, transmission and distribution processes that deliver final energy to end-use sectors).[3] In the framework of climate change, decarbonizing electricity generation is a key feature of cost-effective mitigation strategies in achieving low-stabilization levels (430–530 ppm CO_2 eq.).[3] Following the Sustainable Development Goal 7 (SDG7, *Affordable and Clean Energy*)[4] recommendation and according to the 2030 Climate & Energy Framework,[5] the European Union (EU) aims at reaching two targets by 2030: (i) at least 32% share for renewable energy and (ii) at least 32.5% improvement in energy efficiency.

For many years, financing entities perceived renewables (*e.g.*, first-generation solar cells made of ultrapure silicon metal) as risky because of the high cost of production, leading to high lending rates for individuals and businesses requiring funding for renewable power generation. However, considering the most recent International Renewable Energy Agency (IRENA) report, this trend is on continuous decline since the

[a]*Department of Chemistry, Università degli Studi di Torino, Via Pietro Giuria 7, 10125 – Turin, Italy. E-mail: matteo.bonomo@unito.it*
[b]*NIS Interdepartmental Centre and INSTM Reference Centre, Università degli Studi di Torino, Via G. Quarello 15A, 10135 – Turin, Italy*
[c]*GAME Lab, Department of Applied Science and Technology, Politecnico di Torino, Corso Duca degli Abruzzi 24, 10129 – Turin, Italy*
[d]*ICxT Interdepartmental Centre, Università degli Studi di Torino, Via Lungo Dora Siena 100, 10153 – Turin, Italy*

last decade, and unsubsidized onshore wind and solar renewables are becoming more and more cost-competitive, with an increasing number of companies entering the renewable energy industry.[6] Specifically, the report showed that the global weighted-average cost of electricity declined by 26% year-on-year for concentrated solar power (CSP), followed by bioenergy (−14%), solar photovoltaics (PV) and onshore wind (both −13%), hydropower (−12%), geothermal and offshore wind (both −1%). Consequently, cheaper renewable energy sources and batteries are expected to lead to wind and solar accounting for at least half of the global electricity generation by 2050.

In a market analysis and forecast from 2019 to 2024, the International Energy Agency (IEA) set the renewable power capacity expansion to 50% led by solar technologies. In particular, the rapid increase in the ability of consumers to generate their own electricity presents new opportunities and challenges for electricity providers and policy makers worldwide; consequently, distributed solar PV systems in homes, commercial buildings and industry will significantly gain a solid position in the market, and their capacity is forecast to increase up to 320 GW, almost half of the total PV growth.[7,8]

The Sun, being a continuous source of electromagnetic radiation that cannot regenerate itself, is technically a flow resource and not a renewable energy source as it cannot be stocked.[9] However, the Sun can be considered as renewable energy since it is (considering the timescale of mankind at least) inexhaustible. Energy from renewable resources can be considered as a feasible starting point toward truly sustainable sources (especially with respect to those produced by fossil fuels[10]) because their exploitation rate is slower than their consumption. Of course, a renewable resource[9] does not necessarily mean a sustainable[11] energy output. In fact, this purpose can be achieved only through efficient technology, where its production and distribution are not compromised by the availability of materials.

Accordingly, emerging PV and specifically dye-sensitized solar cells (DSSCs) can improve the share of energy produced from renewable sources and energy efficiency through their above-listed specific applications, complementing traditional solar panels.

Originally co-invented by O'Regan and Grätzel,[12] DSSCs are photoelectrochemical devices, which belong to the group of emerging PV technologies. For more than two decades they have been developed as a credible alternative to the well-established p–n junction PV devices made from silicon due to their rapid and simple preparation methodology coupled with green and sustainable production.[13] Nowadays, with the strong advent of newly developed perovskite solar cells (PSCs),[14–16] the lead-based thin-film technology that has quickly and significantly outclassed the record PV efficiencies by a factor of two on both rigid and flexible configurations, promising to compete with silicon technology in the near future, outshined the effective role and prospects of DSSCs for utility-scale solar applications. Nevertheless, at present, there are still limited choices of perovskite materials and their stability and toxicity remain extremely challenging issues; thus, DSSCs and other emerging photovoltaic technologies must be considered still viable and can be developed, perhaps concurrently, for many years in the future, offering the possibility to design solar cells with large flexibility in shape, color and transparency.[17] Compared to silicon-based technologies, there are two main issues preventing the widespread commercialization of DSSCs, their lower efficiency and shorter life-time.[18,19] However, despite the sizeable decline in silicon prices,[20] DSSCs still offer the major advantage of remaining functional even under diffuse light.[21] Moreover, they can be realized as transparent devices, and therefore be used as smart, power-generating building blocks.[22]

Nicole Mariotti

Nicole Mariotti graduated cum laude *at the University of Camerino defending a thesis on green and sustainable approaches in the synthesis of nitro-compounds. She was then enrolled in the* Erasmus Traineeship Program *developing green one-pot multicomponent reactions. After her masters degree, she joined the department of Chemistry at the University of Turin where she continued her studies attending an interdisciplinary PhD course in* Innovation for the Circular Economy*, working on sustainable and innovative materials for energy-related application. She is (co)author of 2 peer-reviewed publications.*

Matteo Bonomo

Matteo Bonomo is a post-doctoral researcher at the University of Turin and his work is mainly related to the synthesis and characterization of innovative materials for emerging photovoltaics. More recently, he has been involved in the investigation of structural and electronic properties of ionic liquids and deep eutectic solvents for energetic application. He has received, among others, the Junior "ENERCHEM 2020" prize (for his innovative contribution in the Chemistry for Renewable Energy). He is (co)author of 35 publications (h-index 11, >350 citations) in international peer-reviewed journals.

Indeed, particularly where low production cost and environmental benignity are primary requirements, DSSCs still represent a competitive alternative technology for three main reasons: (i) their simple preparation methods can contribute to exploiting solar energy in a sustainable way, increasing its use and promoting climate change mitigation,[23] (ii) the opportunity to produce devices that do not contain any critical raw materials (CRMs),[24] and (iii) their foreseen exploitation in distributed energy as windows, internet of things (IoT) devices and in indoor applications.[25,26]

However, despite these merits, their commercialization requires much more effort, and thus significant research is focused on the development and optimization of each of the components of DSSC to enhance their lifetime and efficiency, while reducing costs and environmental impact.[19] Accordingly, several comprehensive and informative articles have been published over the last 10 years, which reviewed the improvements and challenges in the field of DSSCs, from the analysis of their different components and the effect of nanostructuration by S. Anandan in 2007,[27] to the fundamentals and current status by K. Sharma *et al.*,[13] as well as the general trends and developments in the field of photoelectrodes, photosensitizers (PS) and electrolytes by Bose *et al.*[28] Different types of sensitizers were thoroughly discussed by Shalini *et al.*,[29] while the work by J. Wu *et al.* chiefly focused on the counter electrode (CE) part of the devices,[30] including metals/alloys, carbons and conductive polymers. D. Sengupta *et al.* gave insights into the key role of the photoanode and the effect of influencing parameters on its PV characteristics.[31] On the other hand, some authors focused on the electrolyte composition and features to reach the best trade-off between efficiency and stability.[32–34]

Thus, by considering and comparing different review articles in the literature, the basic concepts, research history, key materials, techniques and prospects on further development have been comprehensively reviewed.[34–36] However, we found that there is room for highlighting the research that reported the replacement of conventional DSSC materials due to their high cost, limited abundance and uninvestigated sustainability with environmentally friendly, green and sustainable materials. Accordingly, throughout this review, we report the most recent advances towards the implementation of innovative materials for sustainable DSSCs. It should be noted here that we mainly focus on a thorough and critical analysis of the sustainability of constituent materials of classical DSSCs, together with their synthetic and deposition processes. Actually, a valuable discussion on the sustainable routes for the industrial scale-up and commercialization of DSSCs has been recently reported by Parisi *et al.*,[23,37] which is a perfectly complementary approach to the present review.

After the introduction of the working principle of these devices as one of the mandatory steps in improving their sustainability, an overview of the aspects to be considered while assessing the sustainability of materials, with a brief mention of the final product, is offered (section 1.1). Section 2 investigates (i) the use of noble and CRMs, (ii) material cost, (iii) energy consumption for the manufacture of materials, (iv) materials resulting in degradation and (v) design for product integrity and advantageous waste management. These five aspects are linked to the components of DSSCs, and some research trends for their resolution are presented. In the following sections, each component, namely dyes (section 2.1), electrolytes (section 2.2), counter-electrodes (section 2.3) and transparent conductive oxide (TCO)-coated glass (section 2.4), are individually discussed with the aim to present potential ways to improve the sustainability of the exploited materials. The attention is thoroughly focused on environmental issues, but socio-economic aspects at the material and production levels are also mentioned.

It is our precise and straightforward decision not to tackle the analyses of photoanode, as briefly explained in section 1.1, since nanostructured TiO_2, being abundant and relatively safe,[38,39] already represents the best trade-off between high efficiency and sustainability.[40]

Lucia Fagiolari

Lucia Fagiolari graduated cum laude *and received her PhD in Chemical Sciences from the University of Perugia, where she was involved in the synthesis and characterization of heterogeneous catalysts for water splitting application. Currently, she is a post-doctoral researcher at Politecnico of Turin. Her research concerns the development and characterization of dye-sensitized solar cells, with a focus on the use of renewable raw materials as cell components. She is co-author of 5 publications (h-index = 3, >40 citations) in international peer-reviewed journals.*

Nadia Barbero

Nadia Barbero is Assistant Professor in Organic Chemistry at the University of Turin and her research interests are focused on the design and synthesis of new organic and hybrid materials for non-conventional and technological applications (nanotechnology, biotechnology and dye-sensitized solar cells). She has much experience in NIR-DSSC and is currently involved in IMPRESSIVE EU project for the development of transparent solar cells. She is (co)author of 66 publications (h-index 21, >1100 citations).

The proposed approach aims at creating awareness of the features that require investigation when facing sustainability assessments and to offer a comprehensive set of present studies and insightful topics, which can become relevant in the near future.

1.1 Dye-sensitized solar cells: state of art and future challenges

DSSCs were firstly designed with the intent to reproduce the principle of photosynthesis that occurs in the cells of plants. Artificial photosynthesis has existed for decades, but to date, has not been successfully exploited industrially to create renewable energy because it is still a complicated multi-step process that has to be optimized, which often requires expensive and toxic materials.[41,42] DSSC photovoltaic technology can be likened to artificial photosynthesis since it mimics the way nature absorbs energy from sunlight. According to researchers in this field,[43,44] DSSCs are the closest concept we have to photosynthesis due to their greener, smaller, more flexible and eco-friendly features compared to the early-generation solar cells, which require much more energy to manufacture. These advantages are due to the use of a dye as the photosensitive material, which also makes the working mechanism simple.

A DSSC basically consists of four major components, the anode, PS, electrolyte and CE. Its classic representation is illustrated in Fig. 1a, which schematically shows the main components of the state-of-the-art device established by O'Regan and Grätzel, comprising: (i) a porous layer of dye-sensitized nanocrystalline TiO_2 semiconductor as the photoelectrode, (ii) an electrolyte based on the I^-/I_3^- redox couple, and (iii) platinum thin film as the CE.[12,45] This assembly is generally enclosed within a sandwiched structure of two conductive substrates made of fluorine-doped tin oxide (FTO)-coated glass at both the photoanode and the cathode.

The above described cell architecture is typical of conventional DSSCs, namely n-type, which are based on a n-semiconductor, where the charge movement is guaranteed by negative carriers (*i.e.* electrons).

The working principle of DSSCs involves four fundamental processes (Fig. 1d) to convert the electromagnetic radiation coming from the Sun (or any artificial source) into electrical energy: (i) the impingement of sunlight onto the dye provokes photoexcitation; (ii) the photogenerated electrons are then injected in the conduction band (CB) of the photoanode and, then, to the external circuit; (iii) the electrolyte supplies electrons to reduce the dye molecules, thus avoiding their decomposition, through the redox reaction of iodide into triiodide (this reaction has to be rapid to avoid the recombination of injected electrons with the oxidized dye molecules, which causes cell short circuiting) and (iv) at the cathode, triiodide eventually recovers an electron coming from the external load to complete the electronic circuit.

Scientists involved in the field have also deeply investigated the feasibility of a p-type counterpart, in which a sensitized p-semiconductor acts as the working electrode (Fig. 1b [46]). Unfortunately, the photoconversion efficiency of the "inverted" geometry has never approached that of the conventional geometry (lower by one order of magnitude[47]), despite the great efforts in tailoring photocathode materials[48–51] and the development of dedicated sensitizers[52–55] and redox couples.[56,57] This is mainly ascribed to the lower photocurrent powered by p-DSSCs, as expected by their hole-driven charge diffusion processes. In both the *n* and *p* configurations, only one electrode is photoactive (the anode or the cathode, respectively), whereas the other operates as a standard electrode. Some articles reported the exploitation of a tandem geometry, in which both the photoanode and the photocathode, being sensitized, are actively involved in the production of a photocurrent (Fig. 1c).[58–60] This configuration allows higher photovoltages to be obtained compared to the single junction device, but the overall efficiency is still heavily limited by the charge transport properties of the photoanode.

Claudio Gerbaldi

Claudio Gerbaldi (Ph.D. in Materials Science and Technology) is full professor of Chemistry at the Department of Applied Science and Technology (Politecnico di Torino). Leader of the Group for Applied Materials and Electrochemistry (GAME-Lab), he currently coordinates the research activity on innovative polymer electrolytes and nanostructured electrodes for the development of eco-friendly energy storage (chiefly, Li and post-Li batteries) and conversion devices. He has published >140 ISI articles (h-index 48) and, among others, he has received the Piontelli Award for outstanding results in Electrochemistry from the President of the Italian Republic (2015).

Federico Bella

Federico Bella is Associate Professor of Chemistry at Politecnico of Turin and works in the field of hybrid solar cells and secondary batteries, focusing on electrolytes formulation and devices integration. He is author of 80 publications in international peer-reviewed journals (h-index = 49) and he is a board member of the Industrial Chemistry Division of Società Chimica Italiana. He is the 2019 recipient of the RSC Environment, Sustainability & Energy Division Early Career Award for the inventive development of photoinduced polymerization strategies for solar cells and batteries.

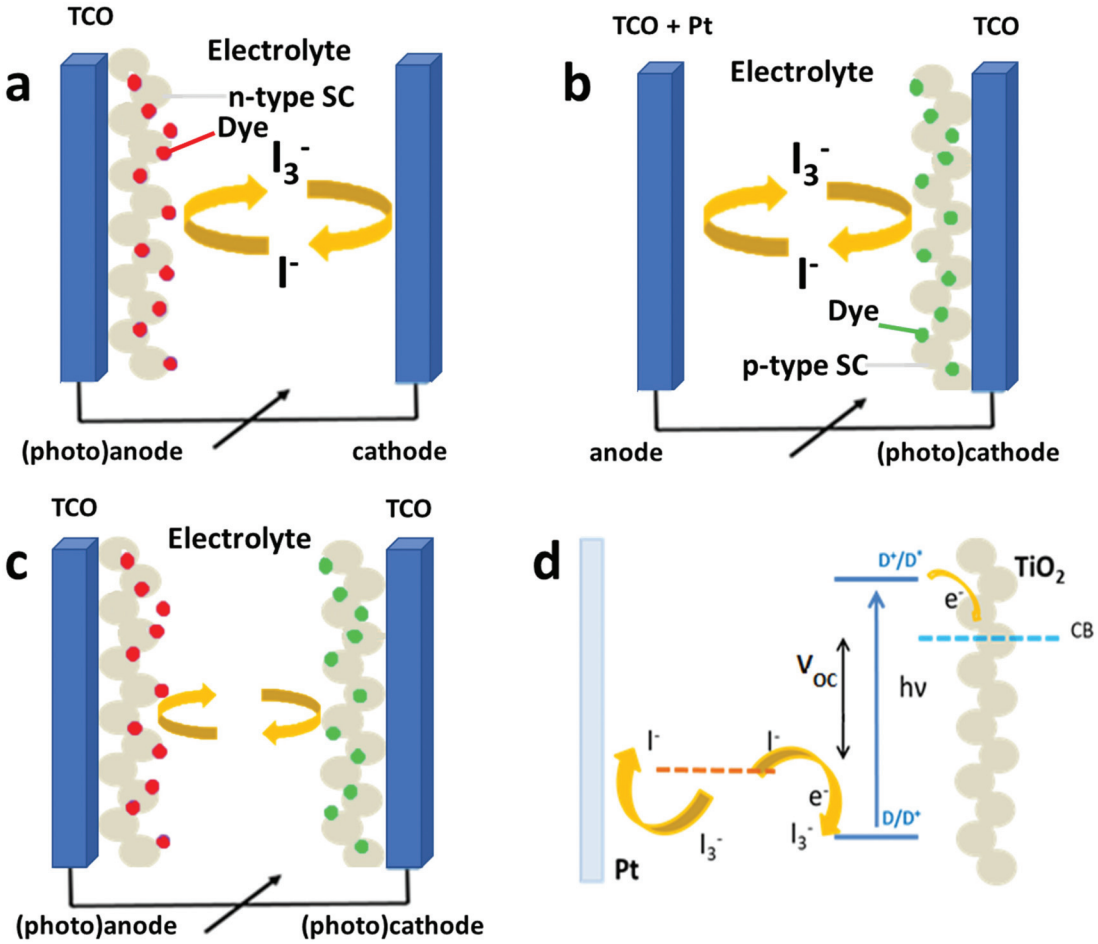

Fig. 1 Schematic representation of (a) classical DSSC, (b) inverted architecture DSSC and (c) tandem device; (d) main electronic processes occurring in a conventional device upon operation.

The specific working principle of each device component will be thoroughly discussed in a dedicated section of this review, with specific attention on the correlation of proposed materials with the physical and chemical phenomena occurring in classical DSSCs. For a deeper approach, please refer to the fundamental review by Hagfeldt *et al.*[36]

DSSCs have aroused significant interest as they offer the possibility to achieve a good conversion of solar energy *via* a simple design at competitive manufacturing cost. The first cell reported by O'Regan and Grätzel showed an efficiency of 7%,[12] and subsequently the work by the Grätzel's team brought it to about 10%.[61] Currently, the best certified result obtained on the laboratory scale is 12.3% (Fig. 2),[62] which is slightly lower than the maximum efficiency obtained by Kakiage *et al.* of around 14%.[63] This enhancement was achieved by the introduction of alternative redox couples (section 2.2), which were developed in conjunction with properly designed sensitizers (section 2.1). As highlighted by L. Peter in 2011,[64] "*if DSSCs are to progress, we do not need just more research; we need better focused research*". Indeed, a specific component should be designed considering its interplay with other cell components, and if the best material does not exist, we should aim to determine the best photoanode/dye/electrolyte/counter-electrode set. Accordingly, computer modelling, machine learning and also the use of specific software for material selection are key

Claudia Barolo

Claudia Barolo is Associate Professor of Industrial Chemistry at the Department of Chemistry of the University of Torino. Her research interest is focussed mostly on the synthesis and characterization of organic and hybrid functional materials (from molecules to polymers) able to interact with light and their possible application in energy related fields (opto-electronics, lighting and solar cells). She is also vice-coordinator of the PhD Programme in Innovation for the Circular Economy at the University of Turin. Her work resulted in more than 110 publications (h-index 32, >3400 citations).

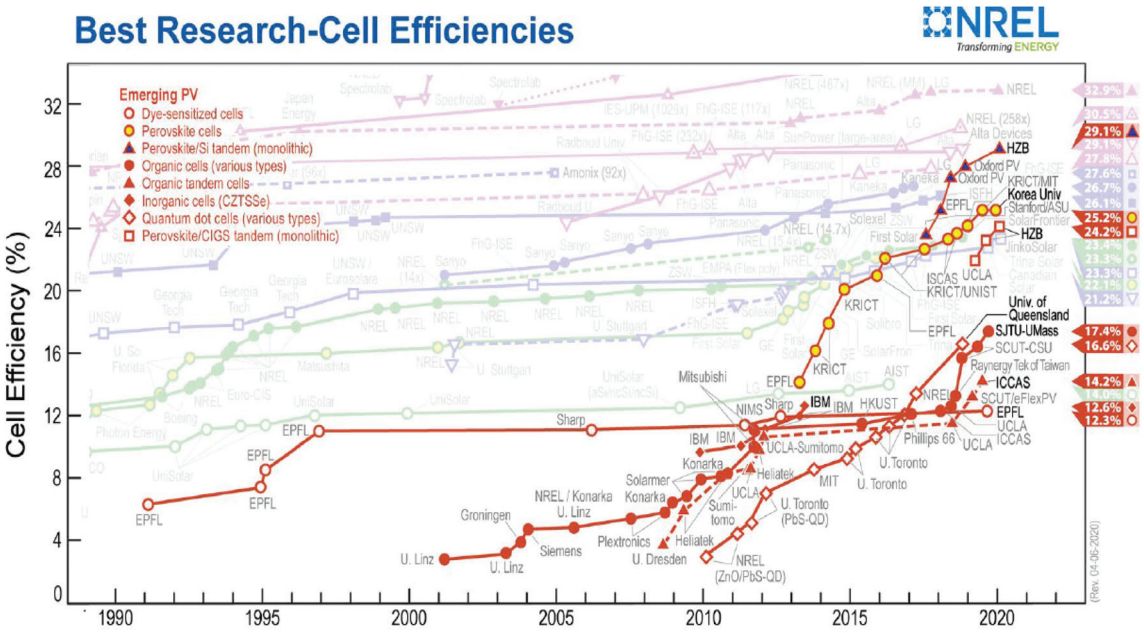

Fig. 2 NREL chart of record performances, showing the highest certified power conversion efficiencies for different types of emerging photovoltaic technologies from 1990 to the present.

to allow better understanding of the processes in DSSCs.[25,65–68] Actually, the improvement in device sustainability should proceed on two parallel (but interconnect) paths aimed at finding the most suitable materials and guaranteeing the best trade-off between sustainability and efficiency.

The photoconversion values sensibly increase if a low intensity light source, simulating indoor application, is employed,[26] where the highest efficiency reported to date is close to 32% (1000 lux),[69] outperforming OPVs,[70] whereas better performances can be obtained by using PSCs.[71] However, regarding indoor application, the presence of lead is a serious issue to be solved. In the case of commercial modules, the maximum reported efficiency is about 8.2%.[72] One of the parameters that should be chiefly monitored is the effect of degradation on performance, where laboratory experiments have shown a decrease in efficiency, which can reach 5% after 1000 h stress at 80 °C or 60 °C in the dark or under the Sun, respectively. In the case of commercial modules, less than 15% degradation in four years has been demonstrated.[73] It is worth mentioning that indoor application will reduce the ageing conditions of the device, leading to better stability. Presenting prospects for the future (*i.e.* next 5–10 years) is very challenging since the further development of DSSCs is bound to that of PSCs. Nonetheless, theoretical calculation showed that a 20–25% efficiency is feasible for single-junction DSSCs,[74,75] whereas the Shockley–Queisser limit (*i.e.* 33.8%)[76] is still far from being reached.

Due to their characteristics of transparency, flexibility, robustness and lightness, DSSCs are well conceived to be integrated in the construction of buildings.[77] They can be applied to windows, walls and roofs of new and existing buildings. Furthermore, besides their ability to generate electricity even indoor or under low illumination conditions, they also have positive aesthetic features. The implementation of this technology in construction is possible due to the wide range of dyes, operation temperatures and almost insensitivity to the angle of incidence of light. Not limited to glass, DSSC technology can make skylights, windows, and even building facades (which are exposed to daylight) capable of producing electricity. It is worth mentioning that, before penetrating the building integrated photovoltaics (BIPV) market, DSSC technology may find useful application in decorating urban street tools and rooftop greenhouses, assisting the growth of plants and supplying small electronic devices to power IoT and low voltage devices (*e.g.* sensors).[78,79] Wearable devices are also an opportunity, such as self-energy converting sunglasses based on DSSCs. This interesting and feasible plethora of applications should be considered in terms of the coupling of light-harvesting devices (*e.g.* DSSCs) and energy storage systems (*e.g.* a batteries or a supercapacitors)[80,81] in order to avoid issues related to the intermittent availability of a light source.

It should be noted that almost all the scientific efforts made in the field of DSSCs aimed at obtaining more efficient and/or more stable devices. However, in recent years, increasing attention has been paid to tackle the sustainability and greenness of the developed device components.

2. The concept of sustainability applied to DSSCs

As mentioned in the introduction, a great number of articles and book chapters on DSSCs have been published in the litera-

ture, where leading scientists working in this field extensively reviewed the working principles, architectures, chemistry, physics, materials science, engineering and smart technology behind DSSCs.[13,29,45,46,82–85] The applications of new materials have been explored to enhance the efficiency and the stability of DSSCs; nevertheless, they are sometimes expensive, unsafe, toxic, not environmentally friendly and/or even produced by complicated and energy consuming processes that are difficult to be scaled-up at competitive prices. Actually, the cost for achieving the highest efficient device overwhelms the actual motivation behind developing a particular class of solar cell technology, which must be eco-friendly and competitive in terms of cost manufacturing. Indeed, in recent years, increasing attention has been focused on tackling the sustainability and greenness of the developed device components.[23,86,87]

It is worth recalling that a device that produces energy from a renewable source is not necessarily sustainable. Indeed, the energy produced from renewable sources presents its own emissions[88] and criticalities, such as the use of CRMs in the involved technologies.[89] Therefore, the investigation of the main responsible factors threating the sustainability of a particular technology is of great importance to achieve renewable energy that can be indeed claimed as sustainable.

A powerful tool to examine the environmental sustainability of a product or service is the life cycle assessment (LCA),[88] which allows the evaluation of its environmental impacts and the identification of the main contributors, namely "*hotspots*". LCA results are characterized by uncertainty levels, where the more the life cycle of a product is assessed, the lower the uncertainty.[90] In the case of DSSCs, the large-scale production and the end-of-life (EoL) phase are not mature, which means that the accuracy of the presented results can be improved in the future when more data will be available, and the processes will be better defined. Moreover, many LCAs for DSSCs have been studied in a "*cradle-to-gate*" way, where this approach considers the life cycle of DSSCs from the extraction of raw materials to the production phase (the use phase and the EoL are not considered due to the lack of data for waste management).[91,92] Subsequently, the LCAs presented in literature deal with "*established architecture*", in which conventional (and high performing) materials are employed.[23,91,93] Therefore, the majority of the innovative materials presented throughout this review have not been investigated *via* an effective LCA; nevertheless, if LCA data are available, we critically analysed the preparation procedures of a specific material in dedicated paragraphs. On the other hand, when LCA data are not available, we evidenced eventual "*hotspots*" to be considered in a forthcoming assessment.

Additional indicators considered for PV energy systems are the cumulative energy demand (CED) and the energy payback time (EPBT). CED is defined as an energetic indicator that quantifies the whole energy required during the life cycle of a product. It is obtained by summing both the direct energy (*e.g.*, electricity for manufacturing, and thermal energy) and the indirect energy (embodied energy of materials) contributions.[94] EPBT is an indicator, which is expressed in years, representing the time required to generate the same amount of energy consumed during the production processes and can be considered a quantitative evaluation of the cost-effectiveness of a specific technology (and its constituent materials).[93] The EPBT depends on the CED, the yearly energy output (YEO) and the electrical conversion factor (C), according to the following equation: EPBT = CED YEO^{-1} C^{-1}. Both CED, and, more broadly, EPBT, are parameters readily neglected in the literature when innovative materials are proposed. Throughout this review, we attempt a qualitative analysis (since the actual numbers are not available in literature) of the synthesis and deposition procedures of materials claimed as sustainable (or more generally cost-effective) in order to evidence the main factor(s) that can negatively influence both parameters.

Furthermore, in a sustainability-driven analysis, one cannot only consider the environmental impacts; indeed, socio-economic factors must also be considered. In the European framework, materials classified as CRM, characterized by supply risk and economic importance, should be substituted and their recovery prioritized.

Cost-effectiveness is another important parameter to consider when envisaging the practical exploitation of any device on a large market scale. Actually, it will not be cost-effective to purchase a brand new, top-quality, expensive PC when all is required is surfing the internet sometimes and storing photos. Similarly, it is not convenient to consume large amounts of energy and expensive reactants for the production of new, super ecofriendly materials for DSSCs if their efficiency it is not competitive on the market scale. DSSCs can reach the verge of commercialization only if the manifested cost estimates for the technology approach the projected costs of other leading PV technologies on the market. Accordingly, to render DSSCs more competitive, enhancing device efficiency and stability at significantly reduced material and manufacturing costs is among the most fundamental steps. Generally, we found it very hard to retrieve all the necessary information about the cost and preparation of materials (including chemicals, precursors, and additives) since LCA and LCC analyses are missing in most of the literature reports. Moreover, this is more an industry-related challenge than an academic one because correlating costs for lab-scale production when working with a few milligrams/grams of reactants to industrial scale production (kilos/tons) is often difficult, and normally a linear correlation cannot be drawn easily. Thus, we decided in this work not to specifically focus on the cost-effectiveness of all the materials presented. In each of the following sections, we included some specific details trying also to make a comparison with the corresponding state-of-the-art commercial devices, particularly focusing on the processes for material production and data in terms of related costs. From a practical application viewpoint for predicted large-scale production, this will allow bringing the best possible profits or advantages at the lowest possible costs. Den Hollander *et al.*[95] presented the concept of design for product integrity, where a product should be designed in a way to avoid it becoming obsolete. Accordingly, the lifetime concept is replaced by the concept of

use cycle. This purpose can be achieved through different approaches. In a liquid-state DSSC, for instance, the device can be designed for refurbishment, where this approach is at the product and component level. The chemist, at the material level, should design materials that are stable to last longer and guarantee enhanced resistance to obsolescence, as well as be readily recyclable. On the other hand, the engineer, at the process level, should design scalable and cost-effective processes to produce large-area modules having innovative architectures that are readily disassembled/dismantled, thus favouring material recovery/reuse.[18,19,96]

A thorough analysis of the environmental impact of DSSC deals with a set of different and complementary issues such as materials and/or processes mainly impacting the DSSC life cycle should be deeply investigated, focusing on the main factors affecting stability and lifetime. Moreover, the use of CRMs and precious metals and the employment of expensive synthetic procedures and processes should be completely avoided. It should be noted that, in this context, the analyses will be mainly focused on the laboratory scale due to the lack in availability of data for industrial processes for the production of DSSCs. Indeed, the same concepts can be applied to both scales.

According to different studies,[19,21,37,93,97,98] the critical factors for DSSCs are: (i) use of CRMs or noble metals, (ii) performance degradation due to electrolyte instability, (iii) high energy demanding TCO/glass, and (iv) sustainability concerns related to uncertain waste management. The sustainable exploitation of materials should consider the use of non-toxic, readily available and low cost, waste derived and/or easily recyclable materials. Ruthenium, cobalt, silver and platinum are the most controversial elements in this context. It is worth mentioning that the impact of different materials (and the related procedures) strongly depends on their amount employed to build a complete device. Therefore, sensitizers will be less meaningful in a sustainability-driven analysis with respect to the counter-electrode and/or electrolyte.

Hereafter, the main sustainability issues are briefly presented, but will be more deeply investigated in dedicated sections. Historically, the most widely employed sensitizers are based on ruthenium, resulting in the highest certified efficiency for DSSCs (12.3%). Nonetheless, ruthenium is a scarce material and it has been included in the list of CRMs by the EU.[19,21,97,99] It is costly and its complexes require relatively sophisticated syntheses and solvent-demanding purification steps.[82] Thus, to address these issues, alternative dyes have been developed, such as metal-free organic and natural dyes,[82,100] which should be synthesised following the twelve principles of Green Chemistry,[101] thus allowing the lowest impacts on the lab-scale phase and the possible evaluation through the green chemistry metrics.[102]

The research on alternative electrolytes is important to overcome degradation issues and extend the lifetime of devices.[103] However, the lifetime of DSSCs is affected by different factors as follows: (i) leakage of electrolytes, (ii) corrosion of CE by the redox couple, (iii) electrolyte bleaching and (iv) removal of the adsorbed dye on the surface of TiO_2. To overcome the conventional iodine-based electrolyte-related issue, researchers have tried different routes.[87] For example, alternative redox couples to the traditional I^-/I_3^- have been suggested, which are less prone to evaporation;[104–106] among others, quasi-solid electrolytes in gelled forms and truly solid-state polymer-based electrolytes have been explored;[107–109] and even water,[110] room temperature ionic liquids (RTILs)[111] and deep eutectic solvents (DESs)[112,113] were proposed. Gel electrolytes guarantee the best trade-off between efficiency and durability,[114] while solid-electrolytes, despite providing lower efficiencies, have the remarkable advantages of being non-volatile and non-fluid, thus avoiding evaporation, leakage and related risks of toxic compound inhalation.[115] With respect to redox mediators, cobalt-based couples have been recently exploited as feasible and best performing alternatives to iodine-based couples.[21,116] Issues related to the use of cobalt include its toxicity, and mainly its supply since cobalt is primarily mined in the politically sensitive Democratic Republic of Congo. Its supply regulation is of great importance, as confirmed by the establishment of the Cobalt Institute, an organisation aimed at promoting "the sustainable and responsible use of cobalt in all forms".[117]

The cost of a technology must be considered, not only for economic reasons, but also for complete compliance of the aforementioned sustainability principles. Platinum-based CEs are typically used in DSSCs, but their cost (about \$30 000 kg^{-1})[118] is extremely high due to the presence of a precious metal, which also requires high temperatures for its deposition. Platinum is also correlated with degradation/stability issues because of its electrocatalytic properties and its dissolution in the electrolyte.[19] The suggested alternatives are carbon-based,[119] such as activated carbon[120] and graphene,[121] transition metal-based[122] and composite electrodes.[123]

The energy consumption of a process must be considered when attempting to lower its impacts. In DSSCs, the coated glass is the most relevant component in almost all environmental impacts.[93,97,124] Actually, it is highly impactful in terms of high energy required for its production; in addition, it has a high impact in terms of weight with respect to total mass and overall cost, since glass accounts for 17% of the total device cost.[18] Accordingly, several LCA studies[93,97] have suggested the replacement of glass with plastic materials as a suitable solution because of their lighter weight and lower process temperatures required compared to sintering and glass lamination, which are time and energy consuming.[97] However, exploiting lower temperatures for material processing can lead to worse performances. For instance, it was observed that the TiO_2 sintering performed at lower temperatures over poly(ethylene terephthalate) (PET) resulted in lower efficiencies due to the different morphologies and sizes of TiO_2 particles compared to that obtained through sintering on glass substrates.[97,125] Additionally, electrode fabrication and glass-glass lamination are highly energy demanding processes.[98]

It is worth mentioning that photoanodes are not specifically reviewed here. Indeed, a sustainable alternative to the use

of TiO_2 nanoparticles has not been proposed thus far since they exhibit a low recombination rate for hole–electron pairs, excellent absorption properties, high chemical and thermal stability, corrosion resistance, non-toxicity, large availability, biocompatibility and competitive cost.[40,126] However, it should be noted that some properties of TiO_2 are not ideal; for example, having a band gap of 3.2 eV (in its anatase phase) it absorbs ultraviolet radiation ($\lambda < 380$ nm). This leads to the formation of highly reactive holes, which can degrade some device components. Accordingly, the employment of semiconductors with a wider band gap has been exploited, for example tin oxide, SnO_2, has a larger band gap (3.6 eV), but its more energetic conduction band leads to a sizeable decrease in photovoltage compared to classical devices.[127] On the other hand, zinc oxide, ZnO, has also attracted increasing attention to be employed as a photoelectrode material in DSSCs,[128–130] guaranteeing faster electron mobility compared to TiO_2.[131] However, it does not guarantee improved performances compared to traditional photoanodes, since the electron transport throughout the semiconductor is not a limiting factor for DSSCs under their operational conditions. In summary, alternative semiconducting oxides can operate as photoanodes in DSSCs, but, to the best of our knowledge, their performances have not surpassed that of TiO_2.

The main components of DSSCs along with the corresponding critical materials, related issues and envisaged solutions are summarized in Fig. 3.

Sealing is crucial for both cell stability and waste management,[19,132] where specific materials are used to guarantee perfect sealing (no leakage and/or contamination) of the device during its whole lifespan, but should also be easily removable upon disposal at the end of its operational life. Degradation and stability are two concepts directly bound to the lifetime of a product. Thus, preventing the production of waste is pivotal to prevent the correct functionality of the PV panel from jeopardizing its lifetime, and thus research on new materials that are stable upon operation and in contact with the other cell components is mandatory.

After product disposal, any device becomes waste, and thus must be correctly designed to become a new source of materials. The EoL of any PV device is a fundamental step to consider chiefly when aiming at producing truly sustainable technology. Nowadays, any industrial product must be designed from the initial step of its production process to be suitable for disassembling, thus allowing the recovery of the highest amount of materials as possible, especially precious and rare metals as well as CRMs.

DSSCs are not a fully mature technology. Research in this field is still at the laboratory or pre-industrial scale. This means that researchers are mainly focused on the investigation of the best materials using the standard assembly adopted for conventional PVs. Once efficient and stable materials are obtained, this technology may have structural improvements to increase its sustainability profile. Accordingly, for other PV technologies, delamination is one of the critical aspects in PV waste treatment since it is the first step performed to disassemble the device.[133] At a material level, as already mentioned above, it is worth highlighting the role of sealing in the perspective of dismantling the panel. From a sustainability viewpoint, scientists must consider numerous aspects in choosing the most suitable materials, where they should (i) be derived from available, widespread and fairly managed resources; (ii) be synthesized minimizing waste, avoiding the use of toxic materials and saving energy; and (iii) improve the product integrity and facilitate the waste recovery and disposal at the EoL.

The development of an ideal DSSC, which can establish its position in the market, should not function just on the best efficiency (where this and long-term stability are the key factors to break through the market), but should also consist of inexpensive sensitizers, non-toxic electrolytes, platinum-free CE and recyclable/reusable components/encapsulation systems, resulting in a PV device that can be fabricated by smart and sustainable procedures. The opportunity to use cheap, available and sustainable or waste-derived materials (*e.g.* waste from both the food and agriculture industries) for the conversion of solar energy, together with the smart use of nanomaterials and nanotechnology to replace precious (platinum) and rare (indium, component of indium-doped tin oxide – ITO layer) metals can favor the fabrication of

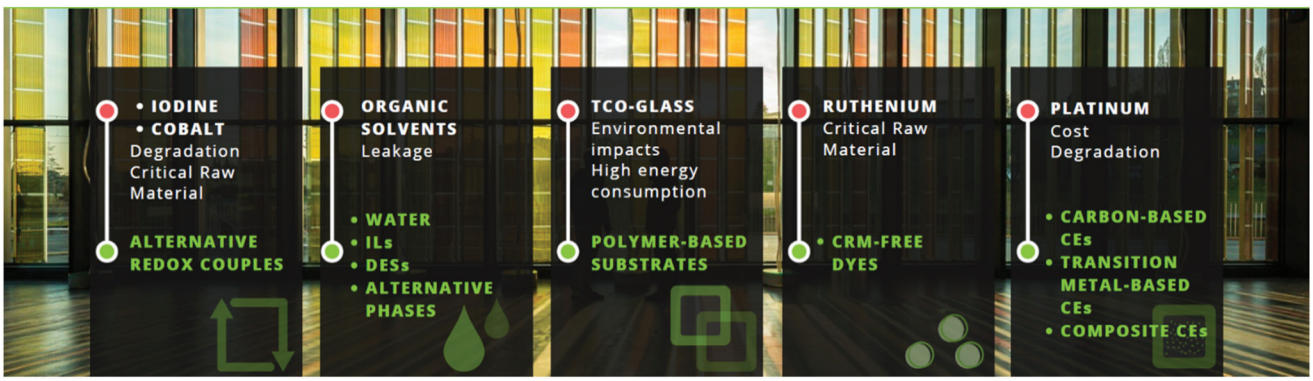

Fig. 3 Main DSSC components, along with corresponding most critical materials, related issues and envisaged solutions.

next-generation solar cells that are much cheaper and simultaneously eco-friendly and sustainable, like the inspiring first idea of Grätzel aimed to achieve.

2.1 Photosensitizers for DSSCs

The photosensitizer (namely, the dye) is one of the most important components of DSSCs since it has the main role of absorbing photons from sunlight, supplying electrons to the semiconductor, and subsequently converting the absorbed sunlight into electrical energy.

To be considered as an efficient PS for DSSCs, a dye should possess several essential requirements, as follows:[134] (i) a high molar extinction coefficient with panchromatic light absorption ability (from the visible (VIS) to the near-infrared (NIR) region); (ii) the ability to strongly bind to the semiconductor through an anchoring group (typically, a carboxylic or hydroxyl group), so that electrons can be efficiently injected into the semiconductor CB; (iii) good highest occupied molecular orbital/lowest unoccupied molecular orbital (HOMO/LUMO) energy alignment with respect to the redox couple and the CB level in the semiconductor, which allows efficient charge injection into the semiconductor, and simultaneously efficient regeneration of the oxidized dye; (iv) the electron transfer rate from the dye sensitizer to the semiconductor must be faster than the decay rate of the PS; and (v) stability under solar light illumination and continuous light soaking. Thus, the specific function and the working mechanism of sensitizers are closely related to both the photoelectrode and the redox mediator. Indeed, the design of an effective PS should not neglect the mutual interactions with both of these components. The adsorption of the PS onto the photoelectrode should lead to the highest surface coverage (to limit the back-transfer reaction between electrons in the CB of the semiconductor and the redox mediator) without giving rise to multilayered structures, which promote self-quenching of the excited state. On the other hand, the LUMO of the sensitizer should be delocalized as close as possible to the anchoring site in order to promote effective charge injection into the semiconductor CB, whereas the opposite is valid for the HOMO, which should be delocalized in the portion of the molecule facing the electrolyte to promote the regeneration process. The overall working principle of a DSSC was presented in section 1.1, but further insight in the mechanism and function of the PS in a DSSC can be found in a series of excellent reviews in the literature.[36]

Among the most efficient sensitizers, we include three main classes of dyes, functionalized oligopyridine metal complexes, Zn-based dyes (Zn-porphyrins and Zn-phthalocyanines) and fully organic dyes. The major issues regarding most of these PSs are (i) the possible release of harmful chemicals as by-products, (ii) the use of toxic reagents/catalysts and the amount of organic solvents needed during their synthesis and purification steps. Moreover, in the case of metal-based molecules, where rare metals such as ruthenium and osmium are employed, the main concern is the use of CRMs, which makes the overall device production highly dependent on rare resources, and thus non-sustainable and uneconomical from a large-scale production viewpoint.[135]

However, according to different LCA[91,93,124] results, the dye contributes a very small part to the overall impact (lower than 3%) and the main reason for its environmental impact is the high consumption of solvents and eluents during its synthesis. Indeed, the quantity of dye necessary for the sensitization of a semiconductor is very limited, since normally the dye loading capacity of a DSSC is around 3×10^{-7} mol cm^{-2}, which means that in the case of N719 and a squaraine dye, 0.35 or 0.20 mg cm^{-2} are needed, respectively.[136] According to the above calculation, it is clear that the overall impact in terms of costs of the whole device is not attributable to the PS, and therefore its replacement with a more sustainable alternative is less urgent. Nevertheless, when considering Ru-based dyes, the metal centre is the most impactful component. It is interesting to observe that in assessing the impacts of YD2-o-C8, D5 and N719 (Zn-porphyrin dye, organic metal-free dye and Ru-based dye, respectively), the latter is the least impactful since its synthesis is well optimized.[93] The optimization of the synthesis of Ru-based dyes is also evident from their availability on the market at very low prices compared to organic dyes, for example 65 € per g for N719 *versus* 400 € per g for a squaraine-based dye.[137]

Moreover, it should be noted that ruthenium-based dyes have been widely investigated and have achieved some of the best PV properties with conversion efficiencies exceeding 11%;[138] they have been already exhaustively reviewed in the literature;[139–145] therefore, their role will not be further investigated here.

However, recently, to overcome the limitations of the use of sensitizers based on rare metal complexes, the scientific community has focused on replacing them with other PSs with comparable efficiencies, which will be briefly discussed in the following paragraphs. On the other hand, the removal of critical elements is not the only parameter to follow in order to achieve a more sustainable dye. This is why it is crucial to combine LCA and green metrics to evaluate the overall environmental impacts.[23]

2.1.1 CRM-free dyes. After DSSCs co-sensitized with two CRM-free organic dyes reached the highest efficiency of 14.3%,[63] CRM-free and fully organic dyes started to be considered the most promising alternatives to replace metal complexes and have been extensively explored due to their numerous advantages.[82] Specifically, their optimal flexibility in molecular design, easy large-scale production and possibility of simple synthetic pathway requiring few and economical purification steps. In addition, they show extremely high molar extinction coefficients (usually exceeding 2.50×10^4 M^{-1} cm^{-1} in the VIS region) for their charge transfer band compared to ruthenium(II) complexes with a tunable absorption,[146] from the VIS to the NIR region. It is impossible to gather all the PSs proposed to date and, therefore, only some examples will be analysed starting from the recent review by Boschloo.[75] Other reviews specifically focused on metal-free PSs can be found in the literature.[143,144]

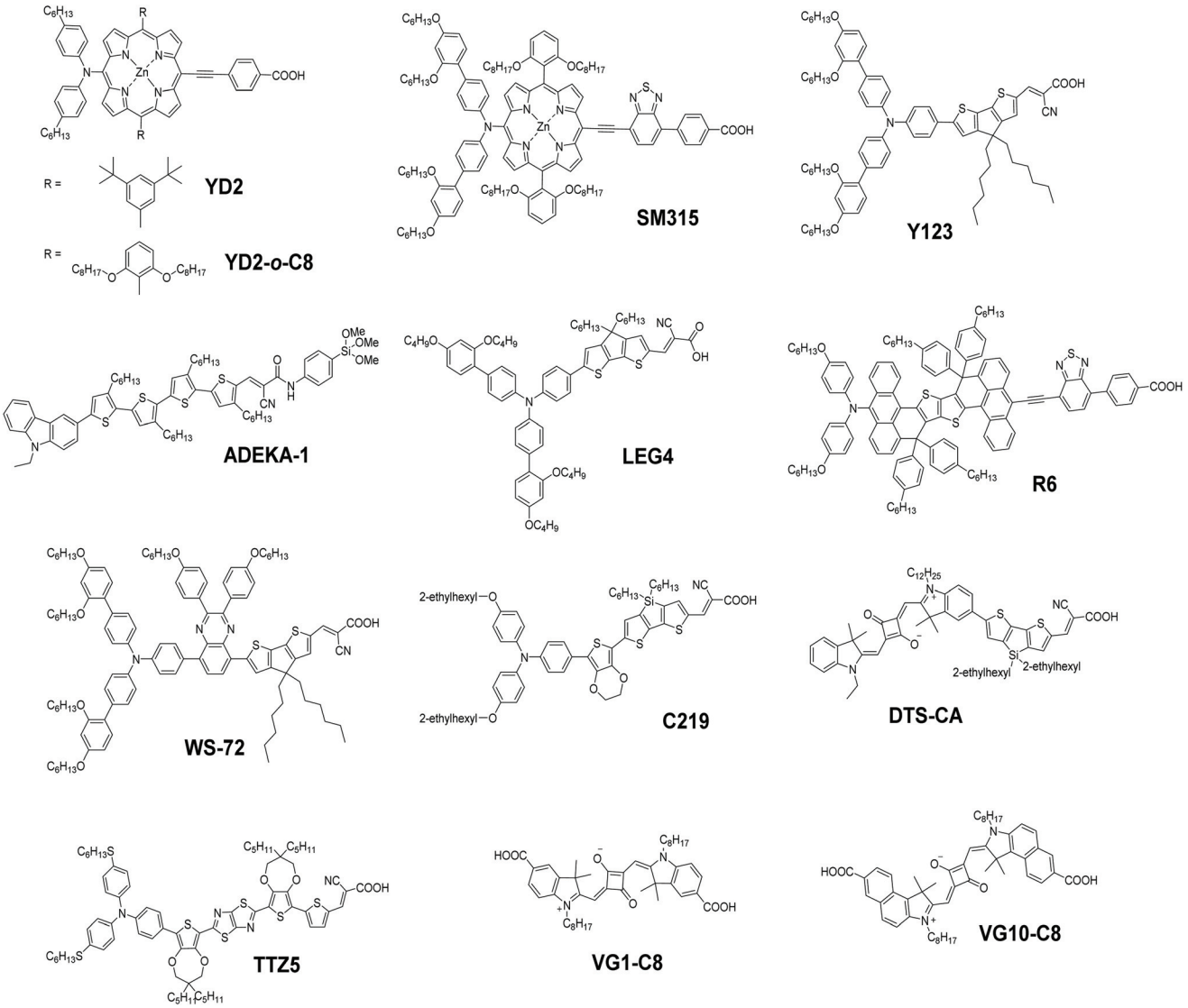

Fig. 4 Structures of various CRM-free photosensitizers: porphyrins (YD2 and YD2-o-C8) and fully organic dyes. All the molecules were drawn using ChemDraw 19.0.

One of the first well-performing porphyrin dyes is the YD-2 dye (Fig. 4), bearing a diarylamino donor group and an ethynylbenzoic acid moiety acceptor group, which reached a photoconversion efficiency (PCE) of 11% when used with an iodide/triiodide-based electrolyte (Table 1, entry 1). The device exhibited a broad absorption in the range of 400 to 750 nm with a peak maximum of over 90% at 675 nm, a short-circuit current density (J_{SC}) of 18.6 mA cm^{-2} and an open-circuit voltage (V_{OC}) of 0.77 V.[147]

In 2011, Yella *et al.*[105] proposed a tailored variant of YD-2, *i.e.* the donor–π-acceptor (D–π-A) Zn porphyrin dye YD2-o-C8 (Fig. 4), which reached a PCE value as high as 11.9% using a cobalt(II/III) tris(bipyridyl)-based redox electrolyte, with a V_{OC} of 965 mV and J_{SC} of 17.3 mA cm^{-2} under standard air mass (AM) 1.5 sunlight at 995 W m^{-2} intensity (Table 1, entry 2). YD2-o-C8 absorbs light over the whole VIS range and bears two octyloxy groups in the *ortho* positions of each *meso*-phenyl ring, impairing the interfacial back electron transfer reaction and leading to enhanced photo-induced charge separation in the DSSC. Moreover, this porphyrin dye reached a power conversion efficiency (PCE) of 12.3% under simulated AM1.5G sunlight when co-sensitized with the Y123 organic D–π-A dye (Fig. 4, Table 1, entry 3). The corresponding cell showed a remarkable panchromatic photocurrent response over the whole VIS range, with a limited 10% to 15% decrease in overall efficiency after continuous (220 h) exposure to full sunlight at 30 °C. The advantage of using a Zn-based PS instead of Ru can be also explained by the higher supply risk of the Ru metal. In fact, the natural abundance of Zn in the Earth's crust is considerably higher (72 ppm *versus* 0.000037 ppm for Ru) and the political stability of top reserve holders make the overall relative supply risk of Zn lower (4.8) compared to Ru (7.6).[148,149]

Table 1 Different classes of dyes, together with name/acronym of the most representative ones, related advantages, critical issues, highest recorded efficiency values and corresponding reference articles

Class	Dye	Pro	Issues[a]	η (%)	Entry[ref.]
Zn-Porphyrin	YD2	• Iodide/triiodide electrolyte • Broad absorption	• Not meaningful	11.1	1[147]
	YD2-o-C8	• High PCE • High stability	• Cobalt-based electrolyte: Co(bpy)$_3^{3+/2+}$	11.9	2[105]
	YD2-o-C8 + Y123	• High PCE • High stability	• Cobalt-based electrolyte: Co(bpy)$_3^{3+/2+}$	12.3	3[105]
	SM315	• Panchromatic absorption • No need of co-sensitization • Very high PCE	• Cobalt-based electrolyte: Co(bpy)$_3^{3+/2+}$	13.0	4[116]
D–π-A	Adeka-1	• High PCE • High stability	• [Co(Cl-phen)$_3$]$^{3+/2+}$	12.5	5[150]
	Adeka-1 + LEG4	• Iodide/triiodide electrolyte	• Not meaningful	11.2	6[63]
	Adeka-1 + LEG4	• Record PCE	• Cobalt-based electrolyte: [Co^{2+}(phen)$_3$](PF$_6^-$)$_2$	14.3	7[63]
	R6	• High PCE • High photostability	• Cobalt-based electrolyte: Co(bpy)$_3^{3+/2+}$	12.6	8[151]
	Y123	• Copper-based electrolyte: Cu(tmp)$_2^{2+/+}$ TFSI	• Not meaningful	13.1	9[69]
	WS72	• Copper-based electrolyte: Cu(tmp)$_2^{2+/+}$ HTM	• Not meaningful	11.6	10[154]
	DTS-CA	• Iodide/triiodide electrolyte	• Not meaningful	8.9	11[155]
Organic squaraine dye	C219	• Iodide/triiodide electrolyte	• Not meaningful	10.1	12[156]
Flavonoids	Anthocyanin from *M. malabathricum*	• Natural PS • Extended π conjugation	• Low stability • Low PCE	1.1	13[172]
Carotenoids	MeO-φ-6-CA	• Natural PS	• Low stability • Low PCE	2.6	14[183]
	PPB + β-carotene	• Natural PS • Iodide/triiodide electrolyte	• Low stability • Co-Sensitization with a chlorophyll derivative • Low PCE	4.2	15[184]
Chlorophylls	Chlorophyll c1 from *Undaria pinnatifida*	• Natural PS	• Low stability • Low PCE	3.4	16[190]
	Chlorophyll c2	• Natural PS	• Low stability • Low PCE	4.6	17[190]
Betalains	SPA	• Natural PS • Iodide/triiodide electrolyte	• Low stability • Low PCE	3.0	18[197]

[a] Issues related to the synthesis of the dyes are omitted for clarity.

A further tailored modification on the zinc-porphyrin structure was proposed in 2014 by Mathew *et al.*,[116] who included a bulky bis(2′,4′-bis(hexyloxy)-[1,1′-biphenyl]-4-yl)amine donor group and proposed a novel benzothiadiazole group as an acceptor. The panchromatic porphyrin sensitizer SM315 (Fig. 4), together with a [Co(bpy)$_3$]$^{2+/3+}$ redox couple, showed an improved J_{SC} (18.1 mA cm^{-2}) with a record 13.0% PCE (Table 1, entry 4) at full sun illumination without the need for a co-sensitizer. The introduction of a novel cobalt(II/III) tris(phenanthroline)-based complex redox electrolyte together with the use of a novel metal-free sensitizing dye, ADEKA-1 (a carbazole/alkyl-functionalized oligothiophene with an alkoxysilyl-anchor moiety, Fig. 4), led to improved light-to-electric energy conversion efficiencies of over 12% (Table 1, entry 5).[150] The same dye demonstrated >14% PCE in the presence of the co-sensitizer LEG4 (a carboxy-anchor organic sensitizing dye, Fig. 4 and Table 1, entries 6 and 7).[63] The benzothiadiazole group was used as acceptor in the organic R6 dye (Fig. 4, Table 1, entry 8), which exhibited a polycyclic aromatic hydrocarbon core with a diarylamine electron donor[151] and a brilliant sapphire color when absorbed on a TiO_2 film with a cobalt (II/III) tris-(bipyridyl)-based redox electrolyte. The resulting DSSC provided an impressive PCE of 12.6% with remarkable photostability. Nevertheless, the use of a cobalt-based electrolyte negatively influences the sustainability of the device, as thoroughly discussed in the following section.

In principle, all of these reported PSs are sustainable since they do not employ CRMs; however, the high efficiency values reported to date have been achieved in the presence of cobalt-based redox couples. Moreover, the synthetic pathways of

Zn-porphyrin dyes should be analyzed and further optimized to diminish the number of required synthetic steps (*i.e.* actually more than ten for SM315 from commercially available starting materials), increase their yields and possibly remove the use of homogeneous noble metal catalysts (*i.e.* several steps required for Pd-based complexes).[152] Indeed, the higher the number of synthetic steps and the lower the reaction yield, the higher the CED of the process.

Examples of more sustainable DSSCs are those using CRM-free PSs coupled with CRM-free copper-based electrolytes, where the use of rare metals and cobalt is avoided. In 2017, Cao *et al.*[153] proposed the well-known Y123 dye using a blend of $[Cu(tmby)_2](TFSI)_2$ and $[Cu(tmby)_2](TFSI)$ as the hole transporting material (HTM) and electrodeposited poly(3,4-ethylenedioxythiophene) (PEDOT) as the CE. Also, in 2018, thanks to the design of an enhanced DSSC architecture, the same group achieved an efficiency of 13.1% on the lab-scale (Table 1, entry 9).[69] A 26% improvement compared to the Y123 reference dye was achieved with the WS-72 dye (Fig. 4), employing a $[Cu(tmby)_2]^{2+/+}$ liquid-junction redox electrolyte.[154] The solidification of the electrolyte for the champion device led to a PCE of 11.7% (J_{SC} = 13.8 mA cm^{-2}, V_{OC} = 1.07 V), which is the highest efficiency reported to date for solid-state DSSCs (Table 1, entry 10).

Among the organic dyes, Marder and his group proposed 4,4-bis(2-ethylhexyl)-4Hsilolo[3,2-*b*:4,5-*b*′]dithiophene (DTS) covalently linked to a squaraine donor, yielding an asymmetrical push–pull D–π-A structure, which provided a PCE of 8.9% with the triiodide/iodide redox couple (Table 1, entry 11).[155] The DTS-CA squaraine dye (Fig. 4) bears two branched 2-ethylhexyl chains out-of-plane, and thus is able to reduce dye aggregation with a considerable improvement in J_{SC}, incident photon-to-electron conversion efficiency (IPCE) and overall cell performance. Another well-performing organic dye featuring more than 10% efficiency is C219 (Fig. 4), which is an amphiphilic push–pull chromophore, consisting of a binary π-conjugated spacer and blocks of a lipophilic alkoxy-substituted triphenylamine electron-donor and a hydrophilic cyanoacrylic acid electron-acceptor. The C219 dye demonstrated a stable performance and high efficiency of 8.9% in a lab-scale solvent-free ionic liquid cell (Table 1, entry 12).[156]

Anyway, even if these fully organic dyes do not bear CRMs, their synthetic procedure can often be non-sustainable. The dyes themselves and the solvents and reagents used for their synthesis can be toxic, hazardous or expensive, and the by-products from their manufacture may be environmental pollutants. Thus, for every synthesis, the calculation of the CED should be undertaken, which is obtained by summing both the direct energy (*e.g.*, electricity) and the indirect energy (embodied energy of materials) contributions. For example, the synthesis of R6 consists of several time/energy consuming steps, including two-fold Suzuki-coupling, double Grignard nucleophilic addition, acid-catalyzed intra-molecular Friedel–Crafts cyclization, Buchwald–Hartwig coupling, monobromination, Sonogashira–Hagihara reaction plus final hydrolysis and acidification.[151] The organic dye C219 is achieved *via* seven synthetic steps, requiring a certain amount of organic solvents and palladium catalysts.[156] The synthesis of the squaraine dye DTS-CA involves an aldehyde protection step, lithiation and stannylation, followed by Knoevenagel condensation.[155] All or most of all these synthetic steps require CRM-based catalysts and an overall large amount of organic solvents, making the final dye non-sustainable, even if it actually does not bear rare metals or CRMs.

An interesting approach to design simpler and more stable dyes that require only a few synthetic steps, and, consequently, a lower amount of energy (lower CED) was proposed by Abbotto *et al.*, designing di-branched di-anchoring sensitizers.[157] A similar idea was also proposed in the case of symmetrical far-RED-NIR sensitizers based on squaraine dyes (VG1-C8 and VG1-C10, Fig. 4).[158,159] The authors were able to obtain a symmetric squaraine and its related non-symmetric structure with comparable efficiencies in DSSCs, but with undoubtedly the advantages of low cost and simple synthesis of the symmetrical structure. The latter approach was further implemented in subsequent years, improving the synthetic yields and lowering the energy request by performing all the synthetic steps within a microwave oven.[160] Unfortunately, photovoltaic efficiencies that surpass that of record Zn-porphyrins and/or metal-free organic dyes reported in Table 1 have not been achieved to date using this approach.

Recently, an approach combining mass-based green metrics and life cycle assessment was applied to identify the best synthetic protocol for the preparation of an organic dye, TTZ5 (Fig. 4),[23] which was previously proposed as sensitizer.[161] New synthetic strategies were compared with the previously reported synthesis. The procedures rely on two different approaches based on a C–H activation/Stille cross-coupling sequence or on a one-pot double C–H activation sequence, and were optimized to allow the production of TTZ5 on a gram scale. The results highlight the contribution of direct energy consumption and purification operations in organic syntheses on the lab scale. It becomes evident how both the new procedures allowed the synthesis to be completed in a more sustainable way than the previous procedure, considering the inferior production of waste, the lower costs and smaller environmental impact. Despite the greater number of steps, surprisingly the C–H/Stille route was revealed to be more sustainable than the one-pot C–H activation route, even though the employment of toxic and/or flammable reagents such as *n*-butyllithium and tin-containing materials increased its eco-scale value, while the application of LCA showed that the drawback of the one-pot C–H activation route procedure is the raw material input for its chromatography setup. Furthermore, this approach demonstrates the usefulness of the environmental multifaceted analytic tool and the power of life cycle assessment to overcome the intrinsic less comprehensive nature of green metrics for the evaluation of organic synthetic protocols.

2.1.2 Natural dyes. To overcome the limitations in the sustainability of using metal complexes and metal-free dyes, natural pigments and dyes found in plants have been proposed as alternatives PSs for DSSCs.[162–164] Here, we stress that

an extremely precise analysis of the cost-effectiveness of natural dyes was not possible despite our efforts, especially since the volume of solvents used for the extraction and the overall yield of this process are usually not reported in literature. The final cost of natural dyes in many cases is difficult to assess since it greatly depends on the availability of their natural sources and the impact of the extraction and purification methods. However, the advantage is that, even if in some cases a large quantity of solvent is needed, it can be easily recovered (with a fixed energy request) downsizing the overall CED and environmental impact of the dye production process due to the minimization of final costs and waste.

To date, despite the limited performance that natural dyes have demonstrated, they have a number of beneficial features, including, among others, high absorption coefficients, simple, low cost and energy saving production, low toxicity, complete biodegradability, ready availability and, most importantly, high reduction in the use of noble metals and CRMs, and thus a negligible environmental impact at lower cost. With respect to the photoconversion efficiency, for all dyes and chiefly for natural dyes, it is important to control the recombination with the electrolyte and with the oxidized dye, since a relatively fast electron/dye cation recombination process has been evidenced.[165] Therefore, the optimization of the interfaces is necessary to improve the V_{OC}, which is usually 200 mV lower compared to that of Ru complexes. Moreover, the IPCE can be affected by the choice of electrolyte, where Co-based complexes may greatly decrease it, while a kinetically faster redox couple such as iodine/iodide seems necessary.

Natural pigments (*e.g.*, anthocyanins, carotenoids, aurones, chlorophylls, tannins, betalains and many others) may be cost effective (depending on their photovoltaic efficiency) when compared to manufactured dyes, since they can easily be extracted from the fruits, flowers, leaves, seeds, roots, barks and various parts of plants utilizing simple extraction processes based on water and simple alcohols (*i.e.* methanol or ethanol), which are environmentally preferable solvents.[166] These dyes and pigments may not contain a solubilising group, which can be temporarily generated during the application.[167] On the other hand, the efficiency obtained using natural dyes as sensitizers is quite low because of their tendency to degrade and lack of panchromatic absorption, which is limited to the range of 400 to 700 nm.[168]

Natural pigments can be grouped into four main families, flavonoids (Fig. 5a), including anthocyanins (Fig. 5b), carotenoids (Fig. 5c), betalains (Fig. 5d) and chlorophylls (Fig. 5e).[169] Flavonoids (Fig. 5a) are important natural products belonging to a class of plant secondary metabolites having a polyphenolic structure, which are widely found in fruits, vegetables, grains, bark, roots, stems, flowers, tea and wine. Flavonoids act as unique ultraviolet (UV) filters, also protecting plants from different biotic and abiotic stresses.[170] From a structural viewpoint, they have a basic C6–C3–C6 skeleton and can be divided into four different classes, *i.e.* flavonoids or bioflavonoids, isoflavonoids and neoflavonoids. They contain a 15-carbon (C15)-based structure with two phenyl rings connected by three carbon bridges, forming a third ring. The degree of phenyl ring oxidation results in their different colours.[168] They can be used as natural PSs for DSSCs,[171] where their adsorption on the mesoporous TiO_2 surface is fast, displacing an OH^- counter ion from the titanium sites, which can combine with a proton coming from the flavonoid structure. Anthocyanins are the most abundant and widespread pigment of the flavonoid family. They exhibit a broad band in the VIS region of the spectrum, which is ascribed to charge transfer transitions, and their compounds can easily bind to the semiconductor *via* their carbonyl and hydroxyl functional groups through a chelation mechanism.[135] DSSCs sensitized by anthocyanin pigments showed efficiencies below 1%, with the exception of a few cases (Table 1, entry 13).[135,163,172,173] The generated IPCE does not exceed 20%, even if charge injection is usually very fast, due to problems related to dye aggregation, electron recombination with the oxidized sensitizer and electron recapture by the iodine/iodide electrolyte. In all of these examples, both the efficiency and stability of lab-scale DSSCs are highly affected by the temperature of the extracting solvent and its nature,[174,175] where mainly its polarity influences the solubility of the pigments. Actually, acidic aqueous dye extracts greatly improved the coloration of the photoanodes for selected eggplant and red grape extracts compared to that obtained from ethanolic solutions.

Carotenoids (Fig. 5c) are an essential component of all photosynthetic organisms due to their eminent photoprotective and antioxidant properties.[176] We counted more than 600 known carotenoids, which can be further categorized into two major classes: xanthophylls (containing oxygen) and carotenes (purely hydrocarbons without oxygen, such as lycopene and carotene). They can be even further classified as primary (*i.e.*, required by plants for the photosynthetic process) and secondary (*i.e.*, localized in fruits and flowers) carotenoids. Normally, they are yellow, orange and red organic pigments produced by plants and algae and several bacteria and fungi. Carotenoids belong to the general family of isoprenoids, having a basic structure made up of eight isoprene units, which results in a C_{40} backbone, allowing them to absorb electromagnetic radiation of short wavelengths ranging from 380 to 550 nm. Their absorptive capability, together with their molar extinction coefficients exceeding 10^5, allows some types of carotenoids to be potential sensitizer materials in PV cells and other artificial photochemical devices. Usually, raw natural dyes are better than their purified or commercial analogues due to the presence of natural extracts, such as alcohols and organic acids, which can improve dye adsorption, prevent electrolyte recombination and decrease dye accumulation.[167,168]

Another promising research direction is the realization of natural, low cost and environmentally friendly DSSCs made from organic waste, leading to a huge decrease in the overall CED. A good example was proposed by Maiaugree *et al.*, where both the dye and counter electrode were prepared from waste mangosteen peel.[177] In particular, a carbonized mangosteen peel film was used with mangosteen peel dye extract as a natural counter electrode and a natural photosensitizer,

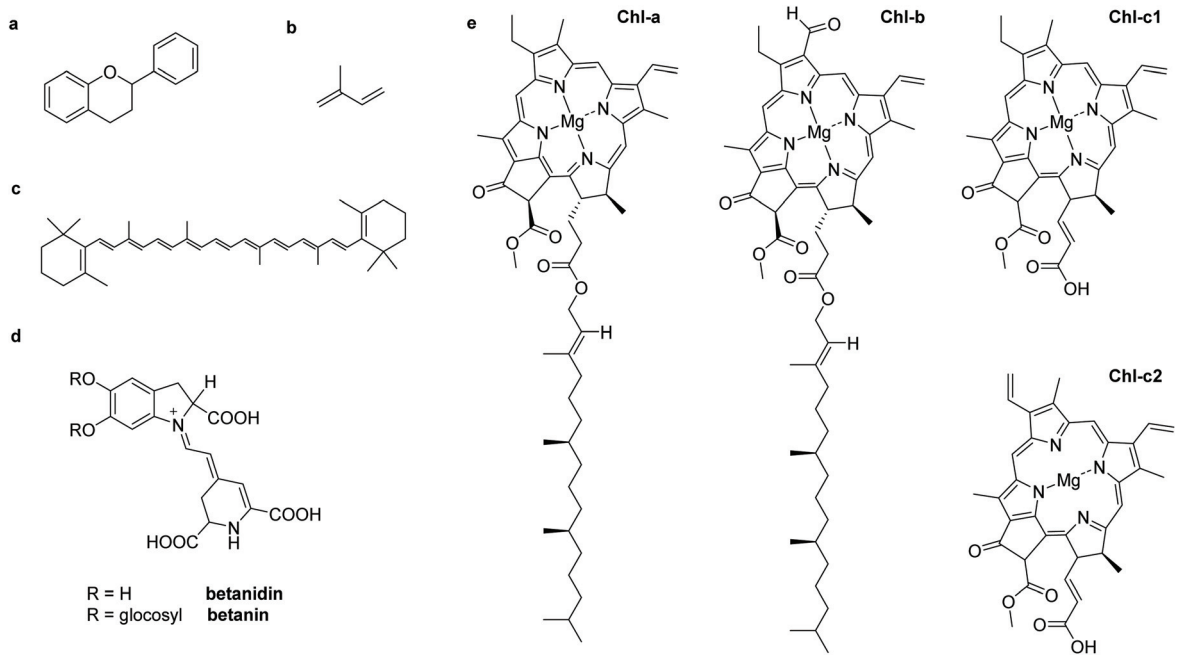

Fig. 5 Chemical structures of natural dyes: (a) basic flavonoid structure, (b) basic structure of an isoprene unit, (c) chemical structure of carotene, (d) structure of betalain derivatives and (e) chemical structures of various chlorophylls. All the molecules were drawn using ChemDraw 19.0.

respectively, to obtain a solar conversion efficiency of 2.63% in combination with an organic disulfide/thiolate mixture as the electrolyte (see section 2.3.1).

Different approaches using carotenoids resulted in the generation of photocurrents upon illumination (usually, around 2 nA cm^{-2}), but the resulting IPCE was very low (<0.4%). The main issue is due to the kinetic limitation of efficient photo-injection and movement of electrons imposed by the short S_1 excited state lifetime (10–50 ps). This was partially solved by Gao *et al.* by directly coordinating a carotenoid, 8′-apo-β-caroten-8′-oic acid substituted with a terminal carboxylate group, to the TiO_2 surface *via* the formation of covalent bonds.[178] The resulting cell showed a J_{SC} of 4.6 mA cm^{-2} with an IPCE of 34% and a V_{OC} of 0.15 V, together with stability for 1 h under continuous irradiation. In fact, carotenoids have not been thoroughly investigated as sensitizers for DSSCs because most of them do not have effective functional groups to bond with the hydroxylic groups of TiO_2. In addition, the strong steric hindrance of their long alkyl chains prevents the dye molecules from arraying efficiently onto the TiO_2 film. Yamazaki *et al.*[179] reported a comparison study between the different photosensitization behaviors of two carotenoids, namely crocetin and crocin. Crocetin, a carotenoid bearing carboxylic groups, exhibited high binding ability to the surface of the semiconductor film and its photoelectrochemical performance (0.56%) was three times or even higher than that of crocin (0.16%). These successful attempts promoted the use of carotenoids as potential new natural sensitizers. Thereafter, carotenoids have been used in DSSCs,[180–182] reaching the highest efficiency of 2.6% with analogues of carotenoic acids (Table 1, entry 14),[183] which increased up to 4.2% in combination with a chlorophyll derivative as the sensitizer (Table 1, entry 15).[184]

Chlorophylls (Fig. 5e) are natural green pigments that are found in natural photosynthetic systems, such as the leaves of most of plants, algae and bacteria.[185] Six different types of chlorophyll pigments exist. Chlorophylls a (Chl-a) and b (Chl-b) are the most common types, which absorb light from the red, blue and violet region with an absorption maximum located at 670 nm.[168] The basic molecular structure of chlorophyll includes a porphyrin ring, which is coordinated to the central atom, together with different side chains and a hydrocarbon tail. Chl-a and Chl-b differ only by the substituent attached to the pyrrole ring on the porphyrin ring opposite to the phytol tail.[135] The absorption spectra of Chl-a and Chl-b are in the range of 400–700 nm and 450–650 nm, respectively, depending on their different side groups. Therefore, chlorophylls and their derivatives are attractive as PSs in DSSCs because of their ability to absorb light in a broad region of the VIS spectrum.

The use of chlorophylls as PSs in DSSCs was recently reviewed.[163,173,186] Their main disadvantage is their long chains, leading to low-electron transferability due to steric hindrance, and in some cases very low adsorption ability onto the semiconductor surface due to the absence of suitable anchoring groups.[187] The most interesting examples utilized chlorophyll extracted from a species of moss bryophyte together with a quasi-solid-state polyacrylonitrile (PAN)-based iodide electrolyte, which led to an efficiency of 1.97% with a J_{SC} of 5.78 mA cm^{-2} and V_{OC} of 0.60 V, covering quite a wide IPCE spectrum from 300 to about 550–600 nm.[188] A further increase (J_{SC} = 5.96 mA cm^{-2} and V_{OC} = 0.58 V with PCE = 2.00%) was

obtained using chlorophyll extracted from the bryophyte *Hyophila involuta*, and a gel electrolyte based on poly(vinyl alcohol) (PVA) and a double salt (KI and tetrapropylammonium iodide). The use of chenodeoxycholic acid (CDCA) as an anti-aggregation agent added to chlorophyll led to a further increase in the light to electricity efficiency of 2.62% with a J_{SC} of 8.44 mA cm^{-2} and V_{OC} of 0.54 V.[189] To the best of our knowledge, chlorophyll c2 extracted from *Undaria pinnatifida*, which was isolated from a brown seaweed, demonstrated the highest efficiency ever recorded among chlorophyll-sensitized DSSCs.[190] Chlorophyll c (Chl-c) was isolated by removing Chl-a and carotenoids, and then the purified Chl-c was subjected to polyethylene column chromatography to isolate Chl-c1 and Chl-c2. Efficiencies of 3.4% and 4.6% were obtained from the Chl-c1- and Chl-c2-sensitized DSSCs, with liquid electrolyte (Table 1, entries 16 and 17), respectively.[190] On the other hand, concerning sustainabiltiy, the additional purification steps counterbalance the gain in efficiency. Moreover, a DSSC prepared using a cocktail of natural dyes (chlorophyll extract of wormwood and anthocyanin extract of purple cabbage) achieved a PCE of 1.95%, V_{OC} of 0.765 V and J_{SC} of 5.83 mA cm^{-2}.[191] However, although chlorophylls have been widely employed as natural sensitizers in DSSCs due to their efficient light-harvesting mechanism and electron-transfer reactions,[169] they lack stability and are highly dependent on the condition of leaves form which they are extracted (whether fresh or dried), which can affect the device performance. Moreover, their absorption is greatly influenced by the solvent and the pH used during pigment extraction.[192]

Betalains (Fig. 5d) are a small group of water-soluble and nitrogen-containing indole-derived glycoside pigments present in the vacuoles of cells of fruits, roots and flowers of plants of the order of *Caryophyllales*. They can be divided into betacyanins and betaxanthins. Red and violet tonalities result from different substitution patterns in betacyanins, while different amino acid or amine side chains determine the color of betaxanthins.[193] Betalains are aromatic indole derivatives and are an alternative to synthetic colorants, which absorb radiation in the VIS range between 476 and 600 nm. Additionally, they show stability over a wide pH range and a high molar extinction coefficient, but they are generally unstable when exposed to light, heat and oxygen.[167] Although only few reports have been published to date on betalain-based DSSCs, the presence of carboxylic functional groups favours their binding to the surface of TiO_2, which makes them promising PSs. The few published examples, reporting efficiencies of around 0.5%[194,195] up to 2%,[196] were thoroughly reviewed by Bartolotta and Calogero,[169] who explained the limitations of using betalains in DSSCs due to their short S_1 lifetime. Recently, Güzel *et al.*[197] reported a betanidin extract, with a very broad absorption in the range of 300 to 700 nm, which showed the highest PCE of 3.04% and excellent stability during solar irradiation when tested in lab-scale DSSCs (Table 1, entry 18). The low performances of betalain-based DSSC are due to their low V_{OC}, similar to other natural dyes, and insufficient electron injection quantum yield. The short S_1 lifetime is responsible for a rapid internal conversion process, and thus the injection is highly affected.[198] Calogero *et al.*[165] observed that it is unlikely that charge injection is the IPCE-limiting process, but recombination losses can be responsible. Unfortunately, a detailed investigation on this issue is still lacking.

The overall performances of DSSCs based on natural dyes and pigments are low compared to other devices where organic or metal–organic dyes are employed as sensitizers. This is chiefly ascribed to the low interaction between dye sensitizers and the semiconductor surface due to the absence of specific anchoring groups and/or presence of bulky groups on the dyes, which results in steric hindrance, preventing the formation of strong bonds with the oxide surface. The low efficiency is also determined by the low V_{OC}, resulting from the inefficient reduction of the oxidized dye. This can be overcome with the use of additives and co-absorbers, but this can have a negative influence on the molar extinction coefficient and the absorption maximum since natural dyes are pH-sensitive.[169] Another important issue is the stability of these devices, which is most often low and insufficient to match the standard devices assembled using other classes of dyes. Other issues include the source of the dyes and pigments, and the solvents employed for their extraction. From the examples reported to date, it is clear that the device performance depends on the polarity and acidity of the solvent or on the extraction temperature,[174] where the solvents used to extract these natural dyes must be carefully selected to achieve high effectiveness in the extraction process, without hampering their sustainable features.[135]

2.1.3 Final remarks on sensitizers. Although the actual quantity of dye used in a DSSC device is very low, making the problem of its cost-effectiveness less impactful, the sustainability of photosensitizers can be substantially enhanced. Starting from the "classical" Ru-based dyes, different directions have been investigated. The substitution of ruthenium with other metals that are not CRM (such as zinc) greatly improved the overall sustainability. A complementary approach involved the design of fully organic sensitizers. However, this elegant approach is usually not classified as sustainable since it is characterized by a sizeable number of synthetic steps and the employment of harmful reactants, solvents and catalysts. Aiming at sustainability, natural dyes can be considered a valid alternative, being environmental-friendly due to their natural occurrence in locally available resources, *i.e.* plants, flowers, fruits and roots. Unfortunately, their performances are lower compared to those of synthetic dyes and they suffer degradation in the presence of sunlight, resulting in great stability problems in DSSCs. Moreover, natural dyes show absorption mainly in the visible region (400–700 nm) of the solar spectrum, losing a consistent energetic contribution from longer wavelengths. Thus, due to the above-mentioned reasons, even if the production of natural dyes is less expensive since it requires simple and direct chemical procedures, they are not cost-effective and synthetic dyes are still more successful and functional. Increasing their light absorption capacity

via co-sensitization is among the most effective possibilities to enhance the DSSC performances of natural dyes because it promotes a synergistic effect in improving electron injection, light harvesting and limitation of electron recombination. This is actually critical for synthetic dyes, which are in principle designed for this specific target, but it becomes much more critical when using natural dyes, which may also bear impurities and functional groups that can affect the functioning of the device. Thus, from a chemical point of view, efforts can be focused on the modification of the design for the production of synthetic dyes, varying the overall approach to their synthesis rather than optimizing the single steps of the conventional protocol, lowering the environmental impact and reducing waste.[23,199] The latter route can lead to well-performing but stable synthetic dyes and can be considered the best trade-off between obtaining cost-effective but sustainable dyes.

2.2 Sustainable electrolytes: beyond iodine, cobalt and organic solvents

As already mentioned in the Introduction, the electrolyte is among the key elements for a well-performing DSSC:[32] it is responsible for the regeneration of the dye after the injection of electrons or holes in n-type and p-type devices, respectively,[200,201] and ensures a good charge transfer through the cell, enabling proper device operation. The electrolyte should have high stability, appropriate redox potential with respect to the HOMO level of the sensitizer, high transparency in the VIS region to avoid competition for light absorption with the dye and low corrosiveness.[32] To further improve the practical application of DSSCs on a large scale, it should also come from abundant, possibly renewable, raw materials. Historically, liquid electrolytes have been firstly exploited for application in DSSCs because they guarantee high charge carrier diffusion and effective permeation of the photoelectrode porous structure. As discussed in detail below (see section 2.2.3), more recently quasi-solid and solid electrolytes have also been investigated to minimize the critical issue of liquid-based devices, typically linked to solvent leakage. Throughout this section, we mainly focus on liquid (both organic, 2.2.1, and aqueous, 2.2.2) electrolytes since they are more thoroughly investigated and considering that the first industries entering in the market proposed DSSCs based on this type of electrolyte. Accordingly, it should be noted that the improved stability guaranteed by quasi-solid and solid electrolytes is not automatically a "*green light*" toward sustainability, and thus proper LCA analyses should be performed.

The most common redox couples of the electrolyte are based on iodine or cobalt. Iodine-based electrolytes are composed of the I^-/I_3^- redox couple, I_3^- being formed through the reaction $I_2 + I^- \rightleftarrows I_3^-$, which offers several advantages, such as fast dye regeneration and charge mobility.[202] Additionally, since I^- is a small anion, it effectively permeates the mesoporous structure of sensitized photoelectrodes, resulting in almost quantitative sensitizer regeneration. On the other hand, this can also favor the recombination reaction with the electrons injected in the VB of TiO_2, which can be efficiently prevented by the insertion of a nanometric "blocking" layer.[203,204] However, I_2 is often corrosive towards commonly used metals (both at the lab-scale and module-scale levels);[205] in particular, when platinum is used as the CE, iodate can be formed, with a depletion of the active species in the electrolyte.[32] This negatively affects the long-term durability of cells, which is also reduced by the volatility of I_2, even if this last issue was partially solved by the use of a quasi-solid electrolyte.[206,207] Moreover, I_2 is colored and absorbs part of the solar radiation, thus competing with the sensitizer.[205] This point is of crucial interest in the development of bifacial devices to be applied in BIVP. In addition, it has a fixed, high redox potential, and thus the V_{OC} is limited between 0.6 and 0.8 V and cannot be tailored as desired.[208] Finally, this redox couple presents a complicated two-electron process, which is analytically described in some review articles.[201]

On the other hand, cobalt-based organometallic complexes offer the possibility of finely tuning the chemical and redox properties of the mediator by varying the ligands on the metal center. However, they are usually sterically hindered molecules, and this results in a mass transportation issue, with slow charge transfer dynamics (*i.e.* for 10^{-6} cm^2 s^{-1} in ACN, which is slower than that of triiodide, $\sim 2 \times 10^{-5}$ cm^2 s^{-1}).[209,210] Cobalt is a CRM and its natural abundance of 0.003% in the Earth's crust and 8×10^{-9}% in the ocean[211] poses a high risk for its future supply according to a recent press release by the European Chemical Society (EuChemS). If the last three months of 2019 are considered, the cost of cobalt hydroxide increased by 55%.[212] Despite the high performance of its complexes as redox pairs, which allowed the highest efficiency values in the field of DSSCs (up to 14.3%),[63] it must be replaced with abundant and renewable raw materials for sustainability. Therefore, although in this context they are not investigated in detail, a recent review excellently summarized their application in DSSCs.[213]

Owing to the disadvantages of iodine- and cobalt-based electrolytes, extensive research has been focused in recent years on the development of alternative redox pairs.[32] In the following subparagraphs, we will briefly review the most interesting developments in this respect, including major outcomes in the last five years, chiefly highlighting specific aspects related to the circular economy of the DSSC market of tomorrow. We strongly believe that a fully sustainable DSSC should be based on innovative electrolytes and related components obtained from renewable sources and not be made up of CRMs, the supply of which can fail in the coming years and the use of which is not justified in terms of overall gain in efficiency output of the device. To our knowledge, there are no literature reports of redox pairs obtained from renewable sources or waste-derived products, as conversely demonstrated for CE (*e.g.*, carbon-based cathodes coming from the food industry waste, *vide infra*). However, we are quite confident that efficient redox pairs based on transition metal complexes may be obtained from waste recovery, and purely organic or sulfur-based shuttles may be readily obtained from biomass or renewable sources.[214]

2.2.1 Alternative redox couple electrolytes. Pseudohalogens are among the first alternative redox couples reported in the literature.[215,216] In particular, the $SeCN^-/(SeCN)_2$ couple can be easily incorporated in a photo-reticulated polymer membrane, which may potentially enhance the long-term stability of devices (*i.e.* the trapping of the redox couple in a polymer matrix greatly reduces the evaporation of the electrolyte solvent), thus representing a step forward towards their commercialization. Pseudohalogen-based redox couples allow *in situ* free-radical polymerization, which is not possible with the traditional iodine-based redox couple due to its radical-quencher nature.[215] Free-radical polymerization is one of the most useful and lucrative fields of chemistry discovered to date, which is tolerant of diverse functionality and can be performed in a wide range of solvents. Particularly, UV and thermally induced methods are rapid, energy saving, and solvent-free, and thus cost-effective and sustainable, and already widely propelled to the commercial scale for the manufacture of diverse polymers starting from oil derivatives. Furthermore, the chemical behavior of pseudohalogens is close to that of halide ions, where the presence of heteroatoms and double bonds does not significantly influence their chemical properties.[215] They often show a more positive redox potential, *e.g.* the redox potential of the $SeCN^-/(SeCN)_2$ shuttle is 0.19 V higher than that of I^-/I_3^-, leading to a higher V_{OC}. It has also been reported that the $SeCN^-/(SeCN)_2$ redox couple possesses good mass transport characteristics, at the level of iodine-based couples.[215] The application of $SeCN^-/(SeCN)_2$ in a UV-crosslinked polymer network was demonstrated, which led to a quasi-solid state system showing a V_{OC} of 550 mV, J_{SC} of 6.68 mA cm^{-2}, fill factor (FF) of 0.53 and PCE of 1.95% (Table 2, entry1). A selenium-based pseudohalogen redox couple was also reported by Lennert *et al.*,[216] who used an RTIL as the electrolyte medium. RTILs are salts in the liquid state at room temperature, which present several advantages, such as low volatility, high chemical and thermal stability, low flammability and rather easy structure tuning to increase the solubility of specific solutes.[217] Consequently, they are potential candidates to replace the high-performing state-of-art organic solvents in DSSC electrolytes. However, although RTILs offer a suitable solution for the replacement of volatile and flammable organic solvents, according to the green chemistry criteria, their synthesis and final disposal at the EoL are still not sustainable[87] and extensive work has still to be done to make them robust alternatives. In the work by Lennert *et al.*, an alkyl-substituted RTIL was used with either selenocyanate or iodide counter anions. Remarkably, the PCE of the selenocyanate-based device was only slightly lower than its iodide-based counterpart (5.00% *vs.* 5.60%, respectively, Table 2, entry 2) mainly due to the slower ionic diffusion and less efficient regeneration at the counter electrode compared to that of its iodine-based counterparts. Overall, despite these promising results, no other relevant work has been done in the development of this redox couple, most likely because selenium is a very rare element in the Earth's crust (5×10^{-6} wt%)[211] and is toxic at high concentrations.[218]

Iron-based redox couples have also been investigated to replace cobalt- and iodine-based electrolytes. Iron is one of the most abundant metals (6.3 wt% in the Earth's crust)[211] and its metal complexes allow for tuning of the redox potential with the use of different ligands. Unfortunately, most of the iron complexes are air sensitive and require dry glove-box confinement for the assembly of the device. This represents a hindrance for the scalability of the manufacturing process, particularly when an easier processability is claimed for DSSC technology with respect to other PV devices. Notably, Fe forms several complexes that are soluble in water, thus its use in green, aqueous-based DSSCs can be envisaged,[104,219] as will be discussed in section 2.2.2. One of the first devices based on iron complexes as redox mediators was reported by Daeneke *et al.*,[104] who demonstrated the use of a ferricyanide/ferrocyanide ($Fe(CN)_6^{4-/3-}$) redox couple, using water as the solvent and proposing this electrolyte as non-corrosive. This redox couple had a similar redox potential to that of I^-/I_3^-, and thus it could be effectively coupled with already existing molecular dyes. A pH buffer and a surfactant were used to regulate the pH of the electrolyte and allow the permeation of the electrolyte into the hydrophobic sensitized TiO_2; unfortunately, the PCE was the half of that of the iodine-based reference (Table 2, entry 3). The same redox couple was adopted by Kokal *et al.*,[220] who reported an aqueous DSSC with an inexpensive magenta dye (new fuchsin) and a platinum-free CE based on CoS deposited on carbon fabric. Here, a remarkable efficiency of 2.88% was reached (Table 2, entry 4), which can be considered, as a first approximation, cost-effective. However, the ($Fe(CN)_6^{4-/3-}$) redox couple has some intrinsic problems that limit its application, for example, since it has a low redox potential, it less effectively regenerates commonly employed dyes and, as a result, more pronounced TiO_2/dye recombination can be expected. In addition, it undergoes to photolysis and photodecomposition under UV and near UV radiation, loosing almost 80% of its initial efficiency just after 5 h of light soaking.[56]

Iron-based organometallic complexes were also exploited in p-type DSSCs.[221] Perera *et al.*[56] successfully employed the $Fe(acac)_3^{0/-1}$ redox couple (acac = acetylacetonate) in a p-type DSSC with NiO as the photocathode. This redox couple showed a remarkably lower redox potential (−0.20 V *vs.* NHE) compared to that of I^-/I_3^- (+0.32 V *vs.* NHE). Consequently, both the V_{OC} and PCE were strongly improved (645 *vs.* 243 mV and +191%, respectively, Table 2, entry 5). However, despite its higher abundance and ready availability compared to cobalt, the results achieved with iron based redox couples are still unsatisfactory, which, added to their O_2 sensitivity, severely limit their widespread exploitation on a large scale.

Copper is intrinsically less toxic,[211] more environmental friendly[208] and two times more abundant than cobalt in the Earth's crust (0.003% *vs.* 0.0068%, respectively).[211] Furthermore, its complexes are generally more stable in air than iron-based ones, which allows their assembly without the use of glove-box conditions. The most common copper-based redox couples are constituted by copper(II/I) organometallic

Table 2 Different classes of alternative redox couple electrolytes, together with constituting material(s), related advantages, critical issues, highest recorded efficiency values *vs.* state-of-art and corresponding reference articles

Class	Material	Pros	Issues	PCE *vs.* reference	Entry[ref.]
Pseudo-halogens	$SeCN^-/(SeCN)_2$ in ACN	• Integration in quasi-solid electrolytes	• Toxicity • Use of organic solvents • Low availability of Se	Not reported	1[215]
	$C_6SeCN/(SeCN)_2$ in alkyl-substituted ionic liquid	• Non-volatile solvent	• Slower regeneration of the dye • Low availability of Se	−10.7%	2[216]
Iron-based complexes	$K_4Fe(CN)_6/K_3Fe(CN)_6$ in water	• Water as solvent	• Use of surfactants	−50.6%	3[104]
	$K_4Fe(CN)_6/K_3Fe(CN)_6$ in water	• Water as solvent	• Low stability	+182% (but using a carbon fabric as CE and not optimizing the condition of I^-/I_3^- with this set up)	4[220]
	$Bu_4N[Fe(acac)_3]/[Fe(acac)_3]$ in ACN	• Natural abundance	• N_2 atmosphere for electrolyte preparation • Use of organic solvent • Low stability	+191% p-type	5[56]
Copper-based complexes	$[Cu(2\text{-mesityl-4,7-dimethyl-1,10-phenanthroline})]^{2+/+}$ in ACN	• Low toxicity	• Organic solvent-based electrolyte • Use of *t*-butyllithium (−78 °C under argon atmosphere in DMF) for the synthesis of the ligand	+2.32% (equimolar) −40.5% (concentrated)	6[208]
	$[Cu(2\text{-alkyl-1,10-phenanthroline})_2]^{2+/+}$	• Low toxicity	• Use of *t*-butyllithium, toluene • Argon condition for the synthesis of the ligand	+7.69% (mesityl) +15.4% (tolyl) −5.77% (phenyl) +9.62% (*n*-butyl)	7[224]
	$[Cu(diimine)_2]^{2+/+}$ in ACN	• Low toxicity	• The synthesis of the ligands is not reported • Organic solvent-based electrolyte	−88.1% −79.3% −61.9%	8[225]
	$Cu(2\text{-mesityl-1,10-phenathroline})_2]^{2+/+}$ and $[Cu(2\text{-mesityl-1,10-phenathroline})_2]^{2+/+}$ in ACN	• Low toxicity • Comparable to Co-based electrolyte	• Use of *t*-butyllithium (−78 °C under argon atmosphere in pentane) for the synthesis of the ligand • Use of toluene for purification • Organic solvent-based electrolyte	−4.8%	9[226]
Other metal-based redox couples	VO(salen) in ACN (the oxidized form of the redox couple is formed *in situ* through $NOBF_4$)	• Abundance of vanadium with respect to cobalt • Non-corrosive	• Synthesis under strictly controlled conditions • Organic solvent-based electrolyte	Not reported	10[231]
	$(Ph_4P)[VO(hybeb)]/Ph_4P[VO(hybeb)]$ in ACN	• Abundance of vanadium with respect to cobalt • Non-corrosive	• Synthesis of the ligand in anhydrous tetrahydrofuran under argon conditions	Not reported	11[205]
	$[TBA]_2Mo_6O_{19}$ and $[TBA]_2W_6O_{19}$ in ACN	• Air stable • Low temperature • Synthesis in water ($Mo_6O_{19}^{2-}$)	• Synthesis in acetic anhydride and DMF	+62.2% ($Mo_6O_{19}^{2-}$) −18.9% ($W_6O_{19}^{2-}$) in p-type DSSC	12[57]

Table 2 *(Contd.)*

Class	Material	Pros	Issues	PCE *vs.* reference	Entry[ref.]
TEMPO-based redox couples	TEMPO/TEMPOBF$_4$ in ACN	• Non-toxic • Easy synthesis • Low temperature	• Organic solvent-based electrolyte	−18.7% (*vs.* Co(II)/Co(III))	13[235]
	TEMPO/TEMPO-BF$_4$ in water	• Non-toxic • Easy synthesis • Low temperature • Aqueous DSSC	• Not relevant	Not reported	14[232]
	TEMPO/TEMPO-BF$_4$ in ACN	• Non-toxic • Easy synthesis • Low temperature	• Organic solvent-based electrolyte	Not reported	15[236]
	TEMPOL/TEMPOL-BF$_4$ in ACN	• Non-toxic • Easy synthesis • Low temperature • Low cost	• Organic solvent-based electrolyte	+1500% (using a Nafion® membrane not optimized for organic electrolyte)	16[238]
Thiolate/ disulfide-based redox couples	T^-/T_2 in ACN (T^- = 5-mercapto-1-methyltetrazole *N*-tetramethylammonium; T_2 = di-5-(1-methyltetrazole disulfide))	• Room temperature	• Argon atmosphere • Organic solvent-based electrolyte	Not reported	17[244]
	T^-/T_2 in ACN (T^- = 5-mercapto-1-methyltetrazole *N*-tetramethylammonium; T_2 = di-5-(1-methyltetrazole disulfide))	• Room temperature	• Argon atmosphere • Organic solvent-based electrolyte	−16% (CE: platinum) −31.8% (CE: PEDOT:PSS) +32.2% (CE: MP carbon)	18[177]
	T^-/T_2 in ACN (T^- = 5-mercapto-1-methyltetrazole *N*-tetramethylammonium; T_2 = di-5-(1-methyltetrazole disulfide))	• Room temperature	• Argon atmosphere • Organic solvent-based electrolyte	−45.8%	19[242]
	T^-/T_2 in ACN(T^- = 1-ethyl-3-methyl-imidaziolium 4-methyl-1,2,4-triazole-3-thiolate; T_2 = 3,3′-dithiobis[4-methyl-(1,2,4)-triazole])	• Low temperature	• Organic solvent-based electrolyte	−53.6%	20[245]
	T^-/T_2 in DMSO/ACN (T^- = 5-methylthio-1,3,4-thiadiazole-2-thiol; T_2 is formed *in situ* through BF_4NO)	• *In situ* generation of the oxidized form (T-commercial)	• Organic solvent-based electrolyte	−37.0%	21[249]
	$T_{ph}^-/(T_{ph})_2$ and $T_{me}^-/(T_{me})_2$ in ACN (T_{ph}^-) = sodium 1-phenyl-1*H*-tetrzole-5-thiolate; $(T_{ph})_2$ = 5,5′-dithiobis(1-phenyl-1*H*-tetrazole); T_{me}^- = sodium 5-mercapto-1-methyltetrazole; $(T_{me})_2$ = di-5-(1-methyltetrazole)disulfide	• Room temperature	• Argon atmosphere • Organic solvent-based electrolyte	Not reported	22[250]
	T^-/T_2 in ACN (T^- = 5-mercapto-1-methyltetrazole *N*-tetramethylammonium; T_2 = di-5-(1-methyltetrazole disulfide))	• Low temperature	• Argon atmosphere • Organic solvent-based electrolyte	Not reported	23[252]
	$[C_{12}MIm][T]/[T_2]$ ($[C_{12}MIm][T]$ = 1-dodecyl-3-methyl-1*H*-imidazol-3-ium 1-methyl-1*H*-tetrazole-5-thiolate; T_2 = di-5-(1-methyl tetrazole))	• Room temperature • Ambient condition • Ionic liquid (non-volatile solvents)	• Chloroform is involved during the synthesis	Not reported	24[253]

DMF = *N*,*N*-dimethylformamide; PSS = poly(styrenesulfonate); MWCNTs = multi-walled carbon nanotubes; and DMSO = dimethyl sulfoxide.

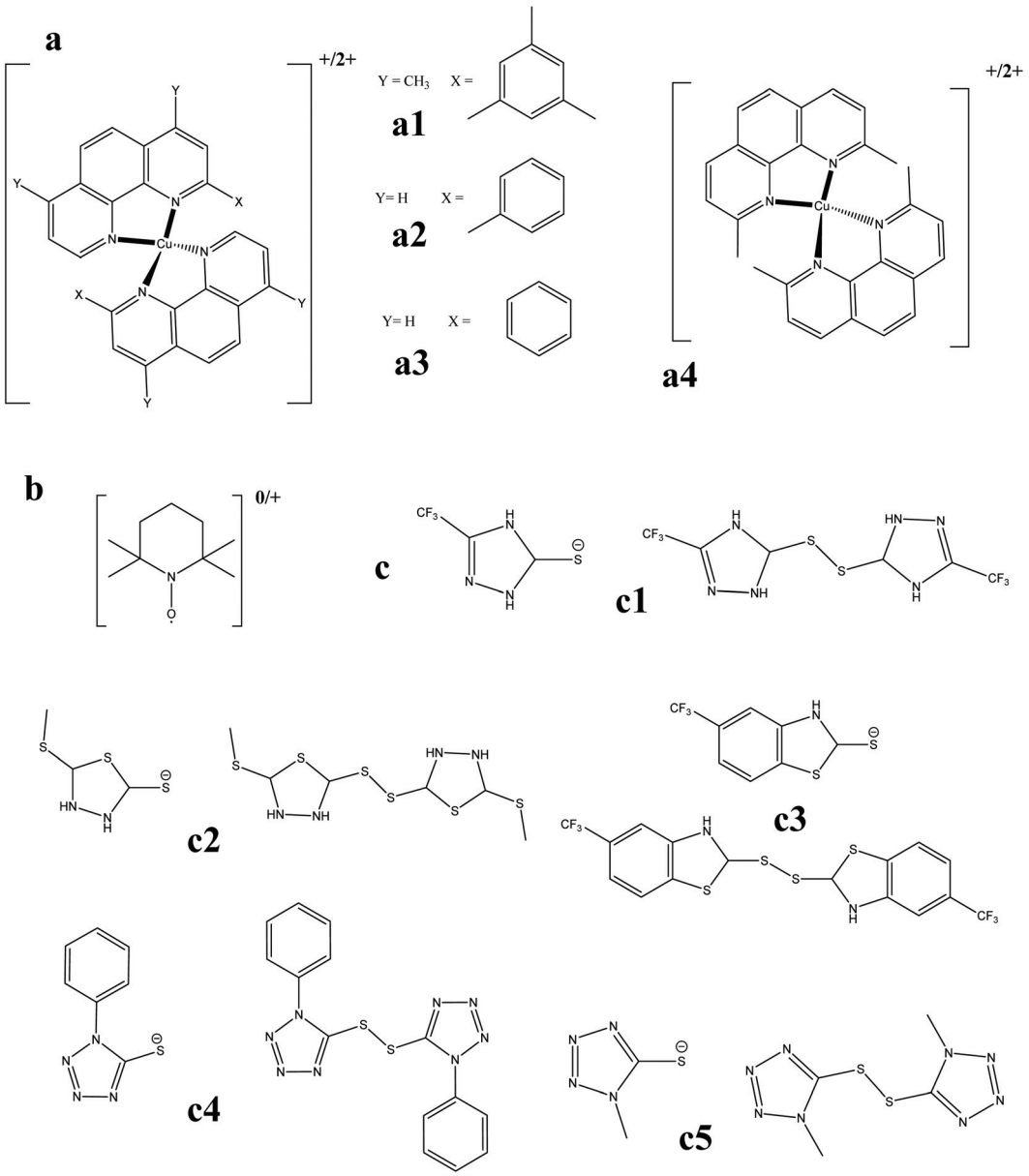

Fig. 6 Chemical structures of various alternative redox couples: (a) copper-based complexes (a1: [Cu(2-mesityl-4,7-dimethyl-1,10-phenanthroline)]$^{+/2+}$; a2: [Cu(2-tolyl-4,7-dimethyl-1,10-phenanthroline)2]$^{+/2+}$; a3: [Cu(2-phenyl-4,7-dimethyl-1,10-phenanthroline)2]$^{+/2+}$; and a4: [Cu(2,9-dimethyl-1,10-phenanthroline)2]$^{+/2+}$), (b) TEMPO$^{0/+}$ (2,2,6,6-tetramethyl-1-piperidinyloxy) and (c) sulphur-based organic molecules: (c1: 2-methyl-5-trifluoromethyl-2*H*-[1,2,4]triazole-3-thiol and 3,3′-dithiobis(2-methyl-5-trifluoromethyl-2*H*-[1,2,4]triazole); c2: 5-(methylthio)-1,3,4-thiadiazolidine-2-thiolate and 1,2-bis(5-(methylthio)-1,3,4-thiadiazolidin-2-yl)disulfane; c3: 5-(trifluoromethyl)-2,3-dihydrobenzo[*d*]thiazole-2-thiolate and 1,2-bis(5-(trifluoromethyl)-2,3-dihydrobenzo[*d*]thiazol-2-yl)disulfane; c4: 1-phenyl-1*H*-tetrazole-5-thiolate and 1,2-bis(1-phenyl-1*H*-tetrazol-5-yl)disulfane; and c5: 5-mercapto-1-methyl tetrazole and di-5-(1-methyltetrazoledisulfide)). All molecules were drawn using ChemDraw 19.0.

complexes with a distorted geometry (Fig. 6a).[208,222–227] This type of complex shows negligible structural changes when switching from the oxidized to reduced form, which means minimal energy loss and fast electron transfer.[220] Their usually more positive redox potential guarantees higher theoretical V_{OC} values compared to that of conventional redox mediators (iodine and cobalt); on the other hand, less efficient dye regeneration can be expected due to the limited ΔG of this process. However, transient absorption spectroscopy confirmed an almost quantitative dye regeneration yield.[224,226] Additionally, from a pure electrochemical point of view, copper-complexes have been proven to be relatively stable.[208]

The main drawback in the use of copper complexes is the presence of the phenanthroline-derived ligand, which requires harsh synthetic conditions despite allowing the realization of complexes with tunable features and low-reorganization energy.[228] Indeed, the 2-substituted phenanthroline ligand is commonly produced *via* the nucleophilic aromatic substi-

tution of the commercially available 1,10-phenanthroline using suitable lithium derivatives. These are produced by transmetallation reaction between the corresponding bromo-derivative and *t*-butyllithium in diethyl ether or pentane at −68 °C, having a negative impact on the CED factor. For the purification of the ligands, toluene is also used. Moreover, the synthesis of the copper complexes is carried out in dry ACN or toluene under an argon atmosphere.[222] Consequently, despite the higher abundance of copper and its reduced toxicity compared to cobalt, the synthesis of copper complexes bearing the 2-substituted phenanthroline ligand is still a significant issue to be solved for the exploitation of this metal as a sustainable redox mediator in DSSCs.

In 2016, Magni *et al.*[208] reported the preparation of [Cu(2-mesityl-4,7-dimethyl-1,10-phenanthroline)]$^{+/2+}$ complexes, which were used as effective redox mediators in ACN solution. They reached an efficiency of 4.4% and 4.1% with the organic G3 dye and platinum and PEDOT as CEs, respectively, proving that these couples could also be effectively regenerated by carbon-based CEs (Table 2, entry 6). Furthermore, to broaden their light harvesting capability, copper-based complexes were coupled with a Zn^{2+} porphyrin bearing cyanoacrylic acid as an anchoring group at the beta-pyrrolic position with an ethynylphenyl bridge. This structure was reported by Colombo *et al.*[223] to be more accessible compared to that of natural porphyrin dyes, allowing a deeper contact with the complexes.

The substituent in the 2-position of the phenanthroline ligands of the [Cu(2-mesityl-4,7-dimethyl-1,10-phenanthroline)]$^{+/2+}$ complexes plays an important role in maintaining a distorted geometry and reducing the internal reorganization energy involved in the redox reaction. In 2018, Benazzi *et al.*[224] introduced different substituents in the 2-position, such as tolyl, phenyl and *n*-butyl. For all these complexes, the regeneration of the dye was effective and faster than interfacial recombination, as demonstrated by transient absorption spectroscopy measurements. No substantial differences were observed in the shape of the *J*–*V* curves of the corresponding devices, with efficiencies in the range of 4.9% to 6.0%, suggesting that all the proposed redox couples may be efficiently used as redox mediators (Table 2, entry 7). Similarly, Karpacheva *et al.*[225] introduced different substituents in phenanthroline ligands, such as methyl, methoxyl and bromophenyl in the *ortho* and *para* positions. However, in this case, the efficiency values were found to be rather low (Table 2, entry 8) compared to that reported by Benazzi *et al.*[224] In 2016, Freitag *et al.*[226] reported a copper complex bearing the dmp ligand (dmp = 2,9-dimethyl-1,10-phenanthroline). The diffusion coefficient of [Cu(dmp)]$^{+/2+}$, determined by cyclic voltammetry, was found to be twice that of the state-of-art [Co(bpy)]$^{2+/3+}$; furthermore, the dye regeneration was four times faster, as confirmed by transient absorption spectroscopy measurements. Consequently, the PCE was high (7.0%) and comparable to that of the best performing cobalt-based devices (Table 2, entry 9). Although the increase in device sustainability is clear, the cost-effectiveness of this redox mediator should be further investigated by means of specific LCA.

Among the metal complexes proposed as redox mediators in DSSCs, oxovanadium-based complexes are worth considering. Even if according to the European Commission vanadium is envisaged as a CRM,[229] it is widely used in other energy fields, such as redox-flow batteries,[230] and was proposed as a valid alternative to cobalt due to its higher abundance in the Earth's crust (0.019% *vs.* 0.003%).[211] In addition, vanadium-based redox shuttles present fast electron transport, as confirmed by paramagnetic resonance spectroscopy and electrochemistry.[205] The first report on an oxovanadium redox couple was published in 2013 by Oyaizu *et al.*[231] The oxovanadium(IV/V) redox couple has an efficient redox mechanism that involves a bimolecular self-exchange reaction. In particular, the authors reported that the [VO(salen)]$^{0/+}$ complex (where salen = *N*,*N*′-ethylenebis(salicylideneiminate)) was highly soluble in ACN electrolyte solvent compared to its homologous. According to its crystal structure, it was found that the [VO(salen)]$^{0/+}$ redox couple experienced slight changes during the redox reaction, highlighting its low rearrangement energy and fast electron exchange. Also, its more positive redox potential compared to the iodine-based electrolyte accounts for its larger V_{OC} (0.74 V). Remarkably, the J_{SC} and PCE were found to be 12.3 mA cm^{-2} and 5.4%, respectively (Table 2, entry 10). Two years later, Apostolopoulou *et al.*[205] reported an oxovanadium complex bearing a tetradentate hybeb ligand (hybeb = [1-(2-hydroxybenzamido)-2-(2-pyridinecarboxamido)benzenato]). Despite the rapidity of the charge exchange process, as demonstrated by electron paramagnetic resonance (EPR), the overall efficiency of the cell (Table 2, entry 11) was definitely low compared to that reported by Oyaizu.[231]

Two other metals have been exploited in the electrolyte of p-type solar cells, namely tungsten and molybdenum. Both of them have a rather low natural abundance of 0.00011% in the Earth's crust, but only tungsten is considered a CRM.[229] Bakker *et al.*[57] reported an excellent V_{OC} improvement using two types of Lindqvist polyoxometalates (POMs), *viz.* $[TBA]_2Mo_6O_{19}$ and $[TBA]_2W_6O_{19}$ (where TBA = tetrabutylammonium), with redox potentials of −0.40 and −0.90 V, respectively (Fig. 7a). These values were remarkably lower than that of I_3^-/I^- (+0.32 V) and $[Co(en)_3]^{3+/2+}$ (−0.03 V). In addition, the two POMs showed negligible molar absorption in the VIS range, thus avoiding any competition for light harvesting with the dye. As expected, the V_{OC} values were found to dramatically increase for both the molybdenum- and tungsten-based electrolytes compared to the iodine- and cobalt-based electrolytes (100 and 80 mV, respectively). Possibly, sluggish diffusion caused a drop in the J_{SC}; therefore, the overall efficiencies of these devices were still unsatisfactory (0.13% and 0.11%, respectively, Table 2, entry 12). The development of alternative redox pairs also involves the synthesis of fully organic electrolytes to completely overcome the issues related to the use of metals, in particular cobalt, in complexes. However, the evaluation of the impacts of each approach should be evaluated. In this respect, Parisi *et al.* observed that the electrolyte does not have a huge impact in the overall device in terms of CED and green metrics.[93] However, their study highlighted the larger

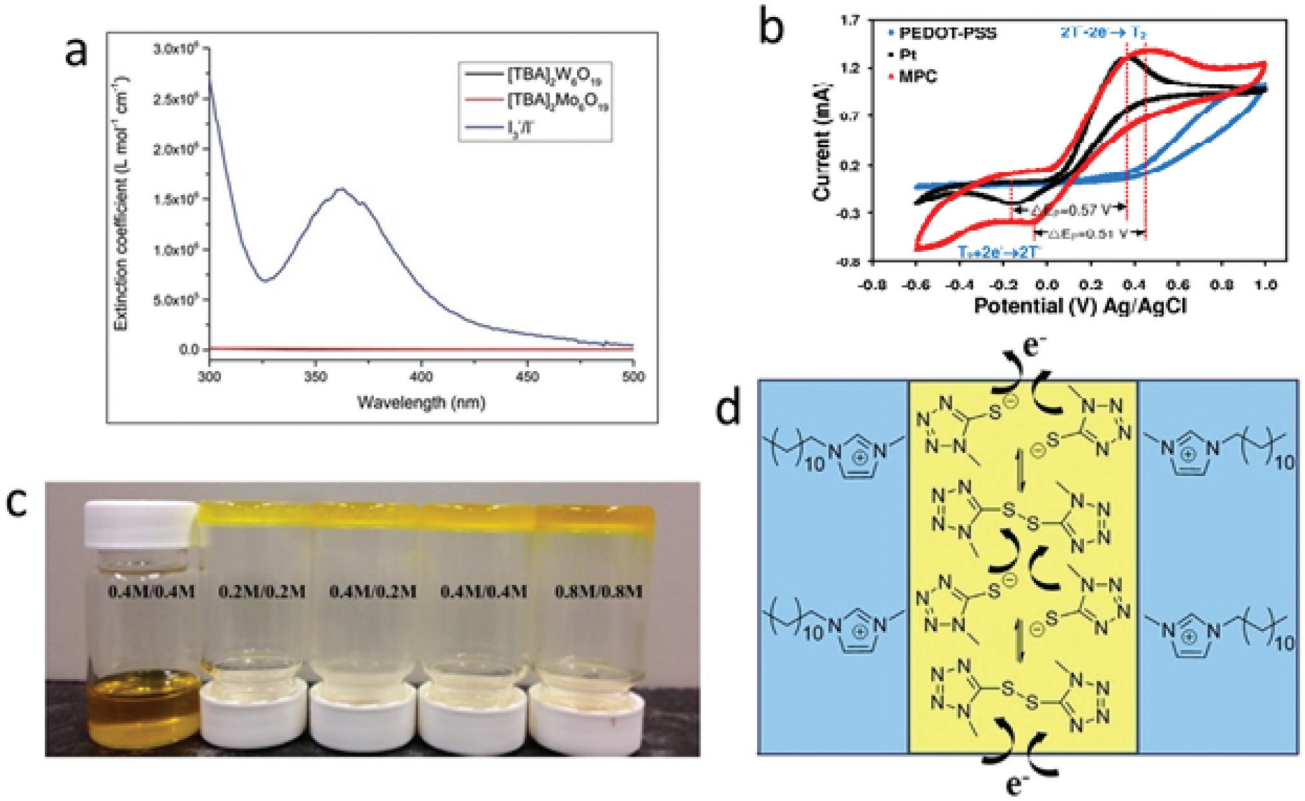

Fig. 7 (a) Absorption spectra of the POM-based electrolytes (black and red) in comparison with the iodine-based electrolytes (blue). The extinction coefficients of the former are negligible. Adapted from ref. 57. (b) Cyclic voltammograms (CV) of MP-derived carbon (red), PEDOT-PSS (light blue) and Pt (black) electrodes (sulphur-based redox couple and 0.1 M $LiClO_4$ in acetonitrile solution). Adapted from ref. 177. (c) Digital photograph of succinonitrile quasi-solid electrolytes. Adapted from ref. 252. (d) Schematic illustration of the electron pathway in the smectic crystal. Adapted from ref. 253.

impacts (ozone depletion) of the iodine-based couple compared to the cobalt-based couple due to the higher requirement of organic solvents. They also suggested an opportunity to achieve lower impacts by shifting towards solid electrolytes. Thus, it will be very interesting to evaluate the impacts of different electrolyte categories.

Besides metal-based redox couples, pure organic couples may be a feasible choice to achieve sustainable, but efficient, DSSCs and to overcome the limitation displayed by metal-based redox couples, namely low diffusion coefficient and complicated charge transfer kinetics (see above). An example of a fully organic electrolyte is TEMPO/$TEMPO^+$ (Fig. 6b), a redox couple with good efficiency in an aqueous environment.[232,233] TEMPO (2,2,6,6-tetramethyl-1-piperidine-1-oxyl) is a commercially available and relatively cheap (3.87 € per g by Merck) nitroxide radical molecule,[234] which can be easily oxidized to $TEMPO^+$. When used in DSSCs, the $TEMPO^{0/+}$ redox couple offers several advantages, such as easy preparation, non-toxicity,[235] no light absorption in the VIS range, fast electron transfer process, rapid mass transport kinetics[236] and highly positive redox potential, which is necessary for achieving high V_{OC}.[232] In 2015, Yang *et al.* tested $TEMPO^{0/+}$ in ACN solution with two different dyes, D149 and LEG4.[235]

Although $TEMPO^{0/+}$ presented a relatively low regeneration driving force (due to its highly positive redox potential), which resulted in regeneration efficiencies of 68% and 87% (with D149 and LEG4 dyes), the authors were able to achieve remarkable efficiency values of 3.29 and 4.70%, respectively (Table 2, entry 13). It showed a diffusion coefficient comparable to that of cobalt complexes in ACN (4.4×10^{-6} cm^2 s^{-1}),[237] suggesting that mass transport is a limiting factor in obtaining a high PCE. Additionally, $TEMPO^{0/+}$ has a smaller electron lifetime compared with the traditional cobalt and iodine-based electrolytes; therefore, some precautions, such as the employment of thinner electrodes should be taken into account to reduce the undesired charge recombination.

To the best of our knowledge, the $TEMPO^{0/+}$ redox couple was applied for the first time in aqueous DSSCs by Yang *et al.*[232] in the same year. As expected, they obtained a high V_{OC} (995 mV), J_{SC} (5.78 mA cm^{-2}), FF (0.75) and, consequently, rather high PCE of 4.14% (Table 2, entry 14). In an elegant work,[236] the TEMPO redox couple was used in combination with ZnO photoanodes, thus avoiding the energy-consuming

high-temperature thermal treatment of traditionally used TiO_2. ZnO was electrochemically deposited at a low temperature, where its morphology consisted of pillars grown vertically to the substrate. It ensured enhanced electron mobility and the resulting lab-scale cell demonstrated an efficiency of 3.92% (Table 2, entry 15). More recently, Kato *et al.*[238] reported a hydrophilic TEMPO derivative (4-hydrox-2,2,6,6-tetramethyl piperidine-1-oxyl, TEMPOL), which was successfully entrapped in a Nafion® polymeric matrix using an aqueous solution to replace ACN, since Nafion® is a good choice to immobilize electro-active cations. Specifically, a Nafion®-coated electrode (NCE) was dipped in an aqueous TEMPOL solution, giving a PCE of 1.6%, which was several times higher than that of its Pt-counterpart (0.11%, Table 2, entry 16). It is worth mentioning that NCE is a CRM-free CE, even if its applicability is limited to Nafion®-based polymeric electrolytes. 4-Hydroxy-TEMPO is less expensive than TEMPO because it is obtained from the cheaper precursor triacetonamine.[239] Overall, although TEMPO is sufficiently inexpensive to be exploited at a laboratory scale, it is not affordable on an industrial scale. Conversely, structurally related analogues (*e.g.*, TEMPOL) can be much less expensive since they are produced from acetone and ammonia, with the latter being seriously considered by the scientific community as an emerging solar fuel.[240] Specifically, for their purification, selective adsorption onto a hydrophobic resin is highly effective, and thus costly azeotropic distillation is avoided. Accordingly, they can be considered a more sustainable choice with respect to TEMPO. Concerning applications, they can be easily incorporated onto/into a solid support to achieve a heterogeneous material for catalysis or electrochemistry.

The $TEMPO^{0/+}$ redox couple and its analogues are very cheap and commercially available materials. The cost of the redox couple should be carefully considered in the design of sustainable, but cost-effective, DSSCs. Actually, in a conventional electrolyte, the redox couple concentration is usually higher than 1 M, and although a modest volume of electrolyte is employed in a conventional device, it can seriously hamper the cost-effectiveness and increase the EPBT of the complete device. Accordingly, $TEMPO^{0/+}$ and its derivatives could be considered as promising cost-effective redox couples in sustainable DSSCs.

The organic thiolate/disulfide couple and its derivatives offer several advantages when used as redox mediators in DSSCs (Fig. 6c), including ease of preparation, non-corrosiveness, negligible light absorption in the VIS range and tunable redox potential. 5-Mercapto-1-methyl tetrazole (T^-) with its dimer di-5-(1-methyltetrazoledisulphide) (T_2) (Fig. 7c) was the first[241] and the most commonly exploited organic sulfur-based redox couple. Sulfur-based electrolytes cannot be used in combination with platinum CE due to the formation of an irreversible S–Pt bond, which contributes to the depletion of both redox active species of the electrolyte and active metal centers of the electrode.[242] Simultaneously, also transition metal compounds (TMCs) seems to be unexploitable in conjunction with these couples due to the likely formation of S–M bonds. Consequently, alternative materials need to be developed, such as PEDOT or carbonaceous materials (section 2.3.1).[243] In 2015, two interesting reports were published using a composite TiC/carbon[244] and a full carbon CE.[242] In particular, the TiC/carbon composite electrode was hydrothermally synthesized using TiC and glucose as the carbon source. Compared to platinum, bare TiC and carbon CEs,[244] the TiC/carbon composite electrode generated the strongest reduction in current density among the electrodes under investigation, suggesting that it was able to effectively reduce T_2. Furthermore, the PV parameters of the TiC/carbon-based cell were comparable to that of the platinum-based cells (PCE = 3.59% *vs.* 3.84%, Table 2, entry 17). In the following example, the carbonaceous material used as the CE was obtained by pyrolysis at 850 °C under the inert atmosphere of a mangosteen peel (MP), an important source of natural phenolic antioxidants.[177] Even if MP is obviously a green and sustainable scaffold, the very high pyrolysis temperature negatively impacts the comprehensive sustainability-driven approach (*i.e.* higher CED). Among the electrode materials tested (platinum and PEDOT), MP resulted in the lowest charge transfer resistance in the symmetrical cell using T^-/T_2 in ACN as the electrolyte (Fig. 7b). Consequently, the MP-based cells reached an average efficiency of 2.63%, remarkably higher than that of the PEDOT:PSS-cells (0.60%) and almost twice that of their platinum counterpart (Table 2, entry 18). The promising prospects of carbon CE combined with T^-/T_2 were further confirmed by Tangtrakarn and co-workers in 2019,[242] who presented a comparison of the electrocatalytic behavior of an annealed carbon-based material obtained by arc evaporation method and platinum (Table 2, entry 19).

In 2012 Tian *et al.*[245] demonstrated that T^-/T_2 was also effective in aqueous electrolyte in combination with two organic dyes, D45 and D51. The efficiency obtained with the aqueous electrolyte (2.6%) was even higher than that reached using the corresponding ACN-based electrolyte (1.1%), which is likely ascribed to the enhanced solubility of the compounds and wettability of the hydrophobic dye-TiO_2 using Triton X as the surfactant. However, these efficiencies were still unsatisfactory compared to that of the iodine-based device (Table 2, entry 20). Actually, the diffusion coefficient of DTT in pure water was much lower than that of the triidiode couple. Furthermore, the regeneration of D45 dye was found to be 4-times slower using TT^-/DTT compared to its iodine-based counterpart. In the following years, the redox and chemical properties of the thiolate/disulfide redox couple were customized *via* the modification of the substituents in the tetrazole ring.[246–248] The main goal was to increase the solubility of these sulfur-based compounds in organic solvents. In fact, the low solubility of T^-/T_2 still represents a sizeable issue in the use of organic sulfur-based redox mediators. Accordingly, it should be noted that to thoughtfully choose a redox couple, a benefit/cost analysis should be also considered, for example, we reported the case of the T^-/T_2 redox mediator. It could be easily substituted with different alkyl moieties (*e.g.* butyl, hexyl, and octyl) by following the same synthetic route and

with almost quantitative yields.[246] However, the alkylthiocyanates employed as precursors have different prices, for example 8 € per g, 5 € per g and 103 € per g for 1-butyl, 1-hexyl and 1-octyl thiocyanate, respectively, where the latter is too high to be considered cost-effective.

With the aim of increasing the redox potential and speeding up the reduction process, Rahman *et al.*[249] reported the easy preparation of 5-methylthio-1,3,4-thiadiazole-2-thiol (MTDT)/5-methylthio-1,3,4-thiadiazolium disulfide dication ($MTDD^{2+}$) as a redox mediator (Fig. 6c), which was then combined with PEDOT CE and indolenine D205 dye or CdS quantum dots (QDs) as sensitizers. The well-matched combination of the MTDT/$MTDD^{2+}$ redox shuttle with PEDOT CE and favorable band alignment of the sensitizers with the redox potential led to efficiency values of 3.55% and 1.20% with D205 and CdS, respectively, which were still lower than that of the reference device (Table 2, entry 21). This was attributed to both ionic conductivity (0.52 S m^{-1}, four times lower) and diffusion issues (D of $MTDD^{2+}$ in ACN is roughly two orders of magnitude lower). Bhargava *et al.*[250] substituted the methyl group with a phenyl group (Fig. 6c) in 5-mercaptotetrazole, which was used in combination with a 20 μm-thick carbon CE. The different substituents on the tetrazole ring had a fundamental effect on the self-assembly properties of the electrolyte; specifically, the 1-phenyl substituted redox couple formed a protective monolayer on the surface of the CE, which worked as a surface-passivating agent to limit corrosion and recombination phenomena at the interface. Under the optimized conditions, an overall efficiency of 4.6% was achieved (Table 2, entry 22). The dual effect of 1-phenyl-5-mercaptotetrazole and its dimeric form was also demonstrated in p-type DSSCs, with sensitized-NiO as the photocathode (PCE = 0.51%).[251]

In conclusion, several alternative redox mediators have been reported, but much work has still to be done in tuning the chemical, electrochemical and physical features of these compounds, considering also the sustainability of the raw materials and the processes involved. It should be noted that the thoughtful development of redox mediators cannot overlook the synergic behavior of both the sensitizer (which needs to be regenerated by the redox mediator) and the counter-electrode (thanks to which the redox mediator is reduced again). Additionally, the above-presented materials have been designed for a specific application in liquid (or at least quasi-solid) electrolyte, whereas a substantially different paradigm is required considering their application in solid-state DSSCs (see section 2.2.3).

Two other examples of the use of T^-/T_2 as a redox mediator are worth mentioning,[252,253] in which the efforts of the authors were devoted to the replacement of organic solvents and the realization of non-volatile, non-flammable and stable electrolytes. In the first case,[252] succinonitrile (SCN) was mixed with T^-/T_2 and used as a quasi-solid electrolyte, having the positive characteristics of ensuring good contact with the electrode materials, maintaining acceptable ionic conductivity, and simultaneously, avoiding the leakage of the electrolyte (Fig. 7c). Specifically, SCN is a solid non-ionic polymer with high polarity, which can dissolve various types of salts. Under the optimized conditions, a remarkable PCE of 3.52% was achieved (Table 2, entry 23).[252]

In the second example,[253] Tan and co-workers firstly demonstrated a crystalline DSSC electrolyte with the T^-/T_2 redox couple, which was obtained in the form of a smectic liquid crystal by mixing 1-dodecyl-3-methyl-1*H*-imidazol-3-ium, 1-methyl-1*H*-tetrazole-5-thiolate ($[C_{12}MIm][T]$) and di-5-(1-methyltetrazole) disulfide in a 2 : 1 ratio (Fig. 7d). The smectic liquid crystal allowed its highly mobile 2D pathways to be exploited, resulting in remarkable PCE of 4.1% (Table 2, entry 24).

2.2.2 On the use of water as an alternative, sustainable electrolyte solvent. Traditional DSSC electrolytes are made of organic solvents, mainly nitrile-based, which are characterized by several drawbacks, primarily including toxicity, related severe environmental impact, high vapor pressure, and in some cases, explosiveness, where this issue affects their safety and seriously limits their practical applications in DSSCs, especially if indoor applications are envisaged.[254] Accordingly, water represents an effective solution due to its strong solvation ability, inertness and low viscosity. However, the DSSC community has historically considered water as a poison for cell stability, and this forced the design of robust encapsulation systems[19] and specifically conceived barrier materials.[110] However, despite these precautions, water traces are always present in the mesopores of the photoanode layer and in the electrolytic solution, where water contamination exponentially increases if plastic/flexible architectures are envisaged. Actually, water permeation in these materials is rather high (*i.e.*, 0.01 g m^{-2} day^{-1}), which may account for a water content exceeding 10 wt% after one year of real outdoor use.[110,255]

Obviously, water is non-toxic compared to organic solvents, and thus intrinsically safe and non-hazardous. Nevertheless, water is a natural resource and its contamination must be carefully considered. Actually, the main issue when using water as a solvent is not represented by its supply, but rather by its purification, recovery and disposal.[256,257] Moreover, to obtain good photoconversion efficiency, ultrapure water is mandatory, leading to a significant increase in the overall cost of the device (mainly due to energy-demanding purification procedures), which in turn lowers its sustainability. Our group is involved in an LCA analysis on the economic impact of the employment of ultrapure water. Indeed, the production process of ultrapure water is highly energy-demanding, affecting the impact of the resulting devices. A more sustainable option may be the employment of wastewater or tap water, but we did not find any report on this topic. Clearly, it is worth highlighting that water displays many attractive features as a solvent, but its use has its own barriers and set of problems,[87] especially when organic molecules are involved. Preliminary investigations towards aqueous DSSCs involved either the use of traditional electrolytes and dyes or the investigation of non-fully aqueous electrolytes comprised of different ratios of water and organic solvents.[258] Nowadays, the trend is

to completely re-think the chemistry aimed at fabricating fully aqueous DSSCs by making use, for instance, of surfactants.[259]

The seminal paper by O'Regan *et al.* in 2010 placed water at the center of the research of a new, truly green DSSC, which exploit it as the main component of the electrolyte. This represented a recent turning point in the research on photoelectrochemical cells.[260] The amount of methoxypropionitrile (MPN) and water was varied when preparing different electrolytes (PMII 2.0 M, I_2 50 mM, GuSCN 0.10 M and TBP 0.5 M; PMII = 1-propyl-3-methylimidazolium iodide; GuSCN = guanidinium thiocyanate; TBP = 4-*tert*-butylpyridine, respectively). Besides, a hydrophobic dye (TG6) was chosen and 1% Triton X-100 surfactant was introduced into the electrolyte to avoid phase separation. The basic functions of the DSSC (injection, regeneration and transport) worked properly at all water concentration levels, even at an H_2O content as high as 80 vol%, and lab-scale cells showed limited losses of 7% and 8% in J_{SC} and V_{OC}, respectively, after 1000 h at 1 sun illumination (35 °C with UV-filter).

In the last decade, the scientific community has spent considerable efforts aimed at using bare water as a solvent. In the context of green chemistry and circular economy milestones, DSSCs fabricated with water-based electrolytes are foreseen to guarantee reduced costs, non-flammability, lower volatility and improved environmental compatibility without neglecting the importance of water as a precious resource. However, this approach is extremely challenging from both the chemical and materials science viewpoints, although an increasing number of electrodes, dyes and electrolyte components has already been proposed for operating in an aqueous environment.[110] This also matches with the initial purpose of the inventors of DSSCs, *viz*. the construction of an artificial photosynthetic system that can convert solar light into electricity; by using only water as the key electrolyte component we will be close to achieving photosynthesis, also paving the way for the widespread distribution of sustainable PV cells in the market. Besides being inexpensive and inherently safe, aqueous DSSCs clearly do not suffer from water contamination issues, with the added value of easily solvating many potential redox mediators. In recent years, photoanode modifications, selection of specifically conceived redox couples, introduction of novel additives and surfactants, preparation of suitable cathodes and jellification of electrolytes have rapidly led to the assembly of 100% aqueous solar cells (see Table 3). Note that 100% aqueous solar cell means water as the only solvent. The wide variety of cell components clearly reveals that a unique strategy to achieve good efficiencies in the presence of aqueous electrolytes is not available to date. Indeed, the TiO_2 electrode structure, dye molecules, redox pairs and related concentration, cathode type and cell thickness are all extremely variable and current efficiency records approaching 7% represent, in principle, a solid milestone considering future optimization in this field.[261]

Among these studies, two of them emerge in terms of sustainability-related aspects, namely the work by Lin *et al.*[265] and Fayad *et al.*[264] The article by Lin *et al.*[265] firstly showed a 100% water-based device bearing a metal-free sensitizer and redox-shuttle. Anthracene/phenothiazine units were used as spacers for the MD3 dye, which in the presence of CDCA, was able to match the performance of N719 in standard lab-scale devices. In an aqueous environment, a dual-TEMPO iodide electrolyte (JC-IL) was proposed, which led to an efficiency of 4.96%. Besides enhancing the V_{OC} to 0.77 V, the TEMPO-based redox couple avoids the use of cobalt, and thus is considered a big step forward to a sustainable path. However, TEMPO is toxic to aquatic life, it is highly persistent and can accumulate in the environment. Even if this is not widely known in the solar harvesting community, in other fields (*e.g.*, catalysis) researchers are placing huge efforts on the reuse/recycling of TEMPO or its immobilization into polymeric matrixes.[269]

The sulfide/polysulfide couple is a valid alternative in aqueous environment. It was investigated by Fayad *et al.*[264] in combination with a zwitterionic and thiocyanate-free dye (namely, T169). The resulting solar cells demonstrated very high current densities (J_{SC} = 13.30 mA cm^{-2}) and a PCE of 4.5%, which were rather stable after 2000 h of aging test (limited 3.3% performance decay). The sustainability of this sulfur-based electrolyte should be fully understood starting from its precursor, *i.e.* 1-(2-hydroxyethyl)-5-mercaptotetrazole, the synthesis of which involves several steps. Even though a couple of LCA studies on DSSCs were published in recent years, further efforts should be focused on the proper understanding of the concrete impact of these alternative redox shuttles. Actually, in some cases, issues related to the use of solvents and energy spent for the whole synthesis place these emerging systems not so far from the traditional systems based on cobalt or organic electrolytes.

Independently from the specific literature articles under analysis, some common aspects related to aqueous DSSCs emerge. Firstly, platinum is still highly used within the aqueous DSSC community; when considering the widespread practical application of these devices on a large-scale, this represents an obstacle to be overcome soon due to cost-related reasons. Secondly, half of the proposed redox couples are based on cobalt, and this is even more critical since it results in safety and environmental issues. Thirdly, a clear strategy to design molecular dyes is still scarce since it requires the development of a photoanode showing good wettability, while concurrently preventing dye desorption by water. Finally, the analysis of solar cell parameters highlights J_{SC} values that are roughly half of those recorded by the corresponding organic electrolyte-based cells. The reason for the low current of water-based DSSCs is still unclear, but likely ascribed to the contributions of weak electrolyte penetration in the whole electrode thickness and the fraction of recombination at the photoanode/electrolyte interface.

A further interesting strategy in the field of aqueous DSSCs deals with the preparation of hydrogel electrolytes, with the aim of increasing cell stability and facilitating device assembly with printing techniques. Notably, the first examples of this type involved the use of polymeric matrices obtained by non-oil-derived sources.[270] Xiang *et al.* and Zhang *et al.* prepared

Table 3 List of the most efficient 100% aqueous DSSCs, characterized under 1 sun irradiation (AM 1.5G), with their main components, advantages, drawbacks, highest recorded efficiencies and corresponding reference articles

Anode	Dye	Electrolyte	Cathode	Pros	Issues	PCE (%)	Entry[ref.]
TiO_2 (4.5 μm) + $TiCl_4$	D149	GuI 8.0 M, I_2 20 mM and CDCA until saturation	Platinum	• Cobalt-free	• High iodide concentration required (8.0 M)	4.1	1[262]
BL + TiO_2 (1.3 μm T + 5 μm SL) + $TiCl_4$	MK-2	$K_4Fe(CN)_6$ 0.40 M, $K_3Fe(CN)_6$ 40 mM, KCl 0.10 M, Trizma-HCl buffer 50 mM (pH 8) and Tween 20 0.1%	Platinum mirror	• Cheap formulation	• Unstable, presence of cyanide	4.1	2[104]
TiO_2 (1 μm T + 3 μm SL)	MK-2	$[Co(bpy)_3]^{2+}$ 0.20 M, $[Co(bpy)_3]^{3+}$ 40 mM, NMBI 0.70 M and PEG 300 1%	Platinum	• Simple photoanode fabrication	• Cobalt-based	4.2	3[263]
TiO_2 (BL + 4 μm T + 4 μm SL) + $TiCl_4$	LEG4	TEMPO 0.15 M, $TEMPOBF_4$ 50 mM, $LiClO_4$ 0.10 M and NMBI 0.20 M	Platinum	• Metal-free redox shuttle	• Acute toxicity of NMBI	4.1	4[232]
$TiCl_4$ + TiO_2 (14 μm + 6 μm SL) + $TiCl_4$	T169	T^-/T_2 0.4/0.4 M, Triton X-100 0.1%, pH 5.0	PEDOT	• Metal-free redox shuttle and cathode	• 25% PCE loss in 2000 h	4.5	5[264]
TiO_2 (9 μm T + 3 μm SL)	MD3	TEMPO 0.40 M, $NOBF_4$ 0.40 M, LiI 0.10 M, I_2 50 mM, DMPII 0.60 M, GuSCN 0.10 M and Tween 20 0.1%	Platinum	• Metal-free redox shuttle	• 8 components in the electrolyte	5.0	6[265]
TiO_2 (1 μm T + 3 μm SL)	MK-2	$[Co(bpy)_3]^{2+}$ 0.20 M, $[Co(bpy)_3]^{3+}$ 40 mM, NMBI 0.70 M and PEG 300 1%	Platinum: ITO	• Lowering Pt amount by adding ITO	• Cobalt-based	5.0	7[263]
TiO_2 (7 μm) + $TiCl_4$	D51	$[Co(bpy\text{-}pz)_3]Cl_2$ 0.13 M, $[Co(bpy\text{-}pz)_3]Cl_3$ 60 mM, NMBI 0.80 M	PEDOT	• Improved solubility of the redox shuttle	• Cobalt-based	5.5	8[266]
TiO_2 (1 μm T + 3 μm SL) + $TiCl_4$	MK-2	$[Co(bpy)_3](NO_3)_2$ 0.20 M, $[Co(bpy)_3](NO_3)_3$ 40 mM, NMBI 0.70 M and PEG 300 1 wt%	Platinum	• Stability (0% PCE decrease in 500 h)	• Cobalt-based	5.6	9[267]
TiO_2 (10 μm)	EO3	JC-IL 0.40 M and $NOBF_4$ 0.40 M	Platinum	• Dual metal-free redox couple	• Stability not demonstrated	6.0	10[268]
TiO_2 (BL + 12.5 μm) + $TiCl_4$	D149	NaI 1.0 M and I_2 10 mM	cPEDOT	• Metal-free redox shuttle, dye and cathode	• Impact of D149 synthesis	7.0	11[261]

GuI = guanidinium iodide; BL = blocking layer; T = transparent layer; SL = scattering layer; PEG = poly(ethylene glycol); NMBI = *N*-methylbenzimidazole; DMPII = 1,2-dimethyl-3-propylimidazolium iodide; and cPEDOT = cationic PEDOT.

hydrogels using gelatin, a widely available, non-toxic and biodegradable polypeptide made by the hydrolytic degradation of collagen.[271,272] In a recent work, the use of cellulose gum, widely known as carboxymethyl cellulose (CMC),[206] allowed the development of homogenous gels with less than 10 wt% CMC in the aqueous electrolyte. The resulting lab-scale devices demonstrated a remarkable efficiency retention of 93% after one month of storage in the dark, and excellent stability when subjected to a further month of thermal aging at 60 °C in an oven.

2.2.3 Beyond liquid-state electrolytes. When screening DSSCs in the literature, a progressive transition clearly emerges from studies focused on liquid electrolytes (during the first years after the 1991 seminal paper) to articles dealing with quasi-solid systems (*i.e.* physically or chemically gelled by means of polymers or nanoparticles);[273] subsequently, completely solid cells were proposed.[35] The rationale behind this evolution is clearly based on the stability issues, as well as on the difficulty of perfectly sealing a liquid electrolyte between two pieces of glass. However, to date, it is rarely discussed in the DSSC community how this is in contrast with the fact that the first industries entering in the market proposed DSSCs (conceived for architectural integration or portable electronics) based on liquid electrolytes.

Considering the aspects strictly related to sustainability, quasi-solid electrolytes do not represent a concrete step forward. In fact, they are usually made of the same salts, solvents and additives used for the preparation of traditional liquid electrolytes. Moreover, in most cases, a thermoplastic polymer derived from oil is used to jellify the system, negatively influencing the sustainability-driven trade-off. Also, considering the working mechanism, there is no substantial difference between quasi-solid and liquid electrolytes, where on one hand, the regeneration of the dye is always based on the electron injection from the redox potential of the mediator to the HOMO level of the dye. On the other hand, the regeneration of the mediator is always based on the mass diffusion of the redox mediator between the cell electrodes. The presence of a polymeric membrane can negatively influence the diffusion of the mediator throughout the electrolyte, but simultaneously, it can protect the latter from unwanted charge recombination at the TiO_2/electrolyte interface. Several reviews have been published on this issue to date,[274,275] from which a good step forward in terms of industrial stability and processa-

bility emerges (*e.g.*, through printing techniques), but this is overall accompanied by a step backward in terms of device sustainability.

Replacing liquid-based systems with solid semiconducting materials started to be concretely possible in 1998, when Bach *et al.* demonstrated the hole-transporting ability of 2,2′,7,7′-tetrakis-(*N*,*N*-di-pmethoxyphenylamine)-9,9′-spirobifluorene (Spiro-OMeTAD).[276] Currently, this represents one of the most attractive solid-state p-type charge transporting layers due to its adequate TiO_2 pore-filling capability and very efficient light-induced charge carrier generation at the heterojunction. Spiro-OMeTAD completely changed the working mechanism of DSSCs, passing from the diffusion of a redox shuttle to the hole-hopping process through a very thin layer separating the electrodes. On the other hand, this solid-state compound led to poor interfacial contacts, causing interface electrostatics to become one of the limiting factors for reproducible, efficient and stable devices.[277] However, the most important issues regarding Spiro-OMeTAD are related to its sensitivity to both moisture and oxygen and its high production costs, mainly due to its lengthy synthesis protocol, which is low yield with a considerable impact in terms of solvents used for the separation and purification steps.[278,279] Furthermore, it necessitates the addition of additives based on lithium and/or cobalt (a well-known CRM) to boost its conductivity and hole mobility, thus making this system far from the sustainability targets of the DSSC scenario. Accordingly, the development of alternatives to Spiro-OMeTAD is now an urgent research topic, mainly in the field of PSCs, where the hole transporting material must be in the solid state.[280]

Plastic crystals, *i.e.* crystals consisting of weakly interacting molecules bearing some conformational or orientational degree of freedom, entered the solid-state DSSCs scenario a few times. After some seminal studies on succinonitrile,[281] some groups proposed organic ionic plastic crystals utilizing pyrrolidinium, phosphonium and quaternary ammonium cations.[282] These systems are solid, show poor volatility and high ionic conductivity (which can be further increased by the addition of SiO_2 nanoparticles), targeting a PCE of close to 8%. They can be liquefied at mild temperature to allow cell filling and then become solid; indeed, plastic crystals function as a solid solvent for the iodine-based redox shuttle. However, the sustainability of this approach is poor (or, at least, not better than that of liquid organic electrolytes). Indeed, the production of succinonitrile involves the addition of HCN to acrylonitrile, which are both strictly connected to impactful industrial preparation protocols.[283]

As a third type of solid DSSC, "zombie solar cells" emerged in recent years when liquid DSSCs based on copper complexes, such as $[Cu(tmby)_2]^{2+/+}$, were dried and the redox shuttle was able to work as a solid hole-conducting species.[284] To date, this approach can give PCE values of up to 11.7%, being the highest ever obtained for solid-state DSSCs.[154] Interestingly, photocurrent dynamics as a function of irradiation intensity showed that the J_{SC} depends linearly on the light power, thus clarifying the absence of mass transport limitations, which can instead be present in the case of copper complexes usually employed in liquid electrolytes. Thus, an LCA study of this approach will be crucial at this stage. In fact, the ability to fabricate solid-state DSSCs based on copper can leads to the simultaneous achievement of sustainability, stability and high efficiencies.

2.2.4 Final remarks on electrolytes. As discussed above, many alternative redox couples have been proposed to date, which can be potentially derived from renewable sources or waste products. This actually limits issues related to the use of CRMs and allows the electrolyte components to be sustainable. However, as reported in Table 3, in most cases, the use of organic solvents in the electrolyte and high energy-consuming synthetic procedures threaten the sustainability of these alternative redox couples. Consequently, extensive research still has to be focused on new materials and reliable procedures. In summary, several alternative redox couples to the traditional iodine and cobalt have been here reported. When using metal-based redox couples, their natural abundance, availability and the eventual recovery must be considered and correlated with their effective properties. As an example, iron is a very abundant metal in the Earth's crust. However, its complexes, when used as redox mediators in DSSCs, resulted in several problems, such as O_2^- sensitivity, photodegradation and high recombination rate. On the other hand, copper complexes present several advantages, such as low light absorption in the visible region, high dye regeneration efficiency, efficient regeneration at the CE, and stability. However, the synthesis of specific ligands (based on phenanthroline) and complexes is far from being "sustainable" since it involves the use of toxic organic solvents and inert N_2 or an Ar atmosphere. In addition to metal-based complexes, completely organic redox mediators were considered, such as $TEMPO^-$ and sulphur-based ones. Concerning the $TEMPO^{0/+}$ redox couple, the main issues are its lower regeneration efficiency and electron lifetime compared to that of the traditional cobalt and iodine. Thus, the use of thinner photoanodes must be considered in order to reduce recombination losses and improve electron collection. Finally, sulphur-based compounds are the most investigated in the wide plethora of alternative redox couples. Actually, they offer several advantages, such as ease of preparation, non-corrosiveness and negligible light absorption in the visible region. Also, although they cannot be used in combination with traditional platinum CEs, they work well with alternative candidates, such as PEDOT or carbonaceous materials.

The choice of the redox pair must also be accompanied by the adequate replacement of organic solvents (in the case of liquid-state DSSCs). Although the long-term stability of aqueous-DSSCs is not unambiguously accepted, water certainly represents a winning choice for this purpose, especially considering that commercial DSSCs are now assembled with liquid electrolytes and the introduction of water as a solvent does not require invasive intervention in production plants. Achieving a truly aqueous solar cell with high efficiency at the level of its organic-based electrolyte counterparts represents the *Holy Grail* for the DSSC community, which is strongly

focused on the development of sustainable, cheap and scalable technology with unique features, especially if indoor and portable objects are envisaged. Accordingly, the issues related to the (ultra)purification of water should be carefully evaluated to classify aqueous DSSCs as truly sustainable technology.

Beside the development of water-based DSSCs, the discovery of the remarkable performance exhibited by the copper-based "Zombie-cell" has opened a new branch in the field of hole transporters. This strategy, which has offered efficiencies of above 11% to date, can became an unprecedent breakthrough in the realization of truly sustainable DSSCs if in-depth LCA studies show adequate figures of merit. To date, this solution has already demonstrated the ability of bypassing the use of CRMs, such as cobalt, while simultaneously offering high efficiency and stability.

2.3 Cost-effective and eco-sustainable counter-electrodes (CEs)

The counter-electrode plays a key role in DSSCs[285] since it catalyses the reduction (also known as regeneration) of the oxidized species of the redox shuttle. Beyond good catalytic activity, CEs should exhibit wide thermal and (photo)chemical stability.[286] With regards to the regeneration mechanism, its kinetics is mainly dependent on the nature of the redox mediator and the physical status of the electrolyte more than on the CE material itself (*vide* section 2.2). Indeed, the latter should present a wide surface area in order to expose a large number of catalytic sites. Accordingly, throughout this section, we mainly focus on the morphological features of the different classes of materials effectively employed as CEs together with their electrochemical properties and relations with other device components. Specific attention is paid on greener and more sustainable synthetic and deposition approaches.

Concerning liquid and quasi-solid electrolytes, the reduction of the redox mediator occurs in three steps as follows: (i) the approaching and absorption of the reduced species onto the surface of the CE; (ii) the regeneration reaction; and (iii) the desorption of the oxidized species from the surface of the CE into the electrolyte solution.[13] Therefore, a good CE should avoid strong chemisorption of the redox species to allow efficient regeneration kinetics. To compare different type of CEs, two main parameters should be analysed, namely the charge transfer resistance (R_{CT}) and limiting current density (J_{lim}). The former, usually obtained from electrochemical impedance spectroscopy (EIS),[287] is a quantitative detector of the resistance experienced by an electron to be transferred from the CE to the oxidized species of the redox couple. The latter is the maximum current density value a CE can support. Thus, to have an efficient counter-electrode, a low R_{CT} and high J_{lim} are required.

Historically, platinum is the CE of choice in DSSCs, but the scientific community is searching for feasible alternative, sustainable materials that are being and more readily available.[288–293] In addition, platinum tends to degrade when in contact with the standard I_3^-/I^- redox mediator, thus restricting its use on a large scale.[294–296] However, due to its superior characteristics of high electrical conductivity and electrocatalytic activity, finding and developing alternative CEs to replace platinum is a significant challenge and huge demand in the community.[297]

Recently, several research works have been focused on the development of cost-effective platinum-free CEs. A plethora of different materials were explored such as carbon-based materials,[298] conducting polymers,[274,299] metal chalcogenides and oxides,[122,300,301] nitrides[302] and metal/carbon composites.[303] Among them, hereafter we focus on carbonaceous materials, metal-based compounds and composites since they are the most effective in terms of both sustainability and scalability. We decided not to discuss polymeric films because despite their good catalytic activity, they usually require rather time- and energy-demanding synthetic procedures and the employment of toxic solvents that increases the CED and lowers the sustainability of the corresponding devices.[304] The most sustainable approaches to obtain efficient CEs are briefly described. It is worth mentioning that a 100% green and sustainable approach is actually unpractical or at least has not been discovered, to the best of our knowledge. Therefore, we referred to papers aiming at reducing the environmental impact in terms of CE production, which avoid the use of CRMs, hazardous solvents or chemicals and harsh procedures, while concurrently demonstrating PCE values close or even higher than that recorded with standard platinum-based reference devices. Furthermore, due to the large number of reports on this topic, we specifically focus on the most recent (*i.e.* last year) papers. Indeed, the purpose of this chapter is to evidence some useful approaches towards sustainable, futuristic cathode materials for DSSCs rather than just give a simple comprehensive overview. It should be noted that a definite verdict on the sustainability of a specific material can be drawn just after a specific LCA.

2.3.1 Carbon-based CEs. Among the different carbonaceous materials,[305,306] graphite was firstly investigated mainly due to its large availability. However, natural graphite has been evaluated as a critical material since 2011 by the EU.[99] This criticality assessment is based on its economic importance, supply risk and proven and readily available substitutes (both from a cost and performance perspective). Graphite is critical especially due to its low substitution potential in refractories, in particular for steel production, and for its large commercial use as an Li-ion battery anode. However, graphite is claimed as a "green" material because of its simple, time/energy saving deposition procedure even under ambient conditions. Pristine graphite shows high electronic conductivity, but its catalytic ability toward triiodide reduction is quite poor. This is mainly ascribable to its limited surface area (*i.e.*, few catalytic sites) and slow electron transfer on the *z*-axis, which results from its intrinsic plane-to-plane structure.[307,308] In contrast, owing to their high surface area-to-volume ratio and stability, the use of both carbon black[309,310] and carbon nanotubes[311] is very promising to obtain excellent performances. Unfortunately, the synthesis of carbon black usually involves operation at very

high temperatures,[312,313] and high surface area CNTs are obtained using rather expensive and harsh templates.[314,315]

It is worth mentioning that even though the eco-friendliness of carbonaceous materials is widely accepted, their sustainability is tightly linked to both the source of their precursors and manufacturing approach, which should be considered in green metrics analyses.[316] Accordingly, the use of harsh solvents and the production of carbon dioxide should be minimized. Moreover, the existing carbon-based CEs still demonstrate unsatisfactory features/performances, and overall, provide lower electrocatalytic activity compared to the standard platinum electrode when classical redox couples are employed. Consequently, further material design and innovation are required to boost the intrinsic electrocatalytic activity of carbonaceous materials. Moreover, it is worth noting that the use of platinum-free CEs is not always cost-effective and environmentally friendly. Sometimes, indeed, the impact of the production process of tailored materials is observed to even exceed that with the use of bare platinum. Thus, to reduce the environmental impact, a valuable approach is to use bio-derived waste as carbon sources and reduce the number of production steps, leading to a lower CED. Recently, different biomass/bio-waste, including coffee waste,[317] corn straw,[318] leaves,[319] mangosteel peels,[177] potato peels and waste residues,[320] were exploited and transformed into biochar for application as CEs.

Very recently, Di and co-workers showed a carbon-based matrix obtained through the pyrolysis of humic acid at high temperature and under an inert atmosphere (Fig. 8a).[321] The precursor was a sub-product of the microbial biodegradation of organic biomass. Even though the process was relatively time consuming (1 day) and required a high pyrolysis temperature (*i.e.*, 900 °C), the use of a secondary raw material made this approach more environmentally sustainable from a circular economy viewpoint compared to that using virgin materials. The electrocatalytic properties (toward the triiodide reduction) of the newly synthesised material were lower than that of platinum. Nonetheless, by cell testing the authors recorded a remarkable PCE of 6.14%, which is only slightly lower than that of the platinum-based reference cell (7.1%), likely because of the lower current density of the carbonaceous matrix (Table 4, entry 1), and suggested improvements include functionalisation with cheap metal atoms (*i.e.*, nickel). The use of waste derived from fruits and vegetables to produce

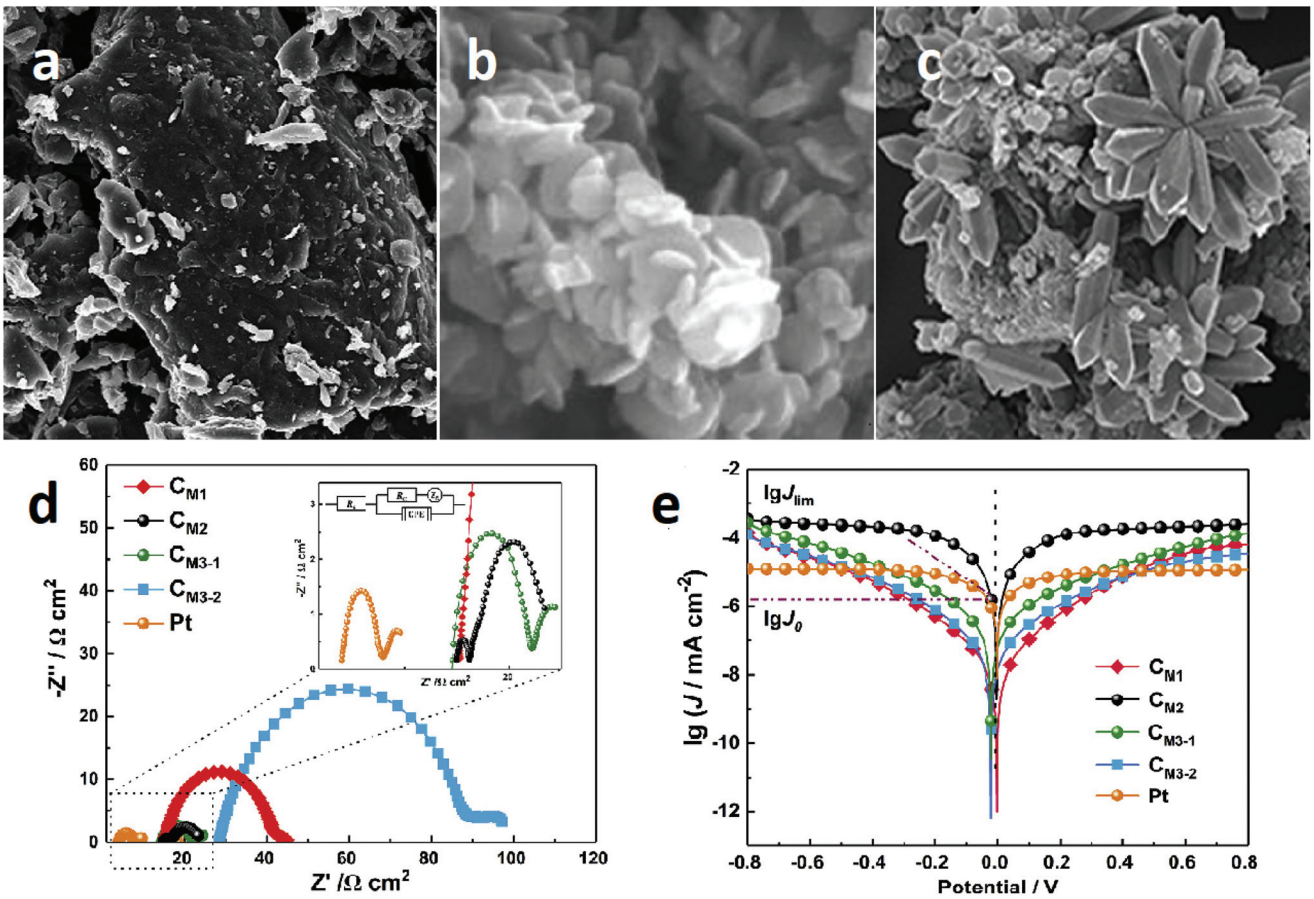

Fig. 8 SEM images of different carbon-based nanostructures derived from waste materials: (a) humic acid (adapted from ref. 321), (b) orange peels (adapted from ref. 322), and (c) pomelo peels (adapted from ref. 323). Electrochemical impedance spectroscopy (EIS, (d)) and Tafel polarization curve (e) of pomelo peel-derived CEs made by different synthetic routes (adapted from ref. 323).

Table 4 Summary of the various materials implemented as the most sustainable CEs in DSSCs

Class	Material	Pros	Issues	PCE *vs.* platinum	Entry[ref.]
Carbonaceous	Humic acid	• Sub-product of biodegradation	• 1 day reaction • High temperature	−13%	1[321]
	Orange fiber	• Waste-derived	• Use of cobalt	n.a.	2[322]
	Pomelo peels	• Waste-derived • CRM-free	• High temperature	Slightly better	3[323]
	2-Methyl-8-hydroxy quinolinol	• Cheap source • CRM-free	• Very high temperature • CO_2 emission • Binders	−27%	4[324]
	Silicon rubber	• Textile-based • Low temperature	• Poor PCE	Very low	5[325]
TM compounds	Co_3S_4/MoS_2	• Low temperature • (Amorphous)	• Use of DMF • Use of cobalt • Argon atmosphere	Slightly better	6[328]
	MoS_2	• Low temperature • Bifacial device • No sintering	• Not relevant	Slightly lower	7[329]
	CoS	• Direct growth • Low temperature • No sintering	• Use of cobalt • 1 day reaction	−11%	8[334]
	Ni/ZnS	• Direct growth • Low temperature • No sintering	• 1 day reaction • Slow I_3^- regeneration	Extremely lower	9[290]
	FeS	• CRM-free • Moderate temperature	• Moderate PCE	Slightly lower	10[336]
	FeS@C	• CRM-free • Glucose as carbon source	• Very high temperature • Long reaction • Argon atmosphere	Slightly better	11[336]
	$NiMoS_4$	• Cheap sources • Low temperature • Water-based	• Use of thiourea	Slightly better	12[338]
	TiS_2	• Direct growth	• High voltage • Use of NH_4F • Sulfidation step	Comparable	13[339]
	NiSe	• Direct growth • Electrodeposition • Water-based	• Use of thiourea	+20%	14[345]
	SnSe	• Direct growth • CRM-free	• High temperature • Argon atmosphere	Extremely lower	15[347]
	Cu/FeSe	• Direct growth • Scalable	• Complex • N_2 atmosphere • Use of oleylamine	Slightly better	16[348]
	VSe_2	• CRMs-free • Low temperature • (Crystalline) • Water-based	• CO_2 emission	+10%	17[340]
	Cu_2O	• CRMs-free • Simple approach	• Low PCE	Lower	18[341]
	$La_{0.7}Ca_{0.3}MnO_3$	• CRM-free	• Use of lanthanum • Use of EDTA • High temperature	Lower	19[342]
	$FeTa_2O_6$	• CRM-free • Moderate temperature	• Low surface area	Lower	20[343]
	$FeTa_2O_6$@C	• CRMs-free • Carbon from waste • Moderate temperature	• Not relevant	Slightly better	21[350]
Composites	MoS_2/rGO	• Low temperature • Hydrogen as reductant • CRM-free	• Long time • Use of DMF	Slightly lower	22[355]
	Ni_3S_4@carbon	• CRM-free • Water-based • Carbon from glucose	• Nitrogen atmosphere	Comparable	23[357]
	Ni_3S_4@carbon/CNFs	• CRM-free • Water-based	• Nitrogen atmosphere • Unknown source of CNFs	Higher	24[357]
	CuS/graphene	• Low temperature • Short time • CRM-free	• Unknown source of graphene	Comparable	25[361]
	Ni/CoP_x@CNTs	• Low temperature • Green precursor	• Use of cobalt • Long time • Unknown source of CNTs	Higher	26[360]

valuable CE materials has been recently investigated. Balanay *et al.*[322] exploited orange peels (Fig. 8b) as starting materials to obtain carbonaceous CEs after grinding with $Co(NO_3)_2$ and following heat treatment at 200/300 °C. The higher the sintering temperature, the better the catalytic performances of the CEs (Table 4, entry 2), even though the slight amelioration did not justify the increase in energy consumption. In a similar approach, Yun and co-workers reported on the employment of pomelo peels as a raw material (Fig. 8c).[323] After washing with water to remove impurities and grinding to finely pulverise the precursor, the authors proposed three different methods to obtain bio-derived carbonaceous films with controllable morphologies. The first method simply consists of a chemical degradation process (to disrupt the macromolecular structure of pomelo peels) followed by microwave pyrolysis (500 W, 6 min), but the as-obtained powders showed an insufficient Brunauer–Emmett–Teller (BET) specific surface area. To better control the morphologies and the surface area of the powder, the authors tested the effect of two consecutive carbonization processes (at 500 °C and 800 °C). From a sustainability viewpoint, the enhancement of the catalytic properties of the materials after pyrolysis was negatively counterbalanced by the higher energy consumption. In the third approach, aiming at reducing both the energy consumption and the use of chemicals, the macromolecular structure was hydrothermally disrupted by avoiding the use of H_3PO_4 and the annealing process was limited to a single step at 500 °C for 2 h. The latter method proved to be the best trade-off between good catalytic activity and improved sustainability. For the final production of the CE (Table 4, entry 3), the powder (dispersed in isopropanol) was sprayed onto FTO and annealed at 400 °C for 30 min.

As already mentioned, the use of carbonaceous materials as CEs in DSSCs has been reported and investigated worldwide, but the sole use of carbon is not sufficient for the resulting CE to be considered truly "sustainable". Indeed, various factors should be considered as follows: (i) the carbonaceous material under use should preferably come from waste or low-cost precursor; (ii) the energy demand and the CO_2 emissions should be minimized during the carbonization process; and (iii) the final material should exhibit good catalytic properties. To exemplify this concept, it is worth reporting the approach by Kumar *et al.*,[324] who carbonized the commercial 2-methyl-8-hydroxy quinolinol under an inert argon atmosphere. The starting material is relatively cheap ($30 per 100 g), but the process required a very high temperature (1200 °C) and it produced more than 4 eq. of carbon dioxide. Moreover, the carbonaceous powder could not be directly deposited onto FTO, which required pre-dispersion in polyvinylpyrrolidone (PVP) followed by doctor-blading. The use of PVP binder forced to an additional sintering step (450 °C, 1 h), leading to a lower PCE compared to the Pt-based device (Table 4, entry 4). This is a clear example of the production of a green, CRM-free material that is hardly sustainable in our opinion, and clearly, it should be evaluated after thorough LCA.

As already discussed early in this section, we decided not to tackle polymer-based CEs due to their barely sustainable synthetic procedures and their poor solubility, which prevents the production of CEs through solution processing. However, compared to both carbonaceous materials and transition metal compounds, polymers are elastic, and thus readily exploitable in flexible and wearable electronics. Accordingly, among the plethora of works on this topic, one example of a truly innovative and sustainable approach, which is the specific aim of this review, is that recently proposed by the Ehrmann's group.[325] They coated a conductive liquid silicone rubber (Powersil® 466 A/B) layer based on polydimethylsiloxane filled with carbon black and graphite on a viscose cotton woven fabric, which was employed as a CE in lab-scale DSSCs after being sintered at 200 °C. Even though the PCE value was found to be rather low (Table 4, entry 5), this work can be effectively considered as the first interesting step toward the development of sustainable textile-based DSSCs.

2.3.2 Transition metal-based CEs. The green characteristics of carbonaceous materials are somehow outshined by their issues in terms of instability towards corrosive iodine-based electrolyte.[326] Consequently, different classes of materials have been exploited as alternative, efficient CEs in DSSCs.[306] Among them, transition metal-based compounds represent the best trade-off between long-term stability, environmental impact and sustainability, resulting in good catalytic activity toward the most commonly employed redox couple, remarkable chemical inertness and good electronic properties.

Among the transition-metal compounds, MoS_2 and more broadly sulphides[290] can be considered the most viable option to replace platinum due to their abundance, low cost and comparable electrocatalytic behaviour. Vikraman *et al.* described a chemical bath method to deposit MoS_2 directly onto FTO-coated glass.[327] However, the performances of the obtained device were strongly dependent on the film deposition time, which was layer grown for less than 20 min and unable to support the current powered by the photoanode, resulting in a very low FF. To enhance the PCE of pure MoS_2, a mixed cobalt/molybdenum sulphur composite was used. Qian *et al.* recently reported on the synthesis of pure MoS_2 and Co_3S_4/MoS_2 nanocubes (Fig. 9a) *via* hydrothermal route (200 °C for 18 h) in an autoclave.[328] They obtained PCE values similar or even better (mixed sulphur) than that of platinum-based devices (Table 4, entry 6) and EIS evidenced a slightly lower charge transfer resistance at the CE/electrolyte interface. Unfortunately, this approach cannot be classified as "green" since it used DMF as the solvent. Moreover, due to requirements in terms of material crystallinity, a further annealing step (350 °C for 1 h under an argon atmosphere) was added, which sensibly increased the overall energy demand of the whole process, thus lowering its sustainability. The (even partial) replacement of molybdenum with cobalt is somehow critical.[87] Unfortunately, the chemical approach for the preparation of the CEs affects the sustainability on a large-scale and also leads to extremely thick substrates, thus affecting the transparency of DSSCs. Accordingly, to overcome these two issues in a

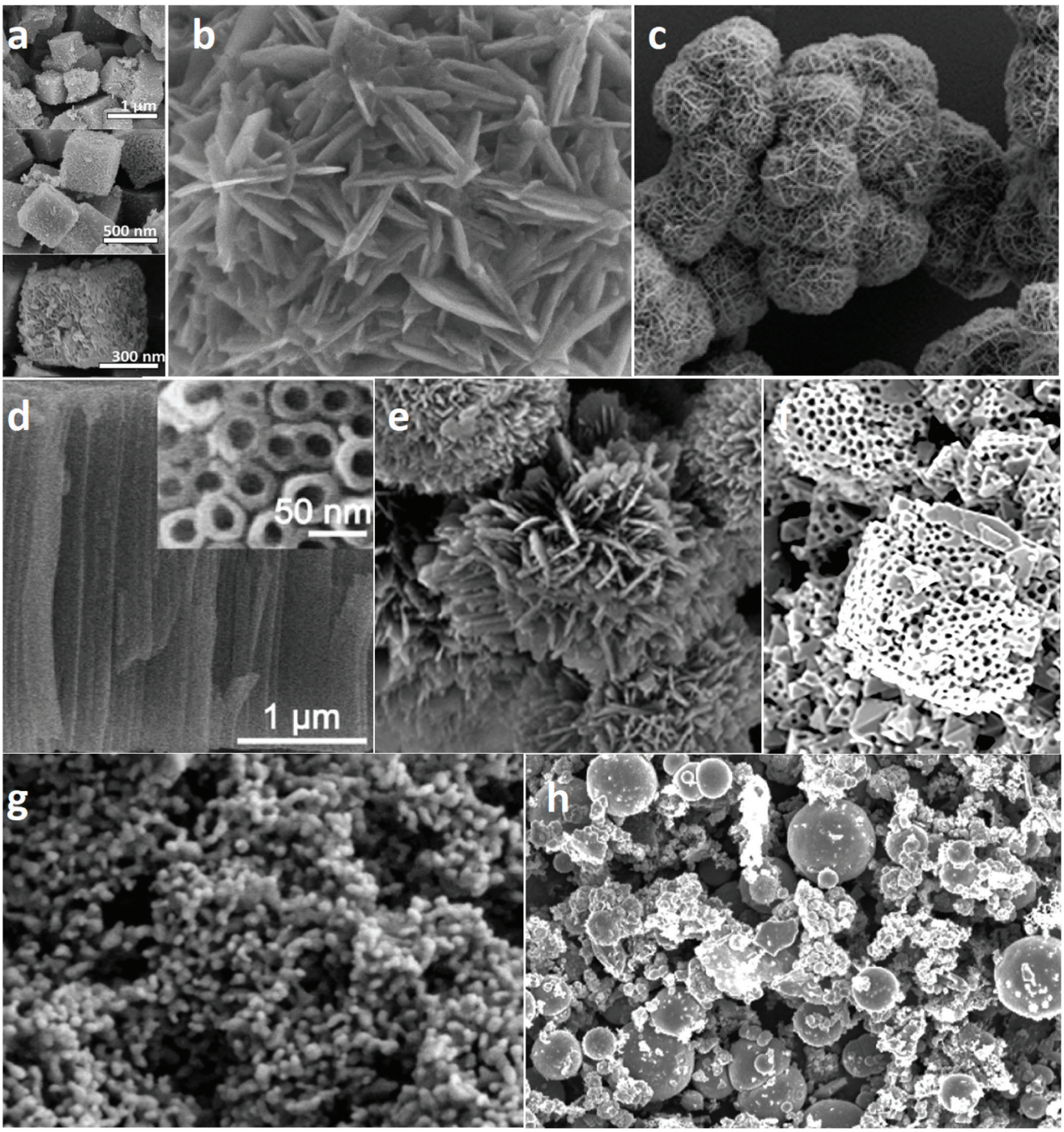

Fig. 9 Transition-metal based nano- and microstructures of: (a) Co_3S_4/MoS_2 nanocubes (adapted from ref. 328), (b) CoS nanoflakes (adapted from ref. 334), (c) Cu_7S_4/CuS nano-hollows (adapted from ref. 337), (d) TiS_2 nanorods (adapted from ref. 339), (e) VSe_2 nanoflakes (adapted from ref. 340), (f) Cu_2O nanosponges (adapted from ref. 341), (g) $La_{0.7}Ca_{0.3}MnO_3$ nanospheres (adapted from ref. 342) and (h) $CuTa_{10}O_{26}$ nanoplates (adapted from ref. 343).

single stage, Jeong and co-workers reported an innovative approach involving low-temperature (below 100 °C) atomic layer deposition of nanometric films to be employed in bifacial devices.[329] The as-obtained films did not require any sintering step, which greatly reduced the total energy consumption for the production of CEs. Remarkably, this material also showed PCE values almost comparable (−8%) to that of the control cells (Table 4, entry 7) due to its relatively high J_{lim} and low R_{CT} (Fig. 10a). On the other hand, CoS nanostructures can be produced *via* simple and cost-effective procedures, with a reduced number of synthetic steps.[330–333] Accordingly, Ashok Kumar *et al.* presented hierarchical CoS structures (Fig. 9b)

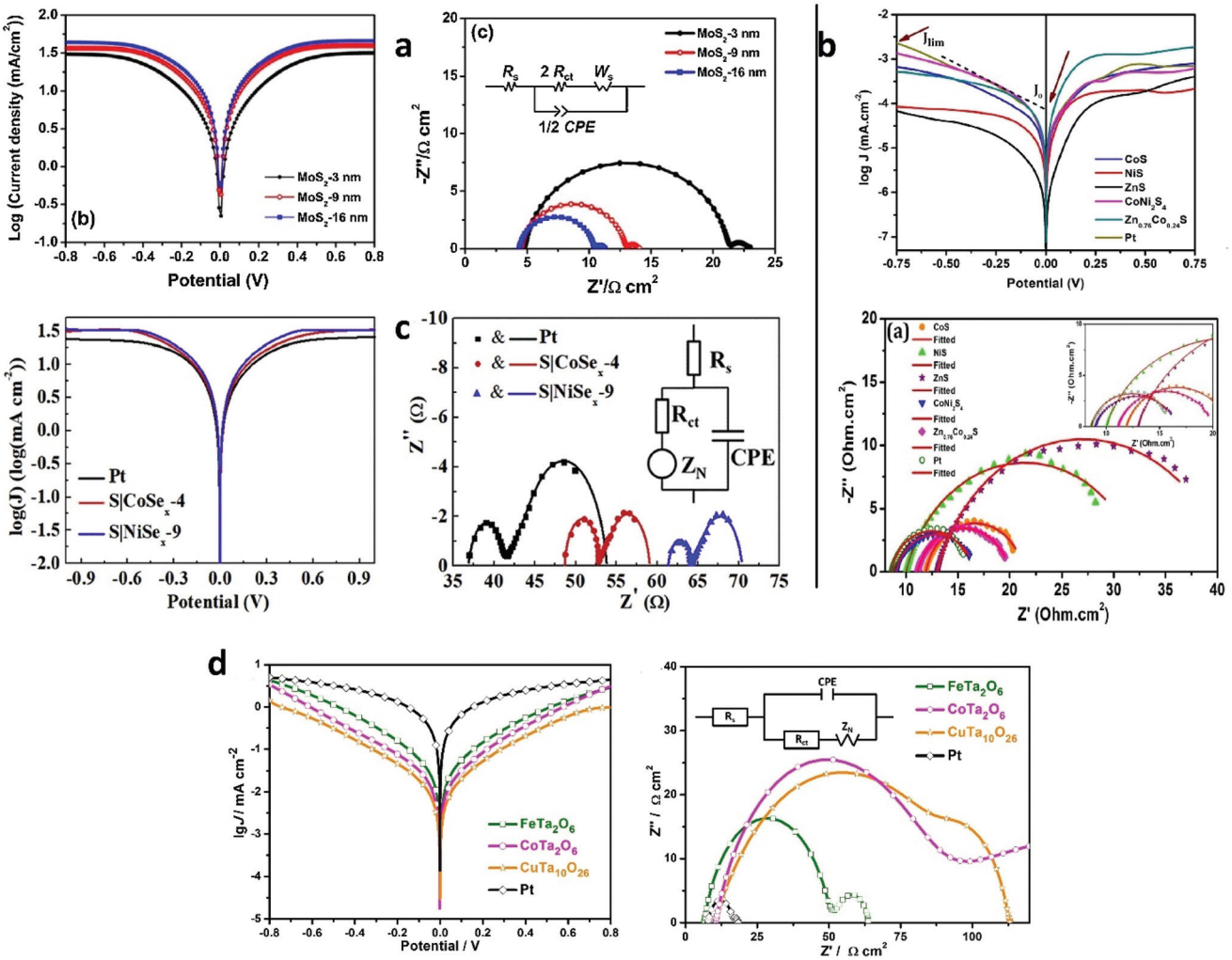

Fig. 10 EIS and Tafel polarization curves of (a) MoS_2 (adapted from ref. 329), (b) different TM sulphides (adapted from ref. 290), (c) cobalt and nickel selenides (adapted from ref. 345) and (d) tantalum-based compounds (adapted from ref. 343).

directly grown on an FTO substrate *via* the hydrothermal method,[334] in which they mixed the reactants (*i.e.*, $CoCl_2$ and thiourea) on the top of an FTO substrate inside a sealed autoclave. The layout was heated at 180 °C for 24 h, thus concurrently growing CoS structures that were tightly anchored onto the conducting film support, avoiding any further deposition step. Then, they tested a similar approach to synthesize a plethora of binary and ternary sulphides, including cobalt, nickel and/or zinc (Table 4, entries 8 and 9).[290] The best results were obtained with the cobalt-containing ternary mixtures, whereas the cobalt-free electrodes mainly suffered from a slow triiodide regeneration reaction, which minimized the current density output (Fig. 10b). To completely avoid the use of CRMs, Park and co-workers focused on the synthesis of crystalline pyrite (*i.e.*, FeS) nanoparticles *via* hot-injection moulding,[335] which required a moderate operating temperature of about 200 °C.[336] FeS nanoparticles were then spin-coated onto FTO glass and used as CEs, giving slightly lower PCEs compared to that of the platinum-based CEs (Table 4, entries 10 and 11). To further improve the efficiency of the newly developed CEs, nanoparticles were supported on amorphous carbon. However, even though the glucose carbon source can be considered "green", the supplementary synthetic procedure was time and energy consuming (high temperature needed) and required a completely inert atmosphere, which actually invalidated the overall sustainability of this approach.

To completely avoid the use of CoS, Li *et al.*[337] focused on the hydrothermal synthesis of Cu_7S_4/CuS nano-hollows (Fig. 9c), which mimicked the behaviour of platinum. The authors reported the complete synthetic approach starting from a copper salt and the use of cheap and less hazardous precursors (*i.e.*, $Cu(NO_3)_2$, NaOH, ascorbic acid, and ethylene glycol) to obtain Cu_2O, avoiding the use of organic solvents; this low-temperature solvothermal synthesis (using Na_2S as the sulphur source) leads to good PCE values in lab-scale devices. These conditions accounted for the true sustainability of this proposed approach, even though it was not definitely confirmed by LCA. Furthermore, when supported on GO, it

showed lower charge transfer resistance and higher limiting current density compared to that of Pt. Yang and Chen[338] employed a low cost and scalable hydrothermal approach to synthesize $NiMoS_4$ compounds using cheap, abundant and very safe reactants (*i.e.*, nickel acetate, sodium molybdate and thiourea as nickel, molybdenum and sulphur sources, respectively) using deionized water as the solvent and relatively low temperature for heat treatment (200 °C for 12 h). Once thoroughly washed and dried, an ethanol solution of the corresponding compound was spin-coated onto FTO glass and then dried at 140 °C. This approach confirms the possibility of obtaining resistant, cheap and catalytically active materials even at relatively low temperatures, effectively avoiding the use of organic solvents (Table 4, entry 12).

Titanium is an abundant and relatively cheap material, and thus usually employed in photoconversion devices. Schmuki and co-workers reported the use of TiS_2 as an efficient alternative to platinum.[339] A titanium thin layer (1 μm) was directly evaporated onto FTO glass and then anodized at room temperature in an EG : H_2O solution of NH_4F (60 V for 10 min; EG = ethylene glycol). The as-obtained titanium oxide layer was thermally converted to the anatase phase (450 °C for 1 h), which showed very poor electrocatalytic properties. A further sulfidation step was then required, which was performed in a quartz tube under an H_2S flow (500 °C). The process took 2 h for completion, and the resulting TiS_2@FTO showed catalytic activity comparable to that of platinum (Fig. 9d, Table 4, entry 13). If we just consider the final material, this approach can be surely classified as green; however, the use of fluorinated compounds, high voltage and a sizeable amount of H_2S does not allow it to be considered truly sustainable.

One of the paradigms of sustainability is to reduce the amount of energy required for the production of materials, especially without a massive transition to renewables. Consider this, it can be very useful to avoid high temperature post-treatments, which are usually required to obtain crystalline materials. Lee and co-workers reported the direct solvothermal growth of CoS nanostructures onto FTO using aniline as the template, ethanol as the solvent and $Co(NO_3)_2$ as the cobalt precursor. The reactants were mixed in an autoclave containing clean FTO slides, and then thiourea was added as the sulphur source and the sealed vessel was heated at 200 °C for 12 h. The as-obtained films were directly employed as CEs, leading to similar results compared to that of the control devices.

Selenium can be effectively used in place of sulphur in binary transition metal compounds due to its similar electronic structure and reactivity.[344] Among the different production methods to directly deposit catalytic films onto the TCO substrate, Jiang and his group[345] focused their efforts on the use of electrodeposition, which is a relatively cheap method that completely avoids the use of harsh solvents and/or toxic materials. Here, thiourea, selenium oxide and nickel chloride in water were used as the sulphur, selenium and nickel sources, respectively. The as-obtained CEs showed outstanding catalytic properties, leading to a PCE of 7.54% (20% higher than that of the control device, Table 4, entry 14) due to an increased J_{SC} and lower charge-transfer resistance, as proven by both the *J–V* and EIS analyses (Fig. 10c). Due to the relatively high PCE coupled with easy and cheap synthetic path, these NiSe CEs can be considered cost-effective. A similar approach was recently exploited by Ahn and co-workers to deposit $CoSe_2$ films.[346] However, compared to previous work, notwithstanding the promising PCE, the use of cobalt in place of nickel reduces the sustainability of this route.

The green features of selenium-based materials are undisputed, especially when coupled to inexpensive, abundant and hazardless cations, such as tin. However, their sustainability is still under debate. As an example, Kishore Kumar and co-workers[347] deposited SnSe films *via* manual screen-printing onto FTO glass and annealed them in an inert atmosphere at 900 °C similar to platinum-CEs (Table 4, entry 15). Even though avoiding the use of platinum looks like a great improvement in terms of sustainability of the devices, the production of SnSe is far from sustainable since the reaction is carried out in a quartz tube at 900 °C for 24 h (relatively high CED). Actually, the use of an extreme temperature seriously increases the energy consumption of the overall process, undermining the sustainability of these SnSe films.

The *in situ* hydrothermal growth method surely provides a feasible, even if hardly scalable, approach for the fabrication of MSe_x films, which have good adhesion to FTO glass. Recently, Chen *et al.*[348] reported an economic and scalable hot-injection approach to produce copper/iron mixed selenide nanocubes (Table 4, entry 16). The acetylacetonate precursor salts of both metals were mixed in oleylamine and heated at 150 °C under a controlled nitrogen atmosphere to avoid oxidation. Then, a selenium precursor solution was added, and the temperature was increased to 250 °C. The excess oleylamine was removed by ion exchange reaction and the surfactant-free $CuFeS_2$ nanocubes were drop-casted onto FTO glass and dried at 60 °C. In our opinion, the only drawback of this approach is the replacement of water (a green solvent) with oleylamine, which is still questionable in terms of environmental impact. The as-obtained film demonstrated lower charge transfer resistance and comparable limiting current density compared to that of platinum, leading to almost identical PCE values.

An innovative approach was recently proposed by Ho and co-workers[340] based on the use of VSe_2 as an electrocatalytic material. Indeed, both vanadium and selenium and the resulting VSe_2 are not CRMs; moreover, the synthetic procedure is relatively easy, and it does not require very high temperature (*i.e.* 220 °C) or even hazardous reactants or solvent. Notably, crystalline materials were obtained without any treatment at high temperature (Fig. 9e). The only drawback of this approach is the high 13 : 1 ratio of moles of CO_2 per mole of VSe_2 produced, starting from SeO_2, V_2O_5 and $C_2H_2O_4{\cdot}2H_2O$ precursors dissolved in deionized water (Table 4, entry 17). Therefore, alternative routes should be investigated with the aim to reduce the amount of produced carbon dioxide without undermining the good catalytic properties of the material.

Compared to both selenides and sulphides, oxides are more stable and cheaper CEs to produce. Interestingly, Miclau and co-workers proposed a "full-copper" device, where Cu_2O was used as both the photocathode and CE,[341] in which some metallic copper nanoparticles (Fig. 9f) were dispersed to enhance the catalytic activity toward the reduction of the redox shuttle. The authors simply employed copper acetate as the starting material and the synthesis was conducted in an autoclave (180 °C for 24 h). Since both electrodes were fabricated using a p-type semiconductor, their PCE was relatively low (Table 4, entry 18), but the simple and inexpensive synthetic route made this approach appealing in terms of sustainability of the final device. Alami and co-workers[349] attempted complementary approaches to obtain Cu_xO@Cu films. Among them, electrodeposition required the use of a strong oxidizing acid (*i.e.*, H_2SO_4), but a very short deposition time of 15 min. The chemical bath approach led to a mixed oxide/hydroxide, thus limiting the scalability of the procedure; however, the very low sintering temperature (60 °C) sensibly reduced the overall energy consumption. Finally, they carried out chemical ageing (an ammonia-based water solution) for 24 h followed by baking at 250 °C for 2 h. It should be noted that even if the obtained PCE of the control device was very low mainly because of the non-optimized photoanode, the Cu-based device suffered from a lower FF compared to that of Pt, which can be ascribed to the poor charge transfer at the electrolyte/CE interface.

Li, Jin and co-workers presented a ternary oxide (*i.e.*, $La_{0.7}Ca_{0.3}MnO_3$ with a perovskite structure, (Fig. 9g) as a CE in DSSCs, approaching the PCE of the platinum-based device (Table 4, entry 19).[342] They claimed that their material was inexpensive, but the use of lanthanum, a rare-earth element, ethylenediaminetetraacetic acid (EDTA) as the coordinating molecule and the high (900 °C) calcination temperature seriously affected the sustainability of the proposed approach. Yun *et al.* recently explored the use of tantalum-based bimetallic oxides.[343] They mixed $TaCl_5$ (tantalum precursor) with a nitrate secondary metal precursor (*i.e.*, iron, cobalt and copper) in an ethanol solution, which was hydrothermally treated at 200 °C for 18 h in an autoclave. The as-obtained precipitate was then annealed under nitrogen at 800 °C for 3 h to obtain the corresponding oxides, $FeTa_2O_6$, $CoTa_2O_6$ and $CuTa_{10}O_{26}$, respectively (Fig. 9h, Table 4, entry 20). The latter showed lower catalytic activity compared to the Pt-based CEs, as proved by the electrochemical characterization (Fig. 10d). To improve their photocatalytic properties without significantly impairing the green characteristics of the approach, the oxides were supported on a carbon matrix, which was obtained from bio-sourced aloe peel waste (Table 4, entry 21).[350] Both the pristine and the carbon-based powders were simply dispersed in isopropanol and sprayed onto a heated FTO substrate and annealed at 400 °C (at least 100 °C lower than the annealing temperature for platinum-based CEs). The best efficiency was provided by the iron-modified supported oxide, which outperformed the reference device, thus resulting in a "green" and rather sustainable alternative to platinum.

2.3.3 Composite CEs. The use of composite materials is a valuable approach to concurrently exploit the positive characteristics of different materials.[351] However, as it is known, the complexity of a material negatively affects its recyclability.[352–354] In the field of DSSCs, this seminal approach was reported by Pang and co-workers,[355] who coupled the robustness and eco-friendly features of MoS_2 with the electronic properties of reduced graphene oxide (rGO), where the composite electrode achieved a PCE of 6.7% compared to that of 0.74% and 3.18% for bare MoS_2 and rGO, respectively (Table 4, entry 22). Notwithstanding the better performance compared to the Pt-device, the proposed materials suffered from relatively high series resistance (as proven by EIS), which is a warning signal of the stable adhesion of the film on the FTO substrate. With regards to the synthetic approach, an MoS_2/GO film was hydrothermally synthesized (200 °C for 12 h) starting from a DMF/water solution of GO, Na_2MoO_4 and L-cysteine. The resulting material was then deposited onto FTO through blade-coating (Fig. 11a). A meaningful step toward sustainability involved the use of a hydrogen flux (under moderate vacuum) to reduce GO to rGO, thus completely avoiding hazardous chemical reductants.

The synthesis of composites is usually complicated, often requiring a number of different steps and high temperatures, thus negatively impacting the CED. Hydrothermal synthesis is amongst the least impactful methods due to the small amount of solvent required, good control of the characteristics of the final material structural/morphological and the relatively low energy demand. Metal sulphides usually show high catalytic performances, but poor conductivity and structural instability.[356] Thus, to overcome these issues, they are coupled with carbonaceous materials such as CNTs or graphene, which greatly enhance the overall conductivity of the resulting composite. Li *et al.* exploited a mixture of $Ni(NO_3)_2$, glucose, urea and cysteine to obtain carbon-supported Ni_3S_4 composites, which showed catalytic features comparable to that of Pt (Table 4, entry 23).[357] The synthetic procedure can be considered as a further improvement towards more sustainable DSSCs, even though the autoclave reaction (180 °C, 20 h), and mainly the following sintering at 500 °C under nitrogen somehow impair the green features of this approach. These authors also reported the use of Ni_3S_4@C/CNTs CEs (Fig. 11b), which outperformed the control device. This is mainly ascribed to the increase in both FF and J_{SC} due to the combination of the electrochemical features of sulphur and carbon-based materials. Nonetheless, the claim for the real sustainability of this second approach should be verified after further details on the production of CNTs are provided.

Some very interesting results were reported by Oh and co-workers, who employed a perovskite-based material slightly doped with GO as a very effective CE (Table 4, entries 24 and 25).[358] The best device (4% GO doping) achieved a remarkably high PCE (*i.e.*, 12.5%) even though the authors did not report the value of the reference platinum-based device. It is worth mentioning that GO sheets were synthetized *via* the Hummers' method, which cannot be considered green since it involves

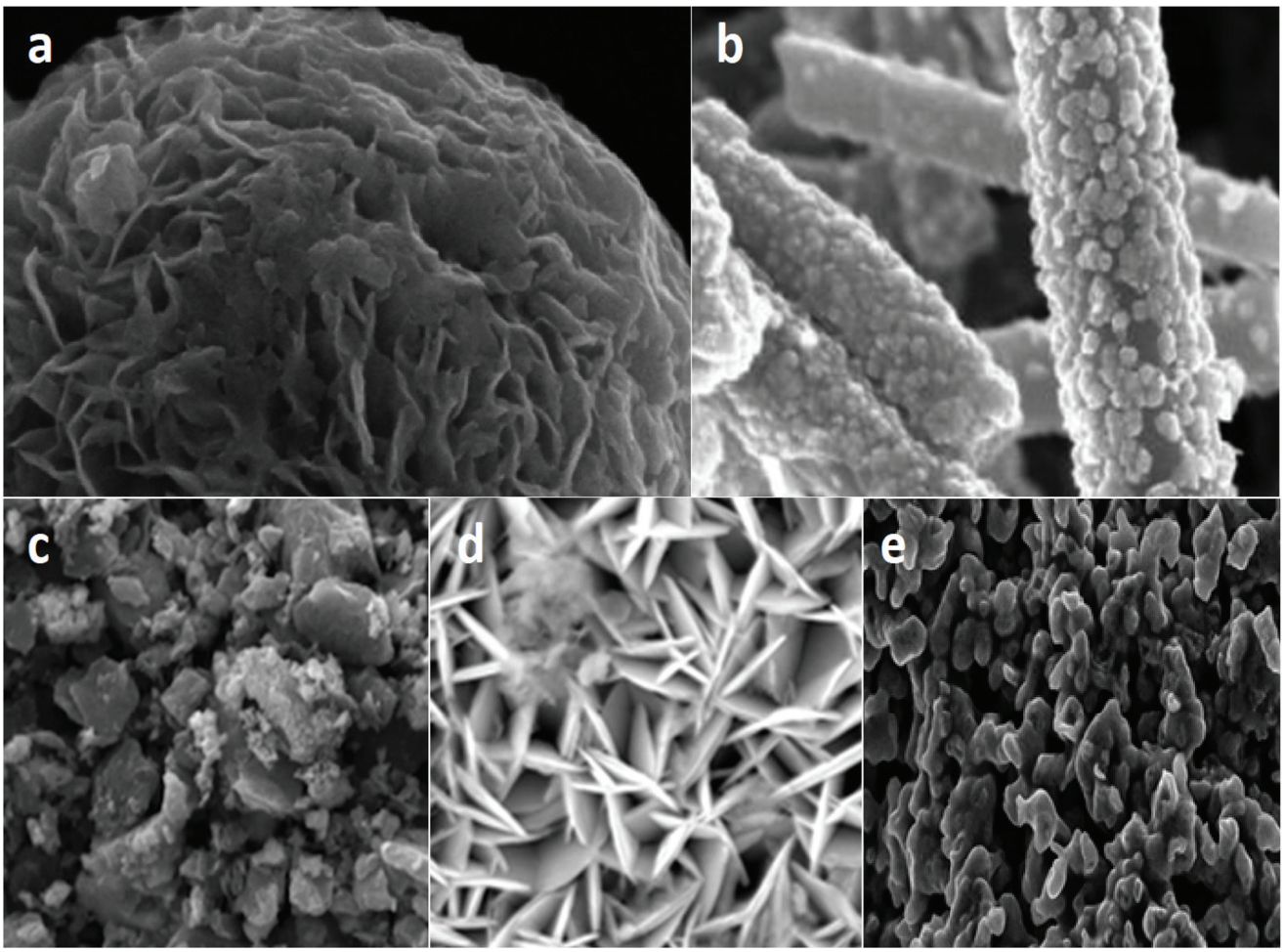

Fig. 11 Nanostructures of composite materials: (a) MoS_2@rGO nanoflakes (adapted from ref. 355), (b) Ni_3S_4 nanospheres supported on carbon nanotubes (adapted from ref. 357), (c) graphene-$La_2CdSnTiO_4$-WSe_2 nanopyramids (adapted from ref. 358), (d) hierarchical NiO@NiS@G nanocomposites (adapted from ref. 359) and (e) Ni/CoP_x@CNTs nanostructures (adapted from ref. 360).

the use of concentrated H_2SO_4, $KMnO_4$, H_2O_2. On the other hand, the relatively small amount of GO used, also coupled with the extremely good performance obtained, counterbalances the rather hazardous approach. Graphene-$La_2CdSnTiO_4$-WSe_2 (G-LCT-W) hybrids (Fig. 11c) were prepared *via* the hydrothermal method by mixing LCT, graphene and WSe_2, followed by heating at 150 °C for 15 h. The precipitate was washed and dried several times, and then dispersed in ethanol to obtain a slurry, which was finally deposited on FTO trough doctor-blading at room temperature.

Rosei *et al.* presented a CuS/graphene composite, which showed catalytic activity comparable to that of platinum (5.73% *vs.* 5.78%, Table 4, entry 25).[361] The most valuable point of this approach is the relatively low sintering temperature required (100 °C for 15 min), even though a complete LCA study is required. Indeed, even if the CuS precursors (*i.e.*, thioacetamide and copper nitrate trihydrate) were actually "green", the authors did not give any useful information about the synthesis of graphene. However, if it was produced *via* a sustainable approach, undoubtedly this work has to be considered as a meaningful milestone in the achievement of 100% green and sustainable CEs. Very recently, Silambarasan and co-workers[359] reported the synthesis of hierarchical NiO@NiS@G nanocomposites (Fig. 11d) coupling the electrochemical ability of cheap NiO with the electronic properties of graphene, thus leading to the fabrication of a more cost-effective and CRM-free CEs, having similar efficiency values compared to that of the platinum-based device.

An innovative composite was recently proposed by Feng and co-workers[360] as an effective CE (Table 4, entry 26), where nickel–cobalt phosphide supported on CNTs (Fig. 11e) was obtained using cheap and green reactants and a sustainable synthetic hydrothermal approach. Specifically, nickel and cobalt oxalates were dissolved in deionized water and added dropwise to a basic solution of CNTs, which was then heated at 100 °C for 24 h in an autoclave. The nickel/cobalt mixed hydroxide@CNT precipitate was obtained *via* a phosphorylation process using NaH_2PO_2, and then heat-treated at 300 °C for 2 h. The performance of the NiO@NiS-based device was partially jeopardized by its lower FF, which can be ascribed to

the adsorption phenomena of both triiodide and iodide anions onto the NiO surface.[362] However, even though the proposed approach avoids the use of critical materials and/or procedures (only cobalt-based issue remains), the sustainability of this approach is not clear because of the lack of information on the precursors and the process for the production of CNTs. If their renewable origin is confirmed, this approach has to be included in the sustainable ways to obtain effective CEs that outperform platinum-based CEs.

2.3.4 Final remarks on CEs. Throughout this section, we discussed some feasible approaches to design and implement environment-friendly, green and sustainable DSSC CEs, some of which are also shown in Fig. 12. The most interesting and valuable ones were summarized, mainly focusing on the type of approach and related sustainability than on the bare PCE, which is nonetheless a meaningful output considering practical application. Considering the plethora of approaches and materials analysed, it is quite difficult to outline a homogenous and straightforward path, and only some general considerations can be drawn.

True understanding of which is the most sustainable CE material is questionable since LCA studies are rarely performed. As the best practice: (i) the use of cobalt should be minimized as much as possible, and most likely completely avoided; (ii) transition-metal based materials should be preferred over carbonaceous ones in terms of better stability, even though the latter are more convenient if "waste-sourced"; (iii) oxides should be preferred over selenides and sulphides because of the reduced number of additional synthetic steps (*i.e.*, selenization or sulfidation); and (iv) composites show the most promising prospects, particularly if the synthetic procedures will be substantially improved in the coming future. All these suggestions should be coupled with a thoughtful choice of the most suitable redox mediator (without neglecting the nature of the solvent and the presence of additives, if any), and to better match the electronic features of the state-of-art electrolyte (see section 2.2), further engineering of the CE can also be considered.

In terms of preparation procedures, among the different approaches, those allowing the direct deposition of CE materials onto TCO glass should be highly preferred, *viz*. electrodeposition and hydrothermal synthesis. Actually, these methods effectively avoid the rather energy demanding anchoring step. It is worth mentioning that a sintering step is always necessary to improve the catalytic performance and the stability of the material, where obviously, the lower the sintering temperature, the higher the relevance and added value of the approach since it will reduce the energy consumption and pave the way for the use of polymeric (and flexible) substrates. The wise development of synthetic and deposition procedures should not neglect future industrialization, and obviously, the proposed approaches should be scalable and easily implemented in existing pilot lines.

It is worth mentioning that the drafted conclusions here refer to standard systems in which iodide/triiodide in organic solvent and glass/FTO are the electrolyte couple and the CE substrate, respectively, which are the most exploited in large-scale devices. Nonetheless, our general considerations can be easily applied to alternative redox couples, greener solvents (*e.g.*, aqueous electrolytes) and innovative substrates (*e.g.*, flexible PET).

2.4 The sustainability issue of TCO/glass substrates

Cradle-to-gate LCA has identified the TCO/glass substrate as one of the main components responsible for the environmental impacts of DSSC modules,[93,363] which can easily ascribed to the following: (i) TCO/glass is the dominant component in terms of mass of a module and (ii) its production is highly energy demanding.

According to a cradle-to-gate LCA,[93] investigation of other substrates to assess the different impacts demonstrated that polymeric substrates, such as PET or PEN (polyethylene naphthalate), decrease the environmental impacts in all the indicators. Replacing glass with polymers results in enhanced performances also in terms of CED and global warming potential within 100 years (GWP100); moreover, the EPBT for DSSCs with polymeric substrates was calculated to be lower than the corresponding DSSCs with glass substrates, even accounting for the lower neat efficiency reachable with a polymeric substrate. Indeed, the trade-off between cost, efficiency, and socio and environmental sustainability should be the final achievement of any process design.

Some representative configurations of polymeric substrates for DSSC are those reported by Yamaguchi and Hsu.[364,365] Both Yamaguchi's and Hsu's groups prepared a plastic substrate photoelectrode starting from ITO/PEN supplied by Oji-Tobi Co. and Pecce Technologies, Inc., respectively (PEN is more thermally stable than PET, but more expensive). Nowadays, the most implemented technology to obtain the conductive substrate is direct magnetron sputtering. Usually, ITO/glass is annealed at 350 °C after the deposition process, but this temperature is too high for plastic substrates. The lower temperature required by polymeric substrates leads to the investigation of alternative deposition techniques, such as pulsed laser deposition and gravure printing process, both proposed as low temperature treatments.[366]

Glass substrates are treated at high temperature for the proper activation of TiO_2 through sintering. The traditional process for the preparation of electrodes involves the sintering of TiO_2 at a temperature in the range of 400–450 °C, while the maximum operational temperature for a plastic substrate is around 150 °C due to its moderate thermal resistance. However, low sintering temperatures do not allow the complete removal of both the binder and the solvent in the TiO_2 paste resulting in insufficient electronic connections between the TiO_2 active material nanoparticles with a corresponding decrease in performance.[367]

Different processes or a combination of processes were investigated to achieve high efficiencies with polymeric substrates. To achieve good adhesion onto TCO/substrates and good interconnection between TiO_2 particles using low temperatures (lower than 200 °C), alternative TiO_2 layer prep-

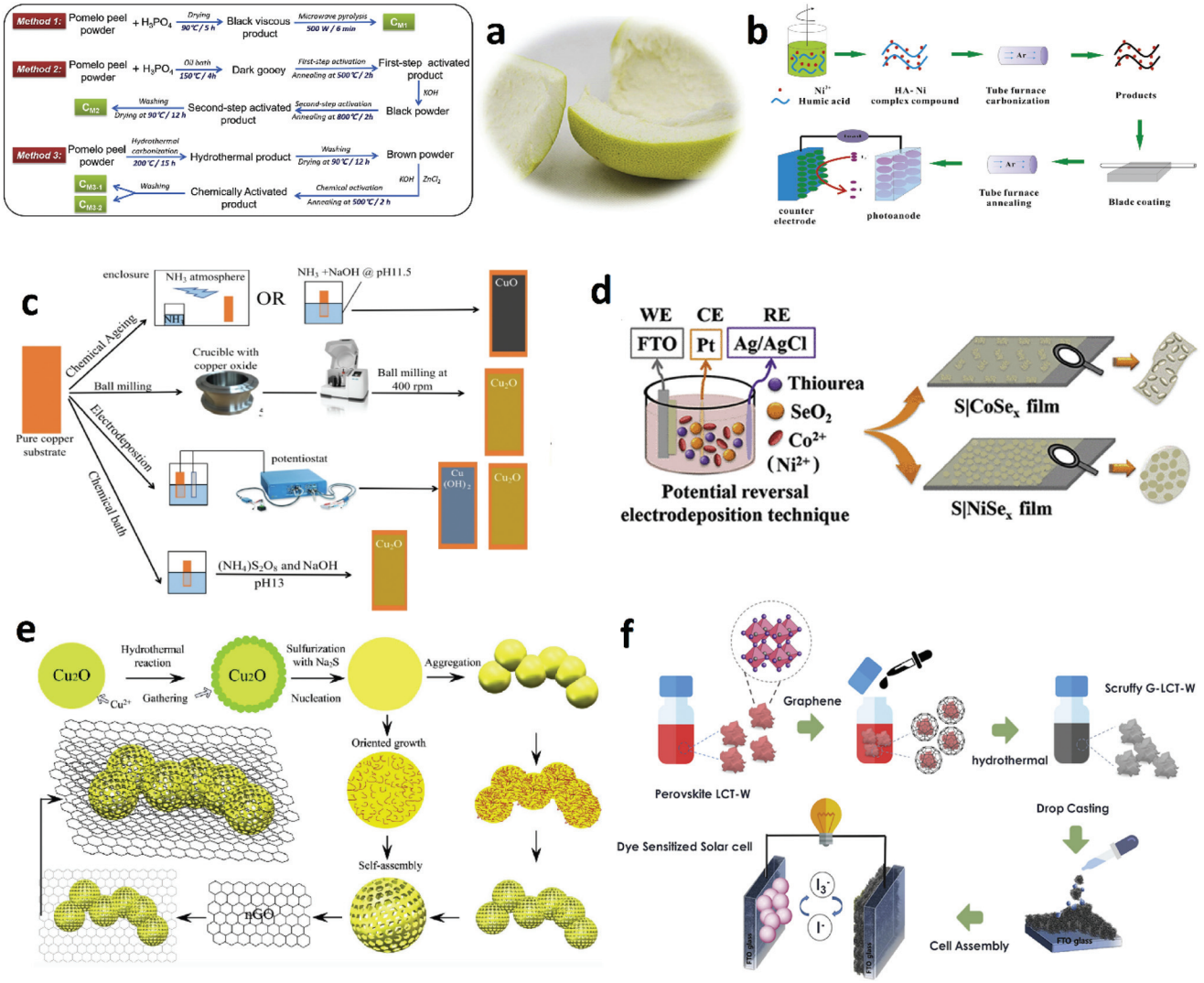

Fig. 12 Some of the most interesting and sustainable approaches to produce green and cost-effective counter-electrodes based on (a and b) waste-derived carbonaceous materials, (c and d) transition metal compounds and (e and f) composite materials. The figures have been adapted from ref. 321, 323, 345, 349, 337 and 358, respectively.

arations were exploited,[125,367,368] which include the press method developed by Hagfeldt *et al.*,[368] lift-off process investigated by Dürr *et al.*,[369] and the combination of UV light exposition with subsequent low temperature heating step by Longo and co-workers.[370] Miyasaka and co-workers explored the combination of electrophoretic deposition and chemical treatments[371] and the preparation of a binder-free paste for the low temperature coating process.[125] An in depth analysis of these approaches is out of the scope of the present review, but we consider that it worth mentioning that these processes exploit a lower temperature compared to the traditional sintering, and hence the energy requirement is lower even if the conditions and chemicals used in each process should be considered for environmental impact evaluation. For instance, Dürr *et al.*[369] exploited a gold layer for the lift-off process, which means that the sustainability as a whole may be impaired by the use of a precious metal. It is clear that one of the most critical aspects to consider comparing glass and plastics is the employed temperature, which significantly affects the final CED. However, the manufacturing process, influence of water, weight, fragility and final application are important aspects to consider when comparing both substrates (Table 5).

Roll-to-roll production is one of the most meaningful added values of polymeric substrates since it allows continuous production instead of the discontinuous process required for glass modules. Polymeric substrates are also superior in term of both light weight and flexibility, where these two aspects allow a high efficiency to weight ratio, lower emission during transportation and reduced risks of breaking during transportation and stocking.[372,373] On the contrary, stability and per-

Table 5 Comparison of the main characteristics of glass *vs.* polymeric DSSC substrates affecting device sustainability

Glass substrate	PET/PEN substrates[364,365]
High environmental impact in a life-to-gate evaluation	Low environmental impacts in a life-to-gate evaluation
Higher thermal stability	Lower thermal stability
Higher efficiency	Lower efficiency
Batch production	Roll-to-roll production
Heavy weight	Light weight
Fragility	Flexibility
Mainly windows as BIPV	Indoor, wearable, portable

meability to water and other small molecules (such as oxygen) are issues for polymeric substrates, where aqueous electrolytes and the exploitation of suitable encapsulants can actually avoid this drawback.

Several studies compared glass and plastics in different fields of application (*e.g.* bottles),[374–376] but a comprehensive study focusing on DSSCs is still missing likely due to the lack of thorough life-cycle knowledge. It should be noted that suitable glass recycling can decrease the overall impact of large-scale DSSC modules. Although considering the *pros* and *cons* of each substrate as a valuable approach, the final application is always pivotal in the definitive choice and sustainability evaluation of a product or service. The future market for DSSCs is more geared towards wearables, portables and indoor application due to the widespread use of PSCs for outdoor applications and the high efficiency of DSSCs under weak and diffuse illumination. However, envisaging the replacement of a traditional window with a DSSC module glass cannot be avoided. In this case, the impacts of glass are partially incorporated in those for window glass production. Again, the best choice in terms of sustainability is a trade-off between many aspects, including environmental impacts, thermal stability, efficiency, ease of manufacturing, weight, fragility and final use, which should be carefully and thoughtfully evaluated.

3. Conclusions and future outlooks

Throughout this review, we analysed the materials proposed for conventional DSSCs chiefly focusing on their sustainability aspects. Indeed, toward the forthcoming commercialization of this class of emerging photovoltaics, the employment of truly sustainable materials cannot be overlooked. Specifically, based on a thorough review of the recent literature, we suggested a set of possible guidelines to generalize the sustainable exploitation of materials, which should be selected and produced strictly focusing on the use of non-toxic, readily available and low cost, possibly waste-derived and/or easily recyclable materials.

The most important issues regarding sustainability in DSSCs involve: (i) the employment of the TCO/glass substrate, which is considered a highly energy-demanding material, and the sustainability concerns of which are mainly related to its uncertain waste management; (ii) the use of CRMs or noble metals including cobalt in the redox shuttle, platinum in the counter-electrode and ruthenium in the sensitizer; and (iii) the limited long-term stability mainly due to the extreme volatility and harshness of organic-based electrolytes.

Photosensitizers should be designed with the aim at avoiding the use of CRMs, where zinc-based porphyrins and some metal-free dyes combine the very high efficiency, typical of metal-based dyes, with a synthetic procedure that can be still improved considering green metrics. It is worth mentioning that the best efficiency has been obtained by using a cocktail of fully organic dyes. Although these molecules do not bear any CRM, their synthetic procedures are usually expensive and not sustainable, requiring multiple steps and the employment of a large amount of toxic and/or hazardous solvents and reagents. For every synthesis, calculation of the CED should be undertaken. To overcome these limitations, scientists proposed natural pigments as effective sensitizers in DSSCs, which may become competitive compared to manufactured dyes since they can easily be extracted from vegetables utilizing simple extraction processes based on green solvents, but only if their efficiency and stability can be further enhanced.

Screening the literature, it is evident that, to date, the best efficiency was obtained using cobalt-based (lab-scale) or iodine-based (modules) redox couples in organic solvents. However, cobalt is a CRM, iodine is quite aggressive towards the other device components and the organic electrolyte, being highly volatile, jeopardizes the long-term stability of the cells. As detailed in section 2.2, copper-based complexes have been proven to be the best trade-off between sustainability and photoconversion efficiency. More recently, the investigation of organic-based redox couples has been successfully exploited, where TEMPO (and its derivatives) allowed a good photoconversion efficiency coupled with relatively long stability to be obtained. The latter is also a prerogative of sulphur-based redox couples; however, in most cases, the synthetic procedures, being highly energy-consuming, threaten the sustainability of these alternative redox couples, and accordingly significant effort should deal with the design of more environmentally friendly and sustainable synthetic routes. It should be noted that these alternative redox couples (both Co/Cu-based and fully organic ones) have been mainly tested in combination with solvents such as ACN or MPN, which undermine their long-term stability. Therefore, some alternative solvents such as ionic liquids, deep eutectic solvents and (simply) water have been proposed and investigated. In the last year, water, which for many years was considered poisonous to the device, has become a resource, where its employment as a solvent led to a photoconversion efficiency approaching 7%. Effortless research is still required, but scientists involved in aqueous DSSCs are very optimistic regarding the possibility of the complete and effective replacement of organic solvents. Truthfully, it should be noted that the sustainability of aqueous-DSSCs is still under debate, where to obtain good photoconversion efficiency, ultra-pure water should be employed, which in turn

negatively impacts the sustainability of the entire production process. The use of wastewater can be proposed, but the relative performances and stability have not been investigated to date.

Counter-electrodes have been the most investigated DSSC components in the last few years. This is mainly due to (i) the necessity to replace platinum since it is expensive, toxic and relatively unstable; and (ii) the practically endless alternative materials. Among them, the best results have been obtained with carbon-based nanostructured materials, resulting in long-term stability and good catalytic properties (mainly toward iodine-based redox couple). However, carbon-based materials cannot be considered sustainable *a priori* and careful investigation must be done regarding their re-use or by-product sources, production processes and effective performances over a relatively long operation lifetime. Unfortunately, the majority of research articles dealing with carbon-based counter-electrodes do not report any meaningful information on their production process, leading to a difficult (and sometimes impossible) sustainability-driven verdict. Another feasible option to replace platinum involves the use of transition-metal based nanostructures. Indeed, transition metals are usually quite abundant and safe (with some exception, *viz.* cobalt); moreover, they can be easily obtained both as sulphides and oxides. The main issue regarding this class of compounds is related to their catalytic activity, which is sizeable only when they are in the nanostructured and crystalline phase. However, nanostructuration often requires high temperature and energy-demanding processes, thus leading to a negative balance in terms of sustainability. Trying to circumvent this issue, scientists resolved to couple the catalytic activity of carbon-based materials with the robustness of transition-metal oxides/sulphides. Accordingly, although still in the early stage of development, the results are very promising, even if only investigated in conjunction with an iodine-based shuttle to date.

Finally, the "problem" of the TCO/glass substrate (only marginally investigated in this review), which is the highest energy-demanding component in conventional DSSCs, should be attentively tackled, where some interesting results have been obtained by the substitution of glass with polymer-based (*e.g.* PEN and PET) or metallic substrates, which consequently open the doors to flexible devices. However, on the one hand, the photoconversion efficiency is significantly lower compared to that of glass-based devices, while, on the other hand, the use of plastic materials requires a complete afterthought of the production processes of both lab- and large-scale devices.

It should be noted that, as briefly mentioned in the above paragraphs, the efforts toward more sustainable materials have been related to a single component (*i.e.* sensitizer, redox couple, electrolyte and counter-electrode) more than complete devices. Indeed, zinc-based porphyrins showed remarkable photoconversion efficiencies when coupled with cobalt- or iodine-based redox couples (dissolved in an organic and highly volatile solvent), whereas copper complexes and/or water environments were not considered. On the other hand, when CRM-free redox couples and aqueous DSSCs were analysed, neither sustainable sensitizers nor platinum-based counter-electrodes were employed. Therefore, a more comprehensive approach is needed, focusing on developing a completely sustainable and cost-effective device.

After the discovery of the DSSC in 1991, scientists and companies involved in this field aimed at obtaining efficient (the former) and stable (the latter) materials toward the actual commercialization of this class of photovoltaic devices. However, after almost 30 years and considering the "energy problem" affecting society currently, the sustainability of the employed materials cannot be considered a worthless spine of the efficiency DSSC. From here on, these three concepts should proceed hand-in-hand, where "stable", "efficient" and "sustainable" should be the adjectives associated with forthcoming innovative materials and processes, considering that a Holy Grail recipe does not exist, but green metrics and LCA can and should drive future research in this field.

4. Abbreviations

4.1 Acronyms and symbols

ACN	Acetonitrile
AM	Air mass
BET	Brunauer–Emmett–Teller
BIPV	Building integrated photovoltaics
C	Electrical conversion factor
CB	Conduction band
CDCA	Chenodeoxycholic acid
CE	Counter electrode
CED	Cumulative energy demand
CMC	Carboxymethyl cellulose
CNT	Carbon nanotubes
CRM	Critical raw material
CSP	Concentrated solar power
DES	Deep eutectic solvents
DMF	Dimethylformamide
DSSC	Dye-sensitized solar cell
D–π-A	Donor–π-acceptor
EC	European commission
EDTA	Ethylenediaminetetraacetic acid
EoL	End-of-life
EPBT	Energy payback time
EuChemS	European chemical society
FF	Fill factor
FTO	Fluorine-doped tin oxide
GO	Graphene oxide
GuSCN	Guanidinium thiocyanate
GWP	Global warming potential
HOMO	Highest occupied molecular orbital
HTM	Hole transport materials
IEA	International energy agency
IPCC	Intergovernmental panel on climate change
IPCE	Incident photon-to-electron conversion efficiency
IR	Infrared
IRENA	International renewable energy agency

J_{SC}	Short-circuit current density
LCA	Life cycle assessment
LCC	Life cycle costing
LUMO	Lowest occupied molecular orbital
MP	Mangosteen peel
MPA	Methoxyacetonitrile
MPN	Methoxypropionitrile
NIR	Near-infrared
PCE	Photoconversion efficiency
PEDOT	Poly(3,4-ethylenedioxythiophene)
PEN	Poly(ethylene naphthalate)
PET	Poly(ethylene terephthalate)
POM	Polyoxometalate
PS	Photosensitizer
PSC	Perovskite solar cell
PV	Photovoltaic
PVA	Poly(vinyl alcohol)
PVP	Poly(vinylpyrrolidone)
QD	Quantum dot
rGO	Reduced graphene oxide
RTIL	Room temperature ionic liquid
SCN	Succinonitrile
SDG	Sustainable development goal
TBA	Tetrabutyl ammonium
TCO	Transparent conductive oxide
TFSI	Bis(trifluoromethanesulfonyl)imide
TM	Transition metal
UV	Ultraviolet
VIS	Visible
V_{OC}	Open-circuit voltage
YEO	Yearly energy output

4.2 Codes of sensitizers and redox couples

ADEKA-1	(*E*)-2-Cyano-3-(5‴-(9-ethyl-9*H*-carbazol-3-yl)-3′,3″,3‴,4-tetrahexyl-[2,2′:5′,2″:5″,2‴-quaterthiophen]-5-yl)-*N*-(4-(trimethoxysilyl)phenyl) acrylamide
[C12MIm][T]	1-Dodecyl-3-methyl-1*H*-imidazol-3-ium-1*H*-tetrazole-5-thiolate
C15	15 Carbons alkyl chain
C6–C3–C6	6 Carbons–3 carbons–6 carbons alkyl chain
Chl-a	Chlorophyll a
Chl-b	Chlorophyll b
D149	5-[[4-[4-(2,2-Diphenylethenyl)phenyl]-1,2,3-3a,4,8b-hexahydrocyclopent[*b*]indol-7-yl]methylene]-2-(3-ethyl-4-oxo-2-thioxo-5-thiazolidinylidene)-4-oxo-3-thiazolidineacetic acid
D45	(*E*)-3-(5-(4-(Bis(2′,4′-dimethoxy-[1,1′-biphenyl]-4-yl)amino)phenyl)thiophen-2-yl)-2-cyanoacrylic acid
D51	(*E*)-3-(6-(4-(Bis(2′,4′-dimethoxy-[1,1′-biphenyl]-4-yl)amino)phenyl)-4,4-dihexyl-4*H*-cyclopenta[2,1-*b*:3,4-*b*′]dithiophen-2-yl)-2-cyanoacrylic acid
dmp	2,9-Dimethyl-1,10-phenanthroline
DTS	4,4-Bis(2-ethylhexyl)-4Hsilolo[3,2-*b*:4,5-*b*′] dithiophene
DTS-CA	(*E*)-4-((6-(6-((*E*)-2-Carboxy-2-cyanovinyl)-4,4-bis(2-ethylhexyl)-4*H*-silolo[3,2-*b*:4,5-*b*′]dithiophen-2-yl)-1-dodecyl-3,3-dimethyl-3*H*-indol-1-ium-2-yl)methylene)-2-((*E*)-(1-ethyl-3,3-dimethylindolin-2-ylidene)methyl)-3-oxocyclobut-1-enolate
EO3	(*E*)-3-(7,10-Bis(4-(2-(2-(2-methoxyethoxy)ethoxy)ethoxy)phenyl)-10*H*-phenothiazin-3-yl)-2-cyanoacrylic acid
hybeb	[1-(2-Hydroxybenzamido)-2-(2-pyridinecarboxamido)benzenato]
LEG4	(*E*)-3-(6-(4-(Bis(2′,4′-dibutoxy-[1,1′-biphenyl]-4-yl)amino)phenyl)-4,4-dihexyl-4*H*-cyclopenta[2,1-*b*:3,4-*b*′]dithiophen-2-yl)-2-cyanoacrylic acid
JC-IL	1-Butyl-3-{2-oxo-2-[(2,2,6,6-tetramethylpiperidin-1-oxyl-4-yl)amino]ethyl}-1*H*-imidazol-3-ium iodide
MeO-φ-6-CA	(2*E*,4*E*,6*E*,8*E*,10*E*,12*E*)-13-(4-Methoxyphenyl)-2,7,11-trimethyltrideca-2,4,6,8,10,12-hexaenoic acid
MK-2	2-Cyano-3-[5‴-(9-ethyl-9*H*-carbazol-3-yl)-3′,3″,3‴,4-tetra-*n*-hexyl-[2,2′,5′,2″,5″,2‴]-quater thiophen-5-yl] acrylic acid
$MTDD2^+$	5-Methylthio-1,3,4-thiadiazolium disulfide dication
MTDT	5-Methylthio-1,3,4-thiadiazole-2-thiol
N719	Di-tetrabutylammonium *cis*–bis(isothiocyanato) bis(2,2′-bipyridyl-4,4′-dicarboxylato)ruthenium (II)
PMII	1-Propyl-3-methylimidazolium iodide
R6	4-(7-((15-(Bis(4-(hexyloxy)phenyl)amino)-9,9,19,19-tetrakis(4-hexylphenyl)-9,19-dihydrobenzo[10′,1′]phenanthro[3′,4′:4,5]thieno[3,2-*b*]benzo[10,1]phenanthro[3,4-*d*]thiophen-5-yl) ethynyl)benzo[*c*][1,2,5]thiadiazol-4-yl)benzoic acid
salen	*N*,*N*′-Ethylenebis(salicylideneiminate)
SPA	Stalk of pokeweed (*Phytolacca americana*) extracts
T-	5-Mercapto-1-methyl-tetrazole
T169	$C_{53}H_{62}N_{12}O_4RuS_2$ index name not yet assigned (CAS 1884649-49-3)
T_2	Di-5-(1-methyltetrazole)
TEMPO	2,2,6,6-Tetramethylpiperidine-1-oxyl
TEMPOL	4-Hydroxy-2,2,6,6-tetramethypiperidine-1-oxyl
TG6	(*cis*–Bis(thiocyanato)(2,2′-bipyridyl-4,4′-dicarboxylato){4,4′-bis[2-(4-hexylsulfanylphenyl)vinyl]-2,2′-bipyridine}ruthenium(II) mono(tetrabutylammonium) salt)
WS-72	(*E*)-3-(6-(8-(4-(Bis(2′,4′-bis(hexyloxy)-[1,1′-biphenyl]-4-yl)amino)phenyl)-2,3-bis(4-(hexyloxy) phenyl)quinoxalin-5-yl)-4,4-dihexyl-4*H*-cyclopenta[2,1-*b*:3,4-*b*′]dithiophen-2-yl)-2-cyanoacrylic acid

Y123	(*E*)-3-(6-(4-(Bis(2′,4′-bis(hexyloxy)-[1,1′-biphenyl]-4-yl)amino)phenyl)-4,4-dihexyl-4*H*-cyclopenta[2,1-*b*:3,4-*b*′]dithiophen-2-yl)-2-cyanoacrylic acid

Conflicts of interest

There are no conflicts to declare.

Acknowledgements

N. M. and M. B. thank Mr Mattia Costamagna for profitable discussion. All the authors acknowledge Ms Ginevra Sorbelli for the rendering of Graphical Abstract. This project has received funding from the European Union's Horizon 2020 research and innovation program under grant agreement no. 826013 (IMPRESSIVE).

References

1 M. Sharmina, C. McGlade, P. Gilbert and A. Larkin, *Mar. Policy*, 2017, **84**, 12–21.
2 Energy Technology Perspectives, https://www.iea.org/topics/energy-technology-perspectives, (accessed 3 February 2020).
3 CoreWritingTeam, *IPCC 2014 Climate Change 2014: Synthesis Report. Contribution of Working Groups I, II and III to the Fifth Assessment Report of the Intergovernmental*, IPCC, Geneva, Switzerland, 2014.
4 Sustainable Development Goals, https://sustainabledevelopment.un.org, (accessed 12 December 2019).
5 2030 climate & energy framework, https://ec.europa.eu/clima/policies/strategies/2030_en, (accessed 19 January 2020).
6 IRENA, *Renewable Power Generation Costs in 2018*, Abu Dhabi, 2019.
7 Market analysis and forecast from 2019 to 2024, https://www.iea.org/reports/renewables-2019, (accessed 3 March 2020).
8 Distributed solar PV capacity growth by country/region, https://www.iea.org/data-and-statistics/charts/distributed-solar-pv-capacity-growth-by-country-region, (accessed 23 January 2020).
9 R. Perman, Y. Ma, J. Mcgilvray and M. Common, *Natural Resource and Environmental Economics*, Addison Wesley, Boston, USA, 2013.
10 Renewable Energy Sources and Climate Change Mitigation, https://www.ipcc.ch/report/renewable-energy-sources-and-climate-change-mitigation, (accessed 11 November 2019).
11 World Commission on Environment and Development, *The Brundtland Report*, 1987.
12 B. O'Regan and M. Grätzel, *Nature*, 1991, **353**, 737–739.
13 K. Sharma, V. Sharma and S. S. Sharma, *Nanoscale Res. Lett.*, 2018, **13**, 381.
14 Y. Dou, Z. Liu, Z. Wu, Y. Liu, J. Li, C. Leng, D. Fang, G. Liang, J. Xiao, W. Li, X. Wei, F. Huang, Y. B. Cheng and J. Zhong, *Nano Energy*, 2020, **71**, 104567.
15 S. He, L. Qiu, L. K. Ono and Y. Qi, *Mater. Sci. Eng., R*, 2020, **140**, 100545.
16 P. Chen, Z. Wang, S. Wang, M. Lyu, M. Hao, M. Ghasemi, M. Xiao, J. H. Yun, Y. Bai and L. Wang, *Nano Energy*, 2020, **69**, 104392.
17 M. Freitag and G. Boschloo, *Curr. Opin. Electrochem.*, 2017, **2**, 111–119.
18 A. Fakharuddin, R. Jose, T. M. Brown, F. Fabregat-Santiago and J. Bisquert, *Energy Environ. Sci.*, 2014, **7**, 3952–3981.
19 S. Mozaffari, M. R. Nateghi and M. B. Zarandi, *Renewable Sustainable Energy Rev.*, 2017, **71**, 675–686.
20 J. E. Trancik and D. Cross-Call, *Environ. Sci. Technol.*, 2013, **47**, 6673–6680.
21 J. Gong, J. Liang and K. Sumathy, *Renewable Sustainable Energy Rev.*, 2012, **16**, 5848–5860.
22 H. Yuan, W. Wang, D. Xu, Q. Xu, J. Xie, X. Chen, T. Zhang, C. Xiong, Y. He, Y. Zhang, Y. Liu and H. Shen, *Sol. Energy*, 2018, **165**, 233–239.
23 M. L. Parisi, A. Dessì, L. Zani, S. Maranghi, S. Mohammadpourasl, M. Calamante, A. Mordini, R. Basosi, G. Reginato and A. Sinicropi, *Front. Chem.*, 2020, **8**, 214.
24 M. Hofmann, H. Hofmann, C. Hagelüken and A. Hool, *Sustainable Mater. Technol.*, 2018, **17**, e00074.
25 H. Michaels, M. Rinderle, R. Freitag, I. Benesperi, T. Edvinsson, R. Socher, A. Gagliardi and M. Freitag, *Chem. Sci.*, 2020, **11**, 2895–2906.
26 A. Venkateswararao, J. K. W. Ho, S. K. So, S. W. Liu and K. T. Wong, *Mater. Sci. Eng., R*, 2020, **139**, 100517.
27 S. Anandan, *Sol. Energy Mater. Sol. Cells*, 2007, **91**, 843–846.
28 S. Bose, V. Soni and K. R. Genwa, *Int. J. Sci. Res. Publ.*, 2015, **5**, 2250–3153.
29 S. Shalini, R. Balasundaraprabhu, T. Satish Kumar, N. Prabavathy, S. Senthilarasu and S. Prasanna, *Int. J. Energy Res.*, 2016, **40**, 1303–1320.
30 J. Wu, Z. Lan, J. Lin, M. Huang, Y. Huang, L. Fan, G. Luo, Y. Lin, Y. Xie and Y. Wei, *Chem. Soc. Rev.*, 2017, **46**, 5975–6023.
31 D. Sengupta, P. Das, B. Mondal and K. Mukherjee, *Renewable Sustainable Energy Rev.*, 2016, **60**, 356–376.
32 J. Wu, Z. Lan, J. Lin, M. Huang, Y. Huang, L. Fan and G. Luo, *Chem. Rev.*, 2015, **115**, 2136–2173.
33 Y. Wang, *Sol. Energy Mater. Sol. Cells*, 2009, **93**, 1167–1175.
34 N. C. D. Nath and J.-J. Lee, *J. Ind. Eng. Chem.*, 2019, **78**, 53–65.
35 M. Ye, X. Wen, M. Wang, J. Iocozzia, N. Zhang, C. Lin and Z. Lin, *Mater. Today*, 2015, **18**, 155–162.
36 A. Hagfeldt, G. Boschloo, L. Sun, L. Kloo and H. Pettersson, *Chem. Rev.*, 2010, **110**, 6595–6663.

37 M. L. L. Parisi, S. Maranghi, L. Vesce, A. Sinicropi, A. Di Carlo and R. Basosi, *Renewable Sustainable Energy Rev.*, 2020, **121**, 109703.
38 E. Baranowska-Wójcik, D. Szwajgier, P. Oleszczuk and A. Winiarska-Mieczan, *Biol. Trace Elem. Res.*, 2020, **193**, 118–129.
39 M. Simonin, A. Richaume, J. P. Guyonnet, A. Dubost, J. M. F. Martins and T. Pommier, *Sci. Rep.*, 2016, **6**, 33643.
40 Y. Bai, I. Mora-Seró, F. De Angelis, J. Bisquert and P. Wang, *Chem. Rev.*, 2014, **114**, 10095–10130.
41 B. Zhang and L. Sun, *Chem. Soc. Rev.*, 2019, **48**, 2216–2264.
42 P. T. Smith, E. M. Nichols, Z. Cao and C. J. Chang, *Acc. Chem. Res.*, 2020, **53**, 575–587.
43 S. James and R. Contractor, *Sci. Rep.*, 2018, **8**, 17032.
44 Z. Wan, C. Jia, Y. Duan, L. Zhou, Y. Lin and Y. Shi, *J. Mater. Chem.*, 2012, **22**, 25140–25147.
45 C. Cavallo, F. Di Pascasio, A. Latini, M. Bonomo and D. Dini, *J. Nanomater.*, 2017, **2017**, 5323164.
46 M. Bonomo, D. Dini and F. Decker, *Front. Chem.*, 2018, **6**, 601.
47 S. Powar, T. Daeneke, M. T. Ma, D. Fu, N. W. Duffy, G. Gotz, M. Weidelener, A. Mishra, P. Bäuerle, L. Spiccia and U. Bach, *Angew. Chem., Int. Ed.*, 2013, **52**, 602–605.
48 D. Xiong, Q. Zhang, S. K. Verma, H. Li, W. Chen and X. Zhao, *J. Alloys Compd.*, 2016, **662**, 374.
49 D. Xiong, Z. Xu, X. Zeng, W. Zhang, W. Chen, X. Xu, M. Wang and Y.-B. Cheng, *J. Mater. Chem.*, 2012, **22**, 24760–24768.
50 T. Jiang, M. Bujoli-Doeuff, Y. Farré, E. Blart, Y. Pellegrin, E. Gautron, M. Boujtita, L. Cario, F. Odobel and S. Jobic, *RSC Adv.*, 2016, **6**, 1549.
51 M. Bonomo, P. Mariani, F. Mura, A. Di Carlo and D. Dini, *J. Electrochem. Soc.*, 2019, **166**, D290–D300.
52 C. H. Chang, Y. C. Chen, C. Y. Hsu, H. H. Chou and J. T. Lin, *Org. Lett.*, 2012, **14**, 4726–4729.
53 M. Bonomo, A. Di Carlo, R. Centore, D. Dini and A. Carella, *Sol. Energy*, 2018, **169**, 237–242.
54 P. Qin, M. Linder, T. Brinck, G. Boschloo, A. Hagfeldt and L. Sun, *Adv. Mater.*, 2009, **21**, 2993–2996.
55 P. Naik, A. Planchat, Y. Pellegrin, F. Odobel and A. V. Adhikari, *Sol. Energy*, 2017, **157**, 1064–1073.
56 I. R. Perera, T. Daeneke, S. Makuta, Z. Yu, Y. Tachibana, A. Mishra, P. Bäuerle, C. A. Ohlin, U. Bach and L. Spiccia, *Angew. Chem., Int. Ed.*, 2015, **54**, 3758–3762.
57 T. M. A. Bakker, S. Mathew and J. N. H. Reek, *Sustainable Energy Fuels*, 2019, **3**, 96–100.
58 Y. Farré, M. Raissi, A. Fihey, Y. Pellegrin, E. Blart, D. Jacquemin and F. Odobel, *ChemSusChem*, 2017, **10**, 2618–2625.
59 M. Hosseinnezhad, S. Moradian and K. Gharanjig, *Prog. Color, Color. Coat.*, 2017, **10**, 239–244.
60 J. He, H. Lindström, A. Hagfeldt and S.-E. Lindquist, *Sol. Energy Mater. Sol. Cells*, 2000, **62**, 265–273.
61 M. K. Nazeeruddin, A. Kay, I. Rodicio, R. Humphry-Baker, E. Müller, P. Liska, N. Vlachopoulos and M. Gratzel, *J. Am. Chem. Soc.*, 1993, **115**, 6382–6390.
62 NREL Research Cells Efficiency Chart 2019, http://www.nrel.gov/ncpv/images/efficiency_chart.jpg, (accessed 5 March 2020).
63 K. Kakiage, Y. Aoyama, T. Yano, K. Oya, J. I. Fujisawa and M. Hanaya, *Chem. Commun.*, 2015, **51**, 15894–15897.
64 L. M. Peter, *The Grätzel cell: Where next?* 2011, vol. 2.
65 K. D. Jayan and V. Sebastian, in *AIP Conference Proceedings*, 2019, vol. 2162, p. 020036.
66 No Title, http://grantadesign.com/language-home/industry/products/ces-selector, (accessed 28 April 2020).
67 J. Gong, K. Sumathy, Q. Qiao and Z. Zhou, *Review on dye-sensitized solar cells (DSSCs): Advanced techniques and research trends*, 2017, vol. 68.
68 M. Soroush and K. K. S. Lau, *Dye-Sensitized solar cells: Mathematical modelling, and materials design and optimization*, 2019.
69 Y. Cao, Y. Liu, S. M. Zakeeruddin, A. Hagfeldt and M. Grätzel, *Joule*, 2018, **2**, 1108–1117.
70 H. K. H. Lee, J. Wu, J. Barbé, S. M. Jain, S. Wood, E. M. Speller, Z. Li, F. A. Castro, J. R. Durrant and W. C. Tsoi, *J. Mater. Chem. A*, 2018, **6**, 5618–5626.
71 M. Li, C. Zhao, Z. K. Wang, C. C. Zhang, H. K. H. Lee, A. Pockett, J. Barbé, W. C. Tsoi, Y. G. Yang, M. J. Carnie, X. Y. Gao, W. X. Yang, J. R. Durrant, L. S. Liao and S. M. Jain, *Adv. Energy Mater.*, 2018, **8**, 1801509.
72 Y. Rong, G. Liu, H. Wang, X. Li and H. Han, *Front. Optoelectron.*, 2013, **6**, 359–372.
73 C. Wu, B. Chen, X. Zheng and S. Priya, *Sol. Energy Mater. Sol. Cells*, 2016, **157**, 438–446.
74 H. J. Snaith, *Adv. Funct. Mater.*, 2010, **20**, 13–19.
75 G. Boschloo, *Front. Chem.*, 2019, **7**, 1–9.
76 W. Shockley and H. J. Queisser, *J. Appl. Phys.*, 1961, **32**, 510–519.
77 S. Yoon, S. Tak, J. Kim, Y. Jun, K. Kang and J. Park, *Build. Environ.*, 2011, **46**, 1899–1904.
78 A. Zaheer and K. George, in 2018 9th IEEE Annual Ubiquitous Computing, Electronics and Mobile Communication Conference, UEMCON, 2018, pp. 917–921.
79 M. Donato, K. Hansen, P. Kalavakuru, M. Kirchgessner, M. Kuster, M. Porro, C. Reckleben and M. Turcato, *J. Instrum.*, 2017, **12**, C03025.
80 A. Scalia, F. Bella, A. Lamberti, C. Gerbaldi and E. Tresso, *Energy*, 2019, **166**, 789–795.
81 L. C. Kin, Z. Liu, O. Astakhov, S. N. Agbo, H. Tempel, S. Yu, H. Kungl, R. A. Eichel, U. Rau, T. Kirchartz and T. Merdzhanova, *ACS Appl. Energy Mater.*, 2020, **3**, 431–439.
82 A. Mishra, M. K. R. Fischer and P. Büuerle, *Angew. Chem., Int. Ed.*, 2009, **48**, 2474–2499.
83 D. Xiong and W. Chen, *Front. Optoelectron.*, 2012, **5**, 371–389.
84 F. Odobel and Y. Pellegrin, *J. Phys. Chem. Lett.*, 2013, **4**, 2551–2564.
85 J. Wu, Z. Lan, J. Lin, M. Huang, Y. Huang, L. Fan and G. Luo, *Chem. Rev.*, 2015, **115**, 2136–2173.

86 P. Liao and E. a. Carter, *Chem. Soc. Rev.*, 2013, **42**, 2401.
87 N. Mariotti, M. Bonomo and C. Barolo, in *Criticisms and Potential Improvements, Reliability and Ecological Aspects of Photovoltaic Modules*, ed. A. Gok, IntechOpen, London, 2020.
88 Varun, I. K. Bhat and R. Prakash, *Renewable Sustainable Energy Rev.*, 2009, **13**, 1067–1073.
89 F. Mathieux, F. Ardente, S. Bobba, P. Nuss, G. Blengini, P. Alves Dias, D. Blagoeva, C. Torres De Matos, D. Wittmer, C. Pavel, T. Hamor, H. Saveyn, B. Gawlik, G. Orveillon, D. Huygens, E. Garbarino, E. Tzimas, F. Bouraoui and S. Solar, *Critical raw materials and the circular economy - Background report*, Publications Office of the European Union, Luxembourg, 2017.
90 P. T. Hsiao, W. T. Hung, Y. C. Chen, L. K. Huang, C. C. Chang, C. F. Chen, H. W. Chen, M. De Lu, Y. P. Lin and Y. L. Tung, *Renewable Energy*, 2020, **152**, 67–74.
91 M. L. Parisi, S. Maranghi, A. Sinicropi and R. Basosi, *Int. J. Heat Technol.*, 2013, **31**, 143–148.
92 M. L. Parisi, A. Sinicropi and R. Basosi, *Int. J. Heat Technol.*, 2011, **29**, 161–169.
93 M. L. Parisi, S. Maranghi and R. Basosi, *Renewable Sustainable Energy Rev.*, 2014, **39**, 124–138.
94 R. Arvidsson and M. Svanström, *Integr. Environ. Assess. Manage.*, 2016, **12**, 429–436.
95 M. C. Den Hollander, C. A. Bakker and E. J. Hultink, *J. Ind. Ecol.*, 2017, **21**, 517–525.
96 A. Kay and M. Grätzel, *Sol. Energy Mater. Sol. Cells*, 1996, **44**, 99–117.
97 M. J. De Wild-Scholten and A. C. Veltkamp, *Environmental life cycle analysis of dye sensitized solar devices. Status and outlook*, Netherlands, 2007.
98 C. Álamo, F. López-Muñoz, P. García-García and S. García-Ramos, *Psychogeriatrics*, 2014, **14**, 261–268.
99 European Commission, *Critical Raw Materials in th EU*, 2017.
100 A. M. Ammar, H. S. H. Mohamed, M. M. K. Yousef, G. M. Abdel-Hafez, A. S. Hassanien and A. S. G. Khalil, *J. Nanomater.*, 2019, **2019**, 1–10.
101 P. T. Anastas and J. C. Warner, *Green chemistry : theory and practice*, Oxford University Press, Oxford [England], New York, 1998.
102 R. A. Sheldon, *ACS Sustainable Chem. Eng.*, 2018, **6**, 32–48.
103 A. Hagfeldt and M. Grätzel, *Acc. Chem. Res.*, 2000, **33**, 269–277.
104 T. Daeneke, Y. Uemura, N. W. Duffy, A. J. Mozer, N. Koumura, U. Bach and L. Spiccia, *Adv. Mater.*, 2012, **24**, 1222–1225.
105 A. Yella, L. Hsuan-Wei, H. N. Tsao, Y. Chenyi, C. Aravind Kumar, M. K. Nazeeruddin, E. W.-G. Diau, C.-Y. Yeh, S. M. Zakeeruddin and M. Grätzel, *Science*, 2011, **334**, 629–634.
106 G. Oskam, B. V. Bergeron, G. J. Meyer and P. C. Searson, *J. Phys. Chem. B*, 2001, **105**, 6867–6873.
107 F. Bella, E. D. Ozzello, A. Sacco, S. Bianco and R. Bongiovanni, *Int. J. Hydrogen Energy*, 2014, **39**, 3036–3045.
108 R. Shanti, F. Bella, Y. S. Salim, S. Y. Chee, S. Ramesh and K. Ramesh, *Mater. Des.*, 2016, **108**, 560–569.
109 F. Bella, J. Popovic, A. Lamberti, E. Tresso, C. Gerbaldi and J. Maier, *ACS Appl. Mater. Interfaces*, 2017, **9**, 37797–37803.
110 F. Bella, C. Gerbaldi, C. Barolo and M. Grätzel, *Chem. Soc. Rev.*, 2015, **44**, 3431–3473.
111 R. Kawano, H. Matsui, C. Matsuyama, A. Sato, M. A. B. H. Susan, N. Tanabe and M. Watanabe, *J. Photochem. Photobiol., A*, 2004, **164**, 87–92.
112 C. L. Boldrini, N. Manfredi, F. M. Perna, V. Trifiletti, V. Capriati and A. Abbotto, *Energy Technol.*, 2017, **5**, 345–353.
113 S. Khandelwal, Y. K. Tailor and M. Kumar, *J. Mol. Liq.*, 2016, **215**, 345–386.
114 F. Bella, E. D. Ozzello, S. Bianco and R. Bongiovanni, *Chem. Eng. J.*, 2013, **225**, 873–879.
115 I. Benesperi, H. Michaels and M. Freitag, *J. Mater. Chem. C*, 2018, **6**, 11903–11942.
116 S. Mathew, A. Yella, P. Gao, R. Humphry-Baker, B. F. E. Curchod, N. Ashari-Astani, I. Tavernelli, U. Rothlisberger, M. K. Nazeeruddin and M. Grätzel, *Nat. Chem.*, 2014, **6**, 242–247.
117 Cobalt Institute, https://www.cobaltinstitute.org/, (accessed 9 March 2020).
118 Live Platinum Price, https://www.kitco.com/charts/liveplatinum.html, (accessed 20 March 2020).
119 H. Wang, J. Gao, J. Zhu, J. Y. Ma, H. Zhou, J. Xiao and M. Wu, *Electrochim. Acta*, 2020, **334**, 135582.
120 K. Imoto, K. Takahashi, T. Yamaguchi, T. Komura, J. I. Nakamura and K. Murata, *Sol. Energy Mater. Sol. Cells*, 2003, **79**, 459–469.
121 J. D. Roy-Mayhew, D. J. Bozym, C. Punckt and I. A. Aksay, *ACS Nano*, 2010, **4**, 6203–6211.
122 C. Gao, Q. Han and M. Wu, *J. Energy Chem.*, 2018, **27**, 703–712.
123 N. A. Karim, U. Mehmood, H. F. Zahid and T. Asif, *Sol. Energy*, 2019, **185**, 165–188.
124 A. C. Veltkamp and M. J. De Wild-Scholten, in *Renewable Energy 2006*, 2006.
125 T. Miyasaka, Y. Kijitori and M. Ikegami, *Electrochemistry*, 2007, **75**, 2–12.
126 Z. Weng, H. Guo, X. Liu, S. Wu, K. W. K. Yeung and P. K. Chu, *RSC Adv.*, 2013, **3**, 24758.
127 Q. Wali, A. Fakharuddin and R. Jose, *J. Power Sources*, 2015, **293**, 1039–1052.
128 H. Minoura and T. Yoshida, *Electrochemistry*, 2008, **76**, 109–117.
129 I. Venditti, N. Barbero, M. V. Russo, A. Di Carlo, F. Decker, I. Fratoddi, C. Barolo and D. Dini, *Mater. Res. Express*, 2014, **1**, 015040.
130 K. Keis, C. Bauer, G. Boschloo, A. Hagfeldt, K. Westermark, H. Rensmo and H. Siegbahn, *J. Photochem. Photobiol., A*, 2002, **148**, 57.
131 S. N. Katea, Š. Hajduk, Z. C. Orel and G. Westin, *Inorg. Chem.*, 2017, **56**, 15150–15158.

132 J. Tao and S. Yu, *Sol. Energy Mater. Sol. Cells*, 2015, **141**, 108–124.
133 K. Komoto and J.-S. Lee, *End-of-Life Management of Photovoltaic Panels: Trends in PV Module Recycling Technologies*, International Energy Agency (EIA), 2018.
134 N. Barbero and F. Sauvage, in *Materials for Sustainable Energy Applications: Conversion, Storage, Transmission, and Consumption*, ed. D. Munoz-Rojas and X. Moya, Jenny Stanford Publishing, New York, 1st edn, 2016.
135 N. T. R. N. Kumara, A. Lim, C. M. Lim, M. I. Petra and P. Ekanayake, *Renewable Sustainable Energy Rev.*, 2017, **78**, 301–317.
136 Y. Hua, L. T. L. Lee, C. Zhang, J. Zhao, T. Chen, W. Y. Wong, W. K. Wong and X. Zhu, *J. Mater. Chem. A*, 2015, **3**, 13848–13855.
137 No Title, https://shop.solaronix.com/.
138 L. Han, A. Islam, H. Chen, C. Malapaka, B. Chiranjeevi, S. Zhang, X. Yang and M. Yanagida, *Energy Environ. Sci.*, 2012, **5**, 6057–6060.
139 B. Happ, A. Winter, M. D. Hager and U. S. Schubert, *Chem. Soc. Rev.*, 2012, **41**, 2222–2255.
140 J. F. Yin, M. Velayudham, D. Bhattacharya, H. C. Lin and K. L. Lu, *Coord. Chem. Rev.*, 2012, **256**, 3008–3035.
141 A. Reynal and E. Palomares, *Eur. J. Inorg. Chem.*, 2011, **29**, 4509–4526.
142 B. Pashaei, H. Shahroosvand, M. Graetzel and M. K. Nazeeruddin, *Chem. Rev.*, 2016, **116**, 9485–9564.
143 S. Bhand and S. Salunke-gawali, *Inorgan. Chim. Acta*, 2019, **495**, 118955.
144 A. Carella, F. Borbone and R. Centore, *Front. Chem.*, 2018, **6**, 481.
145 S. Aghazada and M. Nazeeruddin, *Inorganics*, 2018, **6**, 52.
146 C. P. Lee, C. T. Li and K. C. Ho, *Mater. Today*, 2017, **20**, 267–283.
147 T. Bessho, S. M. Zakeeruddin, C. Y. Yeh, E. W. G. Diau and M. Grätzel, *Angew. Chem., Int. Ed.*, 2010, **49**, 6646–6649.
148 No Title, https://www.rsc.org/periodic-table/element/44/ruthenium, (accessed 1 June 2020).
149 No Title, https://www.rsc.org/periodic-table/element/30/Zinc, (accessed 12 June 2020).
150 K. Kakiage, Y. Aoyama, T. Yano, T. Otsuka, T. Kyomen, M. Unno and M. Hanaya, *Chem. Commun.*, 2014, **50**, 6379–6381.
151 Y. Ren, D. Sun, Y. Cao, H. N. Tsao, Y. Yuan, S. M. Zakeeruddin, P. Wang and M. Grätzel, *J. Am. Chem. Soc.*, 2018, **140**, 2405–2408.
152 P. Gao, Y. J. Kim, J. H. Yum, T. W. Holcombe, M. K. Nazeeruddin and M. Grätzel, *J. Mater. Chem. A*, 2013, **1**, 5535–5544.
153 Y. Cao, Y. Saygili, A. Ummadisingu, J. Teuscher, J. Luo, N. Pellet, F. Giordano, S. M. Zakeeruddin, J.-E. Moser, M. Freitag, A. Hagfeldt and M. Grätzel, *Nat. Commun.*, 2017, **8**, 15390.
154 W. Zhang, Y. Wu, H. W. Bahng, Y. Cao, C. Yi, Y. Saygili, J. Luo, Y. Liu, L. Kavan, J. E. Moser, A. Hagfeldt, H. Tian, S. M. Zakeeruddin, W. H. Zhu and M. Grätzel, *Energy Environ. Sci.*, 2018, **11**, 1779–1787.
155 F. M. Jradi, X. Kang, D. Oneil, G. Pajares, Y. A. Getmanenko, P. Szymanski, T. C. Parker, M. A. El-Sayed and S. R. Marder, *Chem. Mater.*, 2015, **27**, 2480–2487.
156 W. Zeng, Y. Cao, Y. Bai, Y. Wang, Y. Shi, M. Zhang, F. Wang, C. Pan and P. Wang, *Chem. Mater.*, 2010, **22**, 1915–1925.
157 A. Abbotto, N. Manfredi, C. Marinzi, F. De Angelis, E. Mosconi, J. H. Yum, Z. Xianxi, M. K. Nazeeruddin and M. Grätzel, *Energy Environ. Sci.*, 2009, **2**, 1094–1101.
158 J. Park, C. Barolo, F. Sauvage, N. Barbero, C. Benzi, P. Quagliotto, S. Coluccia, D. Di Censo, M. Grätzel, M. K. Nazeeruddin and G. Viscardi, *Chem. Commun.*, 2012, **48**, 2782–2784.
159 J. Park, N. Barbero, J. Yoon, E. Dell'Orto, S. Galliano, R. Borrelli, J.-H. Yum, D. Di Censo, M. Grätzel, M. K. Nazeeruddin, C. Barolo and G. Viscardi, *Phys. Chem. Chem. Phys.*, 2014, **16**, 24173–24177.
160 N. Barbero, C. Magistris, J. Park, D. Saccone, P. Quagliotto, R. Buscaino, C. Medana, C. Barolo and G. Viscardi, *Org. Lett.*, 2015, **17**, 3306–3309.
161 A. Dessì, M. Calamante, A. Mordini, M. Peruzzini, A. Sinicropi, R. Basosi, F. Fabrizi De Biani, M. Taddei, D. Colonna, A. Di Car, G. Reginato and L. Zani, *Chem. Commun.*, 2014, **50**, 13952–13955.
162 H. Hug, M. Bader, P. Mair and T. Glatzel, *Appl. Energy*, 2014, **115**, 216–225.
163 M. Z. Iqbal, S. R. Ali and S. Khan, *Sol. Energy*, 2019, **181**, 490–509.
164 H. A. Maddah, V. Berry and S. K. Behura, *Renewable Sustainable Energy Rev.*, 2020, **121**, 109678.
165 G. Calogero, G. Di Marco, S. Caramori, S. Cazzanti, R. Argazzi and C. A. Bignozzi, *Energy Environ. Sci.*, 2009, **2**, 1162–1172.
166 C. Capello, U. Fischer and K. Hungerbühler, *Green Chem.*, 2007, **9**, 927–934.
167 M. A. M. Al-Alwani, A. B. Mohamad, N. A. Ludin, A. A. H. Kadhum and K. Sopian, *Renewable Sustainable Energy Rev.*, 2016, **65**, 183–213.
168 N. A. Ludin, A. M. Al-Alwani Mahmoud, A. B. Mohamad, A. A. H. Kadhum, K. Sopian and N. S. Abdul Karim, *Renewable Sustainable Energy Rev.*, 2014, **31**, 386–396.
169 A. Bartolotta and G. Calogero, in *Solar Cells and Light Management: Materials, Strategies and Sustainability*, ed. F. Enrichi and G. C. Righini, Elsevier, 2019, pp. 107–161.
170 A. N. Panche, A. D. Diwan and S. R. Chandra, *J. Nutr. Sci.*, 2016, **5**, 65–72.
171 S. Sabagh, M. Izadyar and F. Arkan, *Int. J. Quantum Chem.*, 2020, **120**, e26171.
172 N. Aziz, N. A. Mat Nor and A. K. Arof, *Opt. Quantum Electron.*, 2020, **52**, 1–13.
173 S. Shalini, R. Balasundara Prabhu, S. Prasanna, T. K. Mallick and S. Senthilarasu, *Renewable Sustainable Energy Rev.*, 2015, **51**, 1306–1325.

174 O. Adedokun, Y. K. Sanusi and A. O. Awodugba, *Optik*, 2018, **174**, 497–507.
175 K. Wongcharee, V. Meeyoo and S. Chavadej, *Sol. Energy Mater. Sol. Cells*, 2007, **91**, 566–571.
176 A. Schieber and F. Weber, in *Handbook on Natural Pigments in Food and Beverages Industrial Applications for Improving Food Color*, ed. R. Carle and R. M. Schweiggert, Elsevier, 2016, pp. 100–124.
177 W. Maiaugree, S. Lowpa, M. Towannang, P. Rutphonsan, A. Tangtrakarn, S. Pimanpang, P. Maiaugree, N. Ratchapolthavisin, W. Sang-Aroon, W. Jarernboon and V. Amornkitbamrung, *Sci. Rep.*, 2015, **5**, 15230.
178 F. G. Gao, A. J. Bard and L. D. Kispert, *J. Photochem. Photobiol., A*, 2000, **45130**, 49–56.
179 E. Yamazaki, M. Murayama, N. Nishikawa, N. Hashimoto, M. Shoyama and O. Kurita, *Sol. Energy*, 2007, **81**, 512–516.
180 Y. Koyama, T. Miki, X. F. Wang and H. Nagae, *Int. J. Mol. Sci.*, 2009, **10**, 4575–4622.
181 Y. Koyama, Y. Kakitani and H. Nagae, *Molecules*, 2012, **17**, 2188–2218.
182 X. F. Wang, R. Fujii, S. Ito, Y. Koyama, Y. Yamano, M. Ito, T. Kitamura and S. Yanagida, *Chem. Phys. Lett.*, 2005, **416**, 1–6.
183 X. F. Wang, Y. Koyama, H. Nagae, Y. Yamano, M. Ito and Y. Wada, *Chem. Phys. Lett.*, 2006, **420**, 309–315.
184 X. F. Wang, A. Matsuda, Y. Koyama, H. Nagae, S. Sasaki, H. Tamiaki and Y. Wada, *Chem. Phys. Lett.*, 2006, **423**, 470–475.
185 M. Roca, K. Chen and A. Pérez-Gálvez, in *Handbook on Natural Pigments in Food and Beverages Industrial Applications for Improving Food Color*, ed. R. Carle and R. M. Schweiggert, Elsevier, 2016, pp. 125–158.
186 A. K. Arof and T. L. Ping, in *Chlorophyll*, ed. E. Jacob-Lopes, IntechOpen, 2017, pp. 105–121.
187 A. K. Pandey, M. S. Ahmad, N. A. Rahim, V. V. Tyagi and R. Saidur, in *Environmental Biotechnology: For Sustainable Future*, ed. R. C. Sobti, N. K. Arora and R. Kothari, Springer International Publishing, 2018, pp. 375–401.
188 H. C. Hassan, Z. H. Z. Abidin, M. A. Careem and A. K. Arof, *High Perform. Polym.*, 2014, **26**, 647–652.
189 H. C. Hassan, Z. H. Z. Abidin, F. I. Chowdhury and A. K. Arof, *Int. J. Photoenergy*, 2016, **2016**, 3685210.
190 X. F. Wang, C. H. Zhan, T. Maoka, Y. Wada and Y. Koyama, *Chem. Phys. Lett.*, 2007, **447**, 79–85.
191 H. Chang, M. J. Kao, T. L. Chen, C. H. Chen, K. C. Cho and X. R. Lai, *Int. J. Photoenergy*, 2013, **2013**, 159502.
192 A. K. Arof and T. L. Ping, in *Chlorophyll*, ed. E. Jacob-Lopes, L. Q. Zepka and M. I. Queiroz, IntechOpen, 2017.
193 P. Esquivel, in *Handbook on Natural Pigments in Food and Beverages Industrial Applications for Improving Food Color*, ed. R. Carle and R. M. Schweiggert, Elsevier, 2016, pp. 81–99.
194 D. Zhang, S. M. Lanier, J. A. Downing, J. L. Avent, J. Lum and J. L. McHale, *J. Photochem. Photobiol., A*, 2008, **195**, 72–80.
195 A. R. Hernandez-Martinez, M. Estevez, S. Vargas, F. Quintanilla and R. Rodriguez, *Int. J. Mol. Sci.*, 2011, **12**, 5565–5576.
196 G. Calogero, G. Di Marco, S. Cazzanti, S. Caramori, R. Argazzi, A. Di Carlo and C. A. Bignozzi, *Int. J. Mol. Sci.*, 2010, **11**, 254–267.
197 E. Güzel, B. S. Arslan, V. Durmaz, M. Cesur, Ö. F. Tutar, T. Sarı, M. İşleyen, M. Nebioğlu and İ. Şişman, *Sol. Energy*, 2018, **173**, 34–41.
198 M. Wendel, A. Kumorkiewicz, S. Wybraniec, M. Ziółek and G. Burdziński, *Dyes Pigm.*, 2017, **141**, 306–315.
199 R. Grisorio, L. De Marco, C. Baldisserri, F. Martina, M. Serantoni, G. Gigli and G. P. Suranna, *ACS Sustainable Chem. Eng.*, 2015, **3**, 770–777.
200 M. Bonomo, A. Di Carlo and D. Dini, *J. Electrochem. Soc.*, 2018, **165**, H889–H896.
201 G. Boschloo and A. Hagfeldt, *Acc. Chem. Res.*, 2009, **42**, 1819–1826.
202 F. Bella, S. Galliano, M. Falco, G. Viscardi, C. Barolo, M. Grätzel and C. Gerbaldi, *Chem. Sci.*, 2016, **7**, 4480–4490.
203 P. J. Cameron and L. M. Peter, *J. Phys. Chem. B*, 2005, **109**(15), 7392–7398.
204 P. Ho, S. Thogiti, L. Q. Bao, R. Cheruku, K. S. Ahn and J. H. Kim, *Sol. Energy*, 2018, **161**, 9–16.
205 A. Apostolopoulou, M. Vlasiou, P. A. Tziouris, C. Tsiafoulis, A. C. Tsipis, D. Rehder, T. A. Kabanos, A. D. Keramidas and E. Stathatos, *Inorg. Chem.*, 2015, **54**, 3979–3988.
206 F. Bella, S. Galliano, M. Falco, G. Viscardi, C. Barolo, M. Grätzel and C. Gerbaldi, *Green Chem.*, 2017, **19**, 1043–1051.
207 S. U. Rehman, M. Noman, A. D. Khan, A. Saboor, M. S. Ahmad and H. U. Khan, *Optik*, 2020, **202**, 163591.
208 M. Magni, R. Giannuzzi, A. Colombo, M. P. Cipolla, C. Dragonetti, S. Caramori, S. Carli, R. Grisorio, G. P. Suranna, C. A. Bignozzi, D. Roberto and M. Manca, *Inorg. Chem.*, 2016, **55**, 5245–5253.
209 P. J. Cameron, L. M. Peter, S. M. Zakeeruddin and M. Grätzel, *Coord. Chem. Rev.*, 2004, **248**, 1447–1453.
210 H. Nusbaumer, S. M. Zakeeruddin, J. E. Moser and M. Grätzel, *Chem. – Eur. J.*, 2003, **9**, 3756–3763.
211 Periodic Table data, https://periodictable.com/index.html, (accessed 20 September 2019).
212 Cobalt hydroxide price up 55% in three months, https://www.mining.com/, (accessed 30 December 2019).
213 F. Bella, S. Galliano, C. Gerbaldi and G. Viscardi, *Energies*, 2016, **9**, 384.
214 N. Swain and S. Mishra, *J. Cleaner Prod.*, 2019, **220**, 884–898.
215 F. Bella, A. Sacco, G. P. Salvador, S. Bianco, E. Tresso, C. F. Pirri and R. Bongiovanni, *J. Phys. Chem. C*, 2013, **117**, 20421–20430.
216 A. Lennert, M. Sternberg, K. Meyer, R. D. Costa and D. M. Guldi, *ACS Appl. Mater. Interfaces*, 2017, **9**, 33437–33445.

217 R. Prado and C. C. Weber, in *Application of ionic liquid*, 2016, pp. 1–58.
218 N. Hadrup and G. Ravn-Haren, *J. Trace Elem. Med. Biol.*, 2020, **58**, 126435.
219 K. Salgado-Castro, I. V. Lijanova, D. Jaramillo-Vigueras and J. N. Castillo-Cervantes, *IEEE J. Photovolt.*, 2019, **9**, 1708–1715.
220 R. K. Kokal, S. Bhattacharya, L. S. Cardoso, P. B. Miranda, V. R. Soma, P. Chetti, D. Melepurath and S. S. K. Raavi, *Sol. Energy*, 2019, **188**, 913–923.
221 M. Bonomo and D. Dini, *Energies*, 2016, **9**, 373.
222 A. Colombo, C. Dragonetti, M. Magni, D. Roberto, F. Demartin, S. Caramori and C. A. Bignozzi, *ACS Appl. Mater. Interfaces*, 2014, **6**, 13945–13955.
223 A. Colombo, G. Di Carlo, C. Dragonetti, M. Magni, A. Orbelli Biroli, M. Pizzotti, D. Roberto, F. Tessore, E. Benazzi, C. A. Bignozzi, L. Casarin and S. Caramori, *Inorg. Chem.*, 2017, **56**, 14189–14197.
224 E. Benazzi, M. Magni, A. Colombo, C. Dragonetti, S. Caramori, C. A. Bignozzi, R. Grisorio, G. P. Suranna, M. P. Cipolla, M. Manca and D. Roberto, *Electrochim. Acta*, 2018, **271**, 180–189.
225 M. Karpacheva, F. J. Malzner, C. Wobill, A. Büttner, E. C. Constable and C. E. Housecroft, *Dyes Pigm.*, 2018, **156**, 410–416.
226 M. Freitag, F. Giordano, W. Yang, M. Pazoki, Y. Hao, B. Zietz, M. Grätzel, A. Hagfeldt and G. Boschloo, *J. Phys. Chem. C*, 2016, **120**, 9595–9603.
227 C. Dragonetti, M. Magni, A. Colombo, F. Melchiorre, P. Biagini and D. Roberto, *ACS Appl. Energy Mater.*, 2018, **1**, 751–756.
228 Y. Saygili, M. Söderberg, N. Pellet, F. Giordano, Y. Cao, A. B. Munoz-García, S. M. Zakeeruddin, N. Vlachopoulos, M. Pavone, G. Boschloo, L. Kavan, J. E. Moser, M. Grätzel, A. Hagfeldt and M. Freitag, *J. Am. Chem. Soc.*, 2016, **138**, 15087–15096.
229 Critical Raw Materials, https://ec.europa.eu/growth/sectors/raw-materials/specific-interest/critical_en, (accessed 3 December 2020).
230 K. Lourenssen, J. Williams, F. Ahmadpour, R. Clemmer and S. Tasnim, *J. Energy Storage*, 2019, **25**, 100844.
231 K. Oyaizu, N. Hayo, Y. Sasada, F. Kato and H. Nishide, *Dalton Trans.*, 2013, **42**, 16090–16095.
232 W. Yang, M. Söderberg, A. I. K. Eriksson and G. Boschloo, *RSC Adv.*, 2015, **5**, 26706–26709.
233 M. A. Mercadante, C. B. Kelly, J. M. Bobbitt, L. J. Tilley and N. E. Leadbeater, *Nat. Protoc.*, 2013, **8**, 666–676.
234 TEMPO SDS, https://www.sigmaaldrich.com/Graphics/COfAInfo/SigmaSAPQM/SPEC/21/214000/214000-BULK_ALDRICH.pdf, (accessed 1 March 2020).
235 W. Yang, N. Vlachopoulos, Y. Hao, A. Hagfeldt and G. Boschloo, *Phys. Chem. Chem. Phys.*, 2015, **17**, 15868–15875.
236 R. Ruess, J. Horn, A. Ringleb and D. Schlettwein, *J. Phys. Chem. C*, 2019, **123**, 22074–22082.
237 S. M. Feldt, E. A. Gibson, E. Gabrielsson, L. Sun, G. Boschloo and A. Hagfeldt, *J. Am. Chem. Soc.*, 2010, **132**, 16714–16724.
238 R. Kato, F. Kato, K. Oyaizu and H. Nishide, *Chem. Lett.*, 2014, **43**, 480–482.
239 R. Ciriminna and M. Pagliaro, *Org. Process Res. Dev.*, 2010, **14**, 245–251.
240 D. R. MacFarlane, J. Choi, B. H. R. Suryanto, R. Jalili, M. Chatti, L. M. Azofra and A. N. Simonov, *Adv. Mater.*, 2019, 1904804.
241 M. Wang, N. Chamberland, L. Breau, J. E. Moser, R. Humphry-Baker, B. Marsan, S. M. Zakeeruddin and M. Grätzel, *Nat. Chem.*, 2010, **2**, 385–389.
242 A. Tangtrakarn, W. Maiaugree, P. Uppachai, N. Ratchapolthavisin, K. Moolsarn, E. Swatsitang and V. Amornkitbamrung, *Diamond Relat. Mater.*, 2019, **97**, 107451.
243 R. Peri, P. Mathan Kumar and B. Muthuraaman, *RSC Adv.*, 2020, **10**, 4521–4528.
244 M. Towannang, P. Kumlangwan, W. Maiaugree, K. Ratchaphonsaenwong, V. Harnchana, W. Jarenboon, S. Pimanpang and V. Amornkitbamrung, *Electron. Mater. Lett.*, 2015, **11**, 643–649.
245 H. Tian, E. Gabrielsson, P. W. Lohse, N. Vlachopoulos, L. Kloo, A. Hagfeldt and L. Sun, *Energy Environ. Sci.*, 2012, **5**, 9752–9755.
246 K. Funabiki, Y. Saito, M. Doi, K. Yamada, Y. Yoshikawa, K. Manseki, Y. Kubota and M. Matsui, *Tetrahedron*, 2014, **70**, 6312–6317.
247 A. Hilmi, T. A. Shoker and T. H. Ghaddar, *ACS Appl. Mater. Interfaces*, 2014, **6**, 8744–8753.
248 W. Y. Li, H. K. Zheng, J. W. Wang, L. Le Zhang, H. M. Han and M. X. Wu, *Appl. Phys. A: Mater. Sci. Process.*, 2017, **123**, 541.
249 M. M. Rahman, J. Wang, N. C. D. Nath and J. J. Lee, *Electrochim. Acta*, 2018, **286**, 39–46.
250 R. Bhargava, T. Daeneke, S. J. Thompson, J. Lloyd, C. A. Palma, J. Reichert, J. V. Barth, L. Spiccia and U. Bach, *J. Phys. Chem. C*, 2015, **119**, 19613–19618.
251 S. Powar, R. Bhargava, T. Daeneke, G. Götz, P. Bäuerle, T. Geiger, S. Kuster, F. A. Nüesch, L. Spiccia and U. Bach, *Electrochim. Acta*, 2015, **182**, 458–463.
252 K. Meng and K. R. Thampi, *ACS Appl. Mater. Interfaces*, 2014, **6**, 20768–20775.
253 S. Tan, Z. Zhao, C. Wang and Y. Wu, *Electrochim. Acta*, 2018, **288**, 165–172.
254 F. De Rossi, T. Pontecorvo and T. M. Brown, *Appl. Energy*, 2015, **156**, 413–422.
255 A. S. da Silva Sobrinho, M. Latrèche, G. Czeremuszkin, J. E. Klemberg-Sapieha and M. R. Wertheimer, *J. Vac. Sci. Technol., A*, 1998, **16**, 3190–3198.
256 P. G. Jessop, *Green Chem.*, 2011, **13**, 1391–1398.
257 Ellen MacArthur Foundation, https://www.ellenmacarthurfoundation.org, (accessed 8 May 2019).
258 Z. Hui, Y. Xiong, L. Heng, L. Yuan and W. Yu-Xiang, *Chin. Phys. Lett.*, 2007, **24**, 3272–3275.

259 Y.-S. Jung, B. Yoo, M. K. Lim, S. Y. Lee and K.-J. Kim, *Electrochim. Acta*, 2009, **54**, 6286–6291.
260 C. Law, S. C. Pathirana, X. Li, A. Y. Anderson, P. R. F. Barnes, A. Listorti, T. H. Ghaddar and B. C. ORegan, *Adv. Mater.*, 2010, **22**, 4505–4509.
261 F. Bella, L. Porcarelli, D. Mantione, C. Gerbaldi, C. Barolo, M. Grätzel and D. Mecerreyes, *Chem. Sci.*, 2020, **11**, 1485–1493.
262 C. Law, O. Moudam, S. Villarroya-Lidon and B. O'Regan, *J. Mater. Chem.*, 2012, **22**, 23387–23394.
263 W. Xiang, F. Huang, Y.-B. Cheng, U. Bach and L. Spiccia, *Energy Environ. Sci.*, 2013, **6**, 121–127.
264 R. Fayad, T. A. Shoker and T. H. Ghaddar, *Dalton Trans.*, 2016, **45**, 5622–5628.
265 R. Y. Y. Lin, T. M. Chuang, F. L. Wu, P. Y. Chen, T. C. Chu, J. S. Ni, M. S. Fan, Y. H. Lo, K. C. Ho and J. T. Lin, *ChemSusChem*, 2015, **8**, 105–113.
266 H. Ellis, R. Jiang, S. Ye, A. Hagfeldt and G. Boschloo, *Phys. Chem. Chem. Phys.*, 2016, **18**, 8419–8427.
267 C. Dong, W. Xiang, F. Huang, D. Fu, W. Huang, U. Bach, Y. B. Cheng, X. Li and L. Spiccia, *Angew. Chem., Int. Ed.*, 2014, **53**, 6933–6937.
268 R. Y.-Y. Lin, F.-L. Wu, C.-T. Li, P.-Y. Chen, K.-C. Ho and J. T. Lin, *ChemSusChem*, 2015, **8**, 2503–2513.
269 S. C. Patankar and S. Renneckar, *Green Chem.*, 2017, **19**, 4792–4797.
270 A. T. Vicente, A. Araújo, M. J. Mendes, D. Nunes, M. J. Oliveira, O. Sanchez-Sobrado, M. P. Ferreira, H. Águas, E. Fortunato and R. Martins, *J. Mater. Chem. C*, 2018, **6**, 3143–3181.
271 W. Xiang, D. Chen, R. A. Caruso, Y. B. Cheng, U. Bach and L. Spiccia, *ChemSusChem*, 2015, **8**, 3704–3711.
272 S. Zhang, G. Y. Dong, B. Lin, J. Qu, N. Y. Yuan, J. N. Ding and Z. Gu, *Sol. Energy*, 2016, **127**, 19–27.
273 B. E. Hardin, H. J. Snaith and M. D. McGehee, *Nat. Photonics*, 2012, **6**, 162–169.
274 S. Yun, J. Nei de Freitas, A. F. Nogueira, Y. Wang, S. Ahmad and Z. Wang, *Prog. Polym. Sci.*, 2016, **59**, 1–40.
275 A. A. Mohamad, *Sol. Energy*, 2019, **190**, 434–452.
276 U. Bach, D. Lupo, P. Comte, J. E. Moser, F. Weissörtel, J. Salbeck, H. Spreitzer and M. Grätzel, *Nature*, 1998, **395**, 583–585.
277 A. Singh, E. Radicchi, S. Fantacci, F. Nunzi, F. De Angelis and A. Gagliardi, *J. Phys. Chem. C*, 2019, **123**(24), 14955–14963.
278 A. T. Murray, J. M. Frost, C. H. Hendon, C. D. Molloy, D. R. Carbery and A. Walsh, *Chem. Commun.*, 2015, **51**, 8935–8938.
279 V. Mirruzzo and A. Di Carlo, *Chem*, 2017, **2**, 612–613.
280 C. H. Teh, R. Daik, E. L. Lim, C. C. Yap, M. A. Ibrahim, N. A. Ludin, K. Sopian and M. A. M. Teridi, *J. Mater. Chem. A*, 2016, **4**, 15788–15822.
281 P. Wang, Q. Dai, S. M. Zakeeruddin, M. Forsyth, D. R. MacFarlane and M. Grätzel, *J. Am. Chem. Soc.*, 2004, **126**, 13590–13591.
282 A. Lennert, K. Wagner, R. Yunis, J. M. Pringle, D. M. Guldi and D. L. Officer, *ACS Appl. Mater. Interfaces*, 2018, **10**, 32271–32280.
283 P. Pollak, G. Romeder, F. Hagedorn and H. Gelbke, *Nitriles*, Wiley, 2000.
284 M. Freitag, Q. Daniel, M. Pazoki, K. Sveinbjörnsson, J. Zhang, L. Sun, A. Hagfeldt and G. Boschloo, *Energy Environ. Sci.*, 2015, **8**, 2634–2637.
285 Y. Hou, D. Wang, X. H. Yang, W. Q. Fang, B. Zhang, H. F. Wang, G. Z. Lu, P. Hu, H. J. Zhao and H. G. Yang, *Nat. Commun.*, 2013, **4**, 1583.
286 L. Wang, M. Al-Mamun, P. Liu, Y. Wang, H. G. Yang, H. F. Wang and H. Zhao, *NPG Asia Mater.*, 2015, **7**, e226.
287 M. Adachi, M. Sakamoto, J. Jiu, Y. Ogata and S. Isoda, *J. Phys. Chem. B*, 2006, **110**, 13872–13880.
288 M. Z. Iqbal and S. Khan, *Sol. Energy*, 2018, **160**, 130–152.
289 R. Senthilkumar, M. Balu, S. Ramakrishnan, P. C. Ramamurthy, S. K. Batabyal, D. Kumaresan and N. K. Kothurkar, *J. Electroanal. Chem.*, 2019, **847**, 113236.
290 K. Subalakshmi, K. A. Kumar, O. P. Paul, S. Saraswathy, A. Pandurangan and J. Senthilselvan, *Sol. Energy*, 2019, **193**, 507–518.
291 I. Ahmad, J. E. McCarthy, M. Bari and Y. K. Gun'ko, *Sol. Energy*, 2014, **102**, 152–161.
292 S. H. Hsu, C. T. Li, H. T. Chien, R. R. Salunkhe, N. Suzuki, Y. Yamauchi, K. C. Ho and K. C. W. Wu, *Sci. Rep.*, 2014, **4**, 1–6.
293 M. Wu, X. Lin, Y. Wang, L. Wang, W. Guo, D. Qi, X. Peng, A. Hagfeldt, M. Grätzel and T. Ma, *J. Am. Chem. Soc.*, 2012, **134**, 3419–3428.
294 A. Agresti, S. Pescetelli, E. Gatto, M. Venanzi and A. Di Carlo, *J. Power Sources*, 2015, **287**, 87–95.
295 G. Syrrokostas, A. Siokou, G. Leftheriotis and P. Yianoulis, *Sol. Energy Mater. Sol. Cells*, 2012, **103**, 119–127.
296 E. Olsen, G. Hagen and S. E. Lindquist, *Sol. Energy Mater. Sol. Cells*, 2000, **63**, 267–273.
297 M. Wu and T. Ma, *J. Phys. Chem. C*, 2014, **118**, 16727–16742.
298 H. Wang and Y. H. Hu, *Energy Environ. Sci.*, 2012, **5**, 8182–8188.
299 R. Trevisan, M. Döbbelin, P. P. Boix, E. M. Barea, R. Tena-Zaera, I. Mora-Seró and J. Bisquert, *Adv. Energy Mater.*, 2011, **1**, 781–784.
300 M. Z. Iqbal, S. Alam, M. M. Faisal and S. Khan, *Int. J. Energy Res.*, 2019, **43**, 3058–3079.
301 Z. Jin, M. Zhang, M. Wang, C. Feng and Z. S. Wang, *Acc. Chem. Res.*, 2017, **50**, 895–904.
302 G. R. Li, J. Song, G. L. Pan and X. P. Gao, *Energy Environ. Sci.*, 2011, **4**, 1680–1683.
303 Z. Zhou, S. Sigdel, J. Gong, B. Vaagensmith, H. Elbohy, H. Yang, S. Krishnan, X. F. Wu and Q. Qiao, *Nano Energy*, 2016, **22**, 558–563.
304 S. Yun, J. Nei de Freitas, A. F. Nogueira, Y. Wang, S. Ahmad, Z. S. Wang, J. N. Freitas, A. F. Nogueira, Y. Wang, S. Ahmad and Z. S. Wang, *Prog. Polym. Sci.*, 2016, **59**, 1–40.

305 K. Suzuki, M. Yamaguchi, M. Kumagai and S. Yanagida, *Chem. Lett.*, 2003, **32**, 28–29.
306 M. Chen and L.-L. Shao, *Chem. Eng. J.*, 2016, **304**, 629–645.
307 G. Liu, H. Wang, X. Li, Y. Rong, Z. Ku, M. Xu, L. Liu, M. Hu, Y. Yang, P. Xiang, T. Shu and H. Han, *Electrochim. Acta*, 2012, **69**, 334–339.
308 G. Veerappan, K. Bojan and S. W. Rhee, *ACS Appl. Mater. Interfaces*, 2011, **3**, 857–862.
309 T. N. Murakami, S. Ito, Q. Wang, M. K. Nazeeruddin, T. Bessho, I. Cesar, P. Liska, R. Humphry-Baker, P. Comte, P. Péchy and M. Grätzel, *J. Electrochem. Soc.*, 2006, **153**, A2255–A2261.
310 J. M. Kim and S. W. Rhee, *Electrochim. Acta*, 2012, **83**, 264–270.
311 M. N. Mustafa, S. Shafie, Z. Zainal and Y. Sulaiman, *Mater. Des.*, 2017, **136**, 249–257.
312 I. Drogin, *J. Air Pollut. Control Assoc.*, 1968, **18**, 216–228.
313 Birla Carbon Sustainability Report 2019, https://sustainability.birlacarbon.com/downloads.html, (accessed 30 December 2019).
314 A. Thess, R. Lee, P. Nikolaev, H. Dai, P. Petit, J. Robert, C. Xu, Y. H. Lee, S. G. Kim, A. G. Rinzler, D. T. Colbert, G. E. Scuseria, D. Tománek, J. E. Fischer and R. E. Smalley, *Science*, 1996, **273**, 483–487.
315 S. Ravi Silva, S. Haq and B. O. Boskovic, *US Pat.*, US8715790B2, 2002.
316 M. Wu, M. Sun, H. Zhou, J. Y. Ma and T. Ma, *Adv. Funct. Mater.*, 2020, **30**, 1906451.
317 D. Y. Chung, Y. J. Son, J. M. Yoo, J. S. Kang, C. Y. Ahn, S. Park and Y. E. Sung, *ACS Appl. Mater. Interfaces*, 2017, **9**, 41303–41313.
318 Z. Qiu, Y. Wang, X. Bi, T. Zhou, J. Zhou, J. Zhao, Z. Miao, W. Yi, P. Fu and S. Zhuo, *J. Power Sources*, 2018, **376**, 82–90.
319 S. M. Cha, G. Nagaraju, S. C. C. Sekhar, L. K. K. Bharat and J. S. Yu, *J. Colloid Interface Sci.*, 2018, **513**, 843–851.
320 G. Ma, Q. Yang, K. Sun, H. Peng, F. Ran, X. Zhao and Z. Lei, *Bioresour. Technol.*, 2015, **197**, 137–142.
321 Y. Di, S. Jia, N. Li, C. Hao, H. Zhang and S. Hu, *Org. Electron.*, 2020, **76**, 105395.
322 B. Baptayev, A. Aukenova, D. Mustazheb, M. Kazaliyev and M. P. Balanay, *J. Photochem. Photobiol., A*, 2019, **383**, 111977.
323 C. Wang, S. Yun, H. Xu, Z. Wang, F. Han, Y. Zhang, Y. Si and M. Sun, *Ceram. Int.*, 2020, **46**, 3292–3303.
324 R. Kumar, V. Sahajwalla and P. Bhargava, *Nanoscale Adv.*, 2019, **1**, 3192–3199.
325 S. Müller, D. Wieschollek, I. J. Junger, E. Schwenzfeier-Hellkamp and A. Ehrmann, *Optik*, 2019, **198**, 163243.
326 F. Hao, P. Dong, Q. Luo, J. Li, J. Lou and H. Lin, *Energy Environ. Sci.*, 2013, **6**, 2003.
327 D. Vikraman, S. A. Patil, S. Hussain, N. Mengal, S. H. Jeong, J. Jung, H. J. Park, H.-S. Kim and H.-S. Kim, *J. Ind. Eng. Chem.*, 2019, **69**, 379–386.
328 J. Zhang, W. Wu, C. Zhang, Z. Ren and X. Qian, *Appl. Surf. Sci.*, 2019, **484**, 1111–1117.
329 T. Jeong, S.-Y. Ham, B. Koo, P. Lee, Y.-S. Min, J.-Y. Kim and M. J. Ko, *J. Ind. Eng. Chem.*, 2019, **80**, 106–111.
330 M. Congiu, M. Bonomo, M. L. De Marco, D. P. Dowling, A. Di Carlo, D. Dini and C. F. O. Graeff, *ChemistrySelect*, 2016, **1**, 2808–2815.
331 M. Congiu, F. Decker, D. Dini and C. F. O. Graeff, *Int. J. Adv. Manuf. Technol.*, 2016, 1–9.
332 H. K. Mulmudi, S. K. Batabyal, M. Rao, R. R. Prabhakar, N. Mathews, Y. M. Lam and S. G. Mhaisalkar, *Phys. Chem. Chem. Phys.*, 2011, **13**, 19307–19309.
333 J.-Y. Lin, Y.-T. Tsai, S.-Y. Tai, Y.-T. Lin, C.-C. Wan, Y.-L. Tung and Y.-S. Wu, *J. Electrochem. Soc.*, 2012, **160**, D46–D52.
334 K. Ashok Kumar, A. Pandurangan, S. Arumugam and M. Sathiskumar, *Sci. Rep.*, 2019, **9**, 1228.
335 T. K. Trinh, V. T. H. Pham, N. T. N. Truong, C. D. Kim and C. Park, *J. Cryst. Growth*, 2017, **461**, 53–59.
336 T. Van Nguyen, N. T. N. Truong, P. Ho, T. K. Trinh, J. H. Kim and C. Park, *J. Mater. Sci.: Mater. Electron.*, 2019, **30**, 19752–19759.
337 K. Zhang, M. W. Khan, X. Zuo, Q. Yang, H. Tang, M. Wu and G. Li, *Electrochim. Acta*, 2019, **307**, 64–75.
338 W. Yang, B. Xia, J. Lu, P. Yang and X. Chen, *Nano*, 2019, **14**, 1950048.
339 M. Lickleder, G. Cha, R. Hahn and P. Schmuki, *J. Electrochem. Soc.*, 2019, **166**, H3009–H3013.
340 F. Y. Kuo, F. S. Lin, M. H. Yeh, M. S. Fan, L. Y. Hsiao, J. J. Lin, R. J. Jeng and K. C. Ho, *ACS Appl. Mater. Interfaces*, 2019, **11**, 25090–25099.
341 D. Ursu, M. Vajda and M. Miclau, *J. Alloys Compd.*, 2019, **802**, 86–92.
342 Q. Yang, X. Zuo, J. Yao, K. Zhang, H. Zhang, M. W. Khan, W. Wang, H. Tang, M. Wu, G. Li and S. Jin, *J. Electroanal. Chem.*, 2019, **844**, 34–42.
343 S. Yun, X. Zhou, Y. Zhang, C. Wang and Y. Hou, *Electrochim. Acta*, 2019, **309**, 371–381.
344 R. N. Hanson, R. W. Giese, M. A. Davis, S. M. Costello, R. N. Hanson and M. A. Davis, *J. Med. Chem.*, 1978, **21**, 496–498.
345 Q.-S. Jiang, W. Li, J. Wu, W. Cheng, J. Zhu, T. Zhu, S. Ren and Y. Zhang, *J. Electroanal. Chem.*, 2019, **852**, 113522.
346 V. H. V. Quy, J. H. Park, S. H. Kang, H. Kim and K. S. Ahn, *J. Electrochem. Soc.*, 2019, **166**, H473–H479.
347 D. Kishore Kumar, S. R. Popuri, S. K. Swami, O. R. Onuoha, J.-W. Bos, B. Chen, N. Bennett and H. M. Upadhyaya, *Sol. Energy*, 2019, **190**, 28–33.
348 H. Wang, S. Huang, S. Wang, Z. Hu, G. Ding, X. Qian and Z. Chen, *J. Electroanal. Chem.*, 2019, **834**, 26–32.
349 A. H. Alami, B. Rajab, J. Abed, M. Faraj, A. A. Hawili and H. Alawadhi, *Energy*, 2019, **174**, 526–533.
350 Z. Wang, S. Yun, X. Wang, C. Wang, Y. Si, Y. Zhang and H. Xu, *Ceram. Int.*, 2019, **45**, 4208–4218.

351 P. Arunachalam, in *Rational Design of Solar Cells for Efficient Solar Energy Conversion*, ed. A. Pandikumar and R. Ramaraj, Wiley, 2018, pp. 169–186.
352 A. A. Mohamed Sultan, E. Lou and P. T. Mativenga, *J. Cleaner Prod.*, 2017, **154**, 51–60.
353 J. B. Dahmus and T. G. Gutowski, *Environ. Sci. Technol.*, 2007, **41**, 7543–7550.
354 X. Zeng, J. A. Mathews and J. Li, *Environ. Sci. Technol.*, 2018, **52**, 4835–4841.
355 B. Pang, Y. Shi, S. Lin, Y. Chen, J. Feng, H. Dong, H. Yang, Z. Zhao, L. Yu and L. Dong, *Mater. Res. Bull.*, 2019, **117**, 78–83.
356 S. Ji, L. Zhang, L. Yu, X. Xu and J. Liu, *RSC Adv.*, 2016, **6**, 101752–101759.
357 L. Li, X. Zhang, L. Fu, Q. Wang, S. Ji, M. Wu, H. Wang and W. Zhang, *Composites, Part B*, 2019, **173**, 107026.
358 Y. Areerob, K. Y. Cho, C.-H. Jung and W.-C. Oh, *J. Alloys Compd.*, 2019, **775**, 690–697.
359 K. Silambarasan, J. Archana, S. Athithya, S. Harish, R. Sankar Ganesh, M. Navaneethan, S. Ponnusamy, C. Muthamizhchelvan, K. Hara and Y. Hayakawa, *Appl. Surf. Sci.*, 2020, **501**, 144010.
360 Y. Di, Z. Xiao, Z. Zhao, G. Ru, B. Chen and J. Feng, *J. Alloys Compd.*, 2019, **788**, 198–205.
361 M. Mohammadnezhad, G. S. Selopal, N. Alsayyari, R. Akilimali, F. Navarro-Pardo, Z. M. Wang, B. Stansfield, H. Zhao and F. Rosei, *J. Electrochem. Soc.*, 2019, **166**, H3065–H3073.
362 M. Banomo, D. Dini, A. G. Marrani, M. Bonomo, D. Dini and A. G. Marrani, *Langmuir*, 2016, **32**, 11540–11550.
363 A. C. Veltkamp, Present. 22nd Eur. Photovolt. Sol. Energy Conf. Exhib, 2007, vol. **3**, pp. 3–7.
364 P. Y. Hsu, H. F. Lee, S. M. Yang, Y. T. Chua, Y. L. Tung and J. J. Kai, in *Procedia Engineering*, 2012, vol. 36, pp. 439–445.
365 T. Yamaguchi, N. Tobe, D. Matsumoto, T. Nagai and H. Arakawa, *Sol. Energy Mater. Sol. Cells*, 2010, **94**, 812–816.
366 S. Heusing, P. W. Oliveira, E. Kraker, A. Haase, C. Palfinger and M. Veith, in *Organic Optoelectronics and Photonics III*, 2008, vol. 6999, p. 69992I.
367 A. F. Nogueira, C. Longo and M. De Paoli, *Coord. Chem. Rev.*, 2004, **248**, 1455–1468.
368 G. Boschloo, H. Lindström, E. Magnusson, A. Holmberg and A. Hagfeldt, *J. Photochem. Photobiol., A*, 2002, **148**, 11–15.
369 M. Dürr, A. Schmid, M. Obermaier, S. Rosselli, A. Yasuda and G. Nelles, *Nat. Mater.*, 2005, **4**, 607–611.
370 C. Longo, J. Freitas and M. A. De Paoli, *J. Photochem. Photobiol., A*, 2003, **159**, 33–39.
371 T. Miyasaka, Y. Kijitori, T. N. Murakami, M. Kimura and S. Uegusa, *Chem. Lett.*, 2002, **31**, 1250–1251.
372 R. Zhu, Z. Zhang and Y. Li, *Nanotechnol. Rev.*, 2019, **8**, 452–458.
373 Y. Ogata, K. Iguchi and T. Oya, *Energies*, 2019, **13**, 57.
374 S. Humbert, V. Rossi, M. Margni, O. Jolliet and Y. Loerincik, *Int. J. Life Cycle Assess.*, 2009, **14**, 95–106.
375 R. Accorsi, L. Versari and R. Manzini, *Sustainability*, 2015, **7**, 2818–2840.
376 J. Peng, L. Lu and H. Yang, *Renewable Sustainable Energy Rev.*, 2013, **19**, 255–274.

